BAYESIAN MAXIMUM ENTROPY SPACE/TIME ANALYSIS OF AMBIENT PARTICULATE MATTER AND MORTALITY IN THAILAND

Sitthichok Puangthongthub

A dissertation submitted to the faculty of the University of North Carolina at Chapel Hill in partial fulfillment of the requirements for the degree of Doctor of Philosophy in the Department of Environmental Sciences and Engineering, School of Public Health.

Chapel Hill
2006

Approved by
Advisor: Marc Serre
Reader: Douglas Crawford-Brown
Reader: Richard Kamens
Reader: David Leith
Reader: Dana Loomis
Reader: Karin Yeatts

ABSTRACT

SITTHICHOK PUANGTHONGTHUB: Bayesian Maximum Entropy Space/Time Analysis of Ambient Particulate Matter and Mortality in Thailand
(Under the direction of Marc L. Serre, Ph.D.)

Several epidemiological studies have confirmed the associations and estimated the risk of cardiovascular and pulmonary mortality due to short term exposure to PM_{10}. However the errors introduced by techniques previously used to interpolate PM_{10} in characterizing the strength of the associations remain in question. Therefore we incorporate the Bayesian Maximum Entropy (BME) method of modern spatiotemporal Geostatistics in the exposure assessment to investigate the effect that daily PM_{10} has on cardiovascular and respiratory mortality in different regions of Thailand.

The BME maps show that the PM_{10} field across Thailand exhibits considerable space/time variability. These maps suggest that the PM_{10} daily average concentration did not comply with the PM_{10} standard, which is supported by the maps of PM_{10} daily maximum concentration, and confirmed by BME maps of non-attainment areas. Furthermore, the BME analysis targeted districts in the Northeast region as sites where new monitoring stations should be added in order to improve the Thailand's existing monitoring network.

These maps provided the most accurate estimate of PM_{10} exposure obtained to date for each district location and day for which cardiovascular and respiratory mortality

was reported in Thailand during 1998-2003. The strength of the associations was then investigated through an analysis using a case-crossover design. The observed associations were stronger for pulmonary mortality than for cardiovascular mortality. The high odds ratios observed in Bangkok and the central region were possibly due to industrialization, construction, and traffic emission sources while positive associations found in other regions could be related to sources from agricultural biomass burning, forest fire, wind-blown dust, and sea spray.

Furthermore, a holistochastic human exposure analysis propagated mapping and epidemiologic uncertainty to obtain the lower-bound and upper-bound estimates of the number of deaths from cardiovascular and respiratory causes that resulted from acute health response to short term exposure to PM_{10} across Thailand. An Elasticity uncertainty analysis suggests that the uncertainty in the assessment of the number of deaths caused by PM_{10} can be improved by adding monitoring stations in the Northeastern region, and by improving the epidemiologic study in the Northern region.

ACKNOWLEDGEMENTS

This dissertation could not have been written without the significant contributions of a number of people. I would like to acknowledge my advisor Dr. Marc Serre for his excellence in teaching and advising as well as his unfailing motivation and encouragement. I feel extremely privileged to work with him and I have learned a great deal from him, above and beyond his contributions to my research. I am grateful to my dissertation committee members: Professor Douglas Crawford-Brown, Professor Richard Kamens, Professor David Leith, Professor Dana Loomis and Dr. Karin Yeatts. Each of them offered remarkable guidance, advice, criticism, and insight from his or her unique expertise. The consistent motivation, support, and encouragement from all of my committee members have meant so much to me. Without their support at the initial stage of forming this research prospectus, I would not be able to continue my PhD study. Special thanks go to Maryanne Boundy, a director of the Baity Air and Engineering Lab and Professor Michael Flynn for their support and critical advice when I was trying to continue my PhD study.

As for SAS® programming assistance, my appreciation goes to Chris Weisen of the Odum Institute for Research in Social Science at UNC for his skillful editing, as well as for his useful ideas and thoughts on several issues that made my analysis more efficiently. Without his help, my analysis might have taken many more months to complete. As for traveling assistance, I would like to acknowledge the University Center

for International Studies at UNC for awarding me the Doctoral Research Travel Award which allowed me to meet and present my research proposal to Thai agencies and obtain data sets needed for this study.

Several individual and agencies in Thailand played major roles in making my doctoral research possible. Special acknowledgment goes to Dr. Warangkana Polprasert of Sukhothai Thammathirat Open University for her assistance in obtaining GIS and demographic data. I would like to thank the Pollution Control Department of Ministry of Natural Resources and Environment, the Bureau of Policy and Strategy of The Ministry of Public Health, the National Statistical Office and the Meteorological Department of Ministry of Information and Communication Technology, and the Department of Provincial Administration of Ministry of Interior for providing data sets needed for this research. I also would like to recognize the Office of Civil Service Commission for awarding me a full M-PhD scholarship which gave me an opportunity to experience the world-class teaching and research at UNC for my professional development.

I would like to thank all of my friends, both in Thailand and in the U.S., especially those in Chapel Hill, for their encouragement and support. I am gratified to my lab mates at the BME Lab for their friendship and assistance throughout this analysis. My deep appreciation goes to the Thai community and friends in North Carolina and the university with whom I have developed close friendship. They have made my stay in the U.S. very delightful. This special feeling has been invaluable and has made me feel at "home" while I have been away from my home in Thailand.

Most importantly, I am forever deeply indebted to my parents, Chalong Sriwattananun and Somboon Puangthongthub, as well as my respected and beloved

relatives, Somsak Chaijaroenwatana and Bin Poolprasert. Their unconditional love, inspiration, and motivation have been with me throughout these many years. With all of these wonderful components from them, I was able to maintain a solid foundation for my personal and professional development that has helped me to achieve this goal with joy, enthusiasm and excitement.

TABLE OF CONTENTS

LIST OF TABLES

LIST OF FIGURES

Figure Page

LIST OF ABBREVIATIONS

BPS	Bureau of Policy and Strategy
BME	Bayesian Maximum Entropy
CAP	Criteria Air Pollutants
CI	Confidence Interval
CO	Carbon Monoxide
ICD-10	The International Codes for Diseases: the Tenth Revision
NAAQS	Thai National Ambient Air Quality Standard
NOx	Nitrous Oxide
NO_2	Nitrogen Dioxide
OR	Odds Ratio
PCD	Pollution Control Department
PDF	Probabilistic Density Function
PM_{10}	Particulate Matter with Aerodynamic diameter Equivalent to or Less Than 10 μm
STRF	Space/Time Random Field
SO_2	Sulfur Dioxide
TSP	Total Suspended Particles
US EPA	United States Environmental Protection Agency

I. INTRODUCTION

Significances of PM_{10} and cardiovascular and respiratory mortality

PM_{10} (an ambient particulate with aerodynamic size equivalent to or less than 10 μm) can penetrate into the thoracic part of the human airways. It is considered one of the Criteria Air Pollutants (CAP) by the US Environmental Protection Agency (EPA) since acute and chronic exposures to ambient PM_{10} can result in various respiratory and cardiovascular health problems as well as premature death. In Thailand, daily fluctuating concentration of PM_{10} has been monitored using nation-wide network of stations maintained by the Thai Pollution Control Department (PCD). The PCD has reported that among monitored air pollutants, PM_{10} concentrations have exceeded the Thai National Ambient Air Quality Standard (NAAQS) more frequently than other CAP.

The size of Thailand is comparable with that of France covering 200,009 square miles with a population of 63 million people residing in 925 districts, while capital, Bangkok city, has 6 million residents living in 50 districts. For the past three decades Thailand has had a notable growth of economic activities in different regions, but specifically in the Bangkok metropolitan area and in the central region of the country. There are about 3.5 million automobiles and 2.5 million motorcycles operating in Bangkok, and everyday more than 500 new cars are entering the roads of the country. The high number of vehicles relative to the small road system available in Bangkok city results in a heavily congested traffic with an

average traveling speed of 10 km per hour during the morning and evening rush hours. The rapid growth of the population and industrial activities as well as the ensuing heavy traffic congestion in the central region have resulted in polluted air and health problems. Major manmade PM_{10} emission sources in Thailand are construction, industrial and vehicular combustion, and biomass burning. Poor air quality due to suspended particulate matter in Bangkok and the Northern city has been associated with various health problems. Air quality management strategies and attempts to reduce PM_{10} levels to attain the NAQQS standard have continuously been implemented in Thailand for more than two decades. Improvements and investments in the expanding monitoring network are ongoing issues as PM_{10} - related health effects are serious. Accurately characterizing the spatiotemporal distribution of PM_{10} is an objective of several Thai governmental agencies dealing with the assessment of the population's exposure to ambient PM_{10} and the implementation of efficient PM_{10} abatement strategies.

An important component needed for any risk assessment analysis is the epidemiologic study of the strength of the association between an exposure and its health effect. Hence the epidemiological study of the association between short term exposure to PM_{10} and mortality in Thailand is critical in any effort to assess the health impact of PM_{10} in that country. Numerous studies conducted in the United States and western counties have confirmed the relationship between fluctuations of daily PM_{10} levels and cardiopulmonary mortality. The association between short-term exposure to PM_{10} and the excess risk of death from cardiovascular and respiratory causes has been previously detected among the population living in Bangkok. However epidemiologic results of the analysis of the association between PM_{10} and cardiopulmonary mortality obtained in Bangkok are of limited use for PM_{10} risk assessment in

other regions of Thailand where population, weather pattern, and PM_{10} constituents may be quite different than those of Bangkok. Obtaining regional estimates of the strength in the PM_{10}-cardiopulmonary mortality association could be useful to allocate resources for air pollution control and public health intervention between regions.

Research motivation

Due to the various health effects associated with PM_{10}, compliance to PM_{10} ambient air standards is vital to protect the Thai population and especially its sensitive groups, including asthmatic children, elderly, and patients with pre-existing cardiopulmonary conditions. In any PM_{10} exposure assessment research, a rigorous stochastic method should be utilized to model the spatiotemporal distribution of PM_{10} in order to determine the population exposure to this air pollutant at locations where direct PM_{10} measurements are not available. In addition, an accurate representation of the PM_{10} field across space and time is essential in air quality management to delineate non-attainment areas and to evaluate the adequacy of the existing monitoring network. Therefore, characterizing the space/time distribution of PM_{10} across Thailand is a critical responsibility of Thai authorities. Furthermore the accurate results of an exposure assessment analysis would also be useful in the epidemiologic investigation of the PM_{10}-mortality association.

In research of the investigation of PM_{10}-mortality association, the uncertainty in PM_{10} exposure assessment due to the high natural spatial and temporal variability of the PM_{10} field could considerably affect the estimated strength of PM_{10}-cardiopulmonary mortality association. In many previous epidemiological studies, PM_{10} exposure values at various receptor locations were assumed equivalent to the levels directly read at monitoring stations in

the proximity of the receptor or at those extending over hundreds of square miles. Therefore the errors introduced in the exposure measurements and in the interpolation were likely large. Instead, using exposure mapping methods that can account for the composite space/time variability of the PM_{10} field and the measurement uncertainty of monitoring data could substantially improve the analysis, and allow exploration of the PM_{10} association with mortality over a large geographical area exhibiting spatial gradients of exposure, i.e. it would provide a multi cities study design. Multi-city studies augment the power of the statistical analysis and reduce the likelihood of bias that might result from an analysis focused on a single city. Furthermore by focusing on specific regions of Thailand, the epidemiologic study can provide regional estimates of the association, which would be very useful to assess the excess cardiopulmonary mortality in different regions of Thailand, especially since emission sources and weather pattern are different from region to region.

In population mortality risk assessment research, the framework that assimilates all available knowledge and related uncertainties provides more meaningful and sound estimates, which are critical for use by public health research, policy, management and decision makers. A sound methodological and theoretical risk assessment framework used to evaluate population health impacts should account for various kinds of knowledge bases, such as the physical characteristics of the exposure field, any epidemiological information available, as well as the relevant demographic data, and should rigorously propagate uncertainty from all its main contributing sources (e.g. the uncertainty in exposure estimates, the uncertainty in exposure-health response curves, etc.).

To respond to the needs expressed in the motivation of this work, the powerful Bayesian Maximum Entropy (BME) exposure mapping method is used. BME as a central

component of the space/time PM_{10} estimation framework can account for a wide variety of knowledge bases, including knowledge about the composite space/time variability of PM_{10} and about the measurement error and other uncertainties associated with the monitoring data. As a result, the BME method provides accurate spatiotemporal exposure maps of PM_{10}, which can be used to improve previous research investigating the short-term effect of PM_{10} on cardiovascular and respiratory mortality. The epidemiology component of this work was conducting using a case-crossover design to analyze the PM_{10}-mortality in different regions of Thailand. The case-crossover design is suited to the study of a transient effect of an intermittent exposure on the subsequent risk of an acute-onset health effect thought to occur shortly after exposure. The results of the exposure mapping analysis and of the epidemiological study of the estimates of the strength of the associations between PM_{10} and cardiopulmonary mortality in different regions of Thailand are then used in a risk assessment framework to obtain estimates of the excess mortality caused by PM_{10} across Thailand. The risk assessment analysis is done using the holistochastic human exposure framework presented in previous works, and extended here to provide the lower and upper bounds of the confidence interval for the excess mortality caused by PM_{10} across Thailand.

Statement of study objectives

The primary goal of this study is the analysis of the spatiotemporal distribution of PM_{10} and its health effect on cardiopulmonary mortality using the BME space/time mapping framework. This goal is achieved in three parts, which are the space/time exposure mapping of PM_{10}, the investigation of the PM_{10} – cardiopulmonary mortality association, and the risk assessment

analysis of the of excess cardiopulmonary mortality caused by PM_{10} across Thailand. Each of these 3 parts of the work will lead to an analysis, as follow:

Analysis 1 To characterize the space/time distribution of PM_{10} across Thailand between 1998 and 2003 by constructing BME spatiotemporal maps of PM_{10} daily mean and daily maximum;

To identify non-attainment areas by constructing BME maps identifying areas not attaining the NAAQS; and

To optimize the adequacy of the current PM_{10} monitoring network by indicating target areas for additional monitors on the basis of maps of the BME estimation error and population density.

Analysis 2 To use of BME estimates of daily PM_{10} concentrations to obtain a BME assessment of the short term exposure to PM_{10} for each death reported between 1998 and 2003; and

To use of a case-crossover study design with conditional logistic regression to obtain regional estimates of the strength of the association between short term PM_{10} exposure and cardiovascular as well as respiratory mortality in the five regions of Thailand, as well as pooled estimates of the strength of the association for the whole country.

Analysis 3 To use the BME mapping method and the holistochastic human modeling exposure framework to assess the cardiovascular and respiratory mortality excess risk resulting from the increase in daily PM_{10} above background throughout 2004.

II. MANUSCRIPT 1: MODELING THE SPACE/TIME DISTRIBUTION OF PARTICULATE MATTER IN THAILAND AND OPTIMIZING ITS MONITORING NETWORK

Abstract

The space/time distribution of PM_{10} in Thailand is modeled using the Bayesian maximum entropy (BME) method of modern Geostatistics. Three kinds of BME spatiotemporal maps over Thailand are sought on the most polluted day for each year of a six year period from 1998 to 2003. These three maps are (1) the map of the BME estimate of daily PM_{10}, (2) the map of the associated BME prediction error; and (3) the BME non-attainment map showing areas where the BME estimate does not attain a 68% probability of meeting the ambient standard for PM_{10}. These detailed space/time PM_{10} maps provide invaluable information for decision-makers in air quality management. Knowing accurately the spatiotemporal distribution of PM_{10} is necessary to develop and evaluate strategies used to abate PM_{10} levels. The space/time BME estimate of PM_{10} on the worst day of the year offers a general picture as to where daily PM_{10} levels are not in compliance with the air quality standard. Delineating these areas leads to the BME non-attainment maps, which are useful in identifying unhealthy zones where sensitive population such as asthmatic children, seniors, or those with cardiopulmonary disease should be advised to avoid outdoor activities. The results of the space/time BME analysis of PM_{10} are further extended to assess whether the current monitoring network is adequate. The current distribution of monitoring stations can be evaluated by combining the available demographic information with the BME estimation

error maps. Administrative districts with large population size and high BME normalized estimation error are suggested as the target for adding new monitoring stations.

Introduction

Air quality monitoring results over Thailand during the 1990s indicated that total suspended particles (TSP), PM_{10} (an ambient particulate with aerodynamic size equivalent to or less than 10 μm) and CO were continuously violating the Thai National Ambient Air Quality Standard (NAAQS) and that NOx and hydrocarbons (HC) were reported at increasing levels (*1*). Ozone, a more recent Criteria Air Pollutants (CAP) that results from the chemistry of NOx and HC under sunlight conditions, has begun exceeding the standard at some monitoring stations (*2*). Among the CAP monitored in Thailand, PM_{10} has been reported to exceed the ambient standard most frequently (*2, 3*). Based on results of ambient air monitoring at street curbsides stations, and according to apportionment studies of emission sources, vehicular exhausts are the most important source of PM_{10} exposure for Bangkok residents (*1, 4*). This conclusion agrees with that of Jinsart *et al.* (2002) who found that the PM_{10} correlation was very high with NO_2 but low with SO_2; a finding inferring that automobile emissions are the main PM_{10} source (*5*). PM_{10} accounts for up to 60% of TSP (by weight) in Bangkok and its vicinity. More than 80% of contributing TSP sources (61,000 tons/year) are motor vehicles and re-entrained road dust (*1, 4*). Two-stroke engine motorcycles and aging diesel buses and trucks are the largest contributors to TSP (*1, 4*). Other sources of TSP include industrial boilers, power plants, and construction. However contributions from other common sources such as household burning and cooking, crematorium, and garbage and agricultural waste burning in open space have not been estimated. Emissions from these sources have been contributing PM_{10} in rural areas (*3*).

Improvement and investment in an expanded monitoring network are ongoing issues as PM_{10} - related health effects are enduring (*4, 6-9*). Characterizing the distribution of PM_{10}

across space and time is a critical component of the mission of several Thai government agencies, including the PCD and the Bangkok Metropolitan Administration. These agencies have been monitoring over years the fluctuating trends of PM_{10}. The informative maps of PM_{10} spatiotemporal distribution will help those agencies in developing and improving their PM_{10} abatement strategies especially in non-attainment areas, and evaluate limitations in the current monitoring network.

In Thailand, PM_{10} is known to exceed the ambient standard more frequently than other co-pollutants. Therefore, the extent to which daily PM_{10} concentrations exceed the NAAQS (120 $\mu g/m^3$) across Thailand remains in question. As a result of this study, we consider two research questions related to this issue that are 1) what is the spatiotemporal distribution of PM_{10} across Thailand?, and how do the corresponding non-attainment areas evolve over time; and 2) how can we improve the current monitoring network using the estimation error maps resulting from the BME analysis? Thus we set the following objectives: 1) to characterize the space/time distribution of PM_{10} across Thailand by constructing BME spatiotemporal maps of PM_{10} daily mean and daily maximum; 2) to identify non-attainment areas by constructing BME maps identifying areas not attaining the NAAQS; and 3) to optimize the adequacy of the current PM_{10} monitoring network by indicating target areas for additional monitors on the basis of maps of the BME estimation error and population information.

Methods

BME mapping and non-attainment area delineation

The powerful BME method of modern Geostatistics has been extensively used in the mapping analysis of environmental contaminants in the ground water, surface water, and ambient air (*10-15*). In these studies, the Space/Time Random Field (S/TRF) $Z(\boldsymbol{p})$ is used to represent the uncertainties and natural variability associated with a contaminant Z at space/time point $\boldsymbol{p}=(\boldsymbol{s}, t)$, where $\boldsymbol{s}$ is the geographical coordinate, and t is time. The BME space/time mapping analysis provides a rigorous mathematical framework to process the physical knowledge base K available for PM_{10} in Thailand. This physical knowledge base K is divided in the general knowledge G characterizing global characteristics of the PM_{10} S/TRF, such as its mean trend describing consistent pattern in space and time and its covariance describing the autocorrelation in space and time, and the site specific knowledge base S consisting of the hard and soft data derived from measurements at specific monitoring stations (for example, probabilistic soft data given by $P[\boldsymbol{x}_{\text{soft}}<\boldsymbol{\chi}_{\text{soft}}]=F_S(\boldsymbol{\chi}_{\text{soft}})$. The integration and processing of the physical knowledge base $K = G \cup S$ leads to the posterior BME probabilistic density function (PDF) $f_K(\chi_k)$ providing a full stochastic description of PM_{10} at any estimation point $\boldsymbol{p}_k$ of interest. The BME posterior PDF $f_K(\chi_k)$ can be expressed as (*16, 17*)

$$f_K(\chi_k) = A^{-1} \int d\boldsymbol{\chi}_{\text{soft}} f_S(\boldsymbol{\chi}_{\text{soft}}) f_G(\boldsymbol{\chi}_{\text{hard}}, \boldsymbol{\chi}_{\text{soft}}, \chi_k), \qquad (1)$$

where $\boldsymbol{\chi}_{\text{hard}}$, $\boldsymbol{\chi}_{\text{soft}}$, χ_k represent the S/TRF for PM_{10} at the hard, soft and estimation points, respectively, $f_S(\boldsymbol{\chi}_{\text{soft}})$ is a the so-called soft PDF defined as $f_S(\boldsymbol{\chi}_{\text{soft}})= \partial F_S(\boldsymbol{\chi}_{\text{soft}})/ \partial \boldsymbol{\chi}_{\text{soft}}$ characterizing the data uncertainty at the soft data points, $f_G(.)$ is the general knowledge PDF obtained at the structural stage of the BME analysis, and A=

$\int d\chi_k \int d\boldsymbol{\chi}_{soft} f_S(\boldsymbol{\chi}_{soft}) f_G(\boldsymbol{\chi}_{hard}, \boldsymbol{\chi}_{soft}, \chi_k)$ is a normalization constant. From the posterior PDF $f\kappa(\chi_k)$ we obtain several estimators of PM_{10} at the estimation point $\boldsymbol{p_k}$. A common estimator used in environmental mapping analysis is the BME mean estimator, $\hat{\chi}_{k,mean}$, defined as the expected value of the BME posterior PDF given by the equation

$$\hat{\chi}_{k,mean} = \int_{-\infty}^{\infty} d\chi_k \; \chi_k f\kappa(\chi_k) \tag{2}$$

The variance of the BME posterior PDF provides a useful assessment of the estimation accuracy associated with the BME mean estimator. This BME posterior variance is denoted as $\sigma^2_{k|\kappa}$ and is given by the following equation.

$$\sigma^2_{k|\kappa} = \int_{-\infty}^{\infty} d\chi_k \; (\chi_k - \hat{\chi}_{k,mean})^2 f\kappa(\chi_k) \tag{3}$$

The BME mean estimates of PM_{10} obtained at the mapping nodes of a regular grid covering Thailand are used to construct BME maps showing the spatial distribution of PM_{10}. Then we obtain non-attainment areas by delineating regions where the BME mean estimates of the daily PM_{10} concentration are greater than the standard. Due to randomness and natural variability of the PM_{10} field, these delineated geographical regions correspond to areas where the probability of a violation of the standard is greater than 68%. These areas are typically referred to as being likely in non-attainment, which is useful both for regulatory purposes as well as for designing efficient strategies for pollution abatement.

Targeting districts where to add new monitoring stations

The BME estimation error variance calculated at the nodes of a regular grid covering Thailand provides a spatial description of the mapping accuracy of PM_{10}. By normalizing this BME estimation error variance with the prior error variance that does not account for site-specific data, we obtain a BME normalized estimation error variance that equals to a fraction of one and can be used to compare mapping accuracy across space (*10*). The BME normalized estimation error variance is small where monitoring stations are clustered and provide good quality monitoring data, while it is high where stations are sparsely located or where measurement errors are high. This BME normalized uncertainty spatial map is helpful to assess the adequacy of the existing network of monitoring stations. It can be used to locate new monitoring station where the normalized uncertainty is high, especially for areas with high population density. For illustration purposes, consider the map of Figure 2.1a showing the 1999 population density in the 925 districts of Thailand. This map shows that the central and northeastern parts of the country are the most crowded regions of Thailand. From a public health perspective, these regions of the country should be considered first when selecting sites for new monitoring stations within areas of high normalized mapping uncertainty. The population density in Thailand is highest in Bangkok, where approximately 6 million people live in 610 $mile^2$. In other words, about 10% of country population is living in Bangkok city which size is only 0.3% of Thailand. As almost half of monitoring sites are located in Bangkok city and its proximity, PM_{10} concentration in Bangkok is well monitored with a data quality that is likely to be good and thus the BME normalized estimation error variance is expected to be low relative to that of other parts of the country. However using an aerial unit of study that is too small can lead to very high population densities is some parts

of Bangkok, which would be problematic since they would outweigh the information about the normalized mapping variance, and target areas for new monitoring simply based on the population density. As an alternative, we propose to calculate the BME mean estimate of PM_{10} and obtain the associated normalized estimation variance only at the centroid of each administrative district. As a result the estimation points $\boldsymbol{p}_k$ are now restricted to the district centroids as depicted in Figure 2.1b. Let $V(\boldsymbol{p}_k)$ be the normalized uncertainty level at district centroid $\boldsymbol{p}_k$ (i.e. the ratio of the BME posterior variance over the prior variance not accounting for site specific data near $\boldsymbol{p}_k$), and $P(\boldsymbol{p}_k)$ be the population size for the district with centroid specified by $\boldsymbol{p}_k$. A proposed indicator for assessing the need to install a new monitoring site at some space/time district location $\boldsymbol{p}_k$ is the population prediction error $I(\boldsymbol{p}_k)$ defined as

$$I(\mathbf{p}_k) = V(\mathbf{p}_k)P(\mathbf{p}_k) \qquad (4)$$

This equation is used to locate and install new monitoring sites based on identifying locations with large $I(\boldsymbol{p}_k)$ value. The magnitude of $I(\boldsymbol{p}_k)$ depends on the density of the monitoring network at a given geographical location, the frequency and data quality collected during the time period of interest, and the number of the population affected by the mapping uncertainty. When monitoring stations are added, removed, or relocated, the population prediction error indicators change accordingly. The Thai monitoring network has continually been expanded across Thailand by adding new monitoring stations, and efforts are undergoing to continue expanding and improving the monitoring network in future years. Investigating the value of $I(\boldsymbol{p}_k)$ defined in Eq. (4) on the worst PM_{10} day during the 1998-

2003 time period will provide a sound methodological approach to assess the appropriateness of the monitoring station network. $I(\boldsymbol{p}_k)$ can be used to optimize the network in future years by suggesting changes in the current network, or by indicating optimal geographical locations, sampling frequency, and desirable data quality for new monitoring stations.

Results

The Thailand PM_{10} data set and its exploratory analysis

A comprehensive monitoring dataset of hourly PM_{10} concentration measurements was obtained directly from the Air Quality and Noise Management Bureau, Thai PCD for the time period of January 1, 1998 to June 1, 2004. The PM_{10} measurements were collected using a monitoring network maintained by the PCD that comprises 51 monitoring stations located on road curbsides and residential areas. The hourly PM_{10} measurements were obtained using the Beta gage attenuation method, which has an 8% relative error and a detection limit of 2 $\mu g/m^3$. The original data set of hourly measurements was aggregated to obtain the daily average and daily maximum of PM_{10} for each available monitoring station and for each day of the January 1998- June 2004 time period. This aggregation procedure reduced the number of monitoring time events from 56,242 hours to 2,344 days. Measurements recorded to be below the detection limit of 2 $\mu g/m^3$ were treated as soft data of interval type, i.e. it was assumed for these measurements that the uncertainty associated with the true PM_{10} concentration was described by a PDF corresponding to a uniform distribution between 0 and 2 $\mu g/m^3$. High outliers above the 99 percentile value (441 $\mu g/m^3$) were treated as uncertain and described using a Gaussian PDF with a standard deviation equivalent to the sampling

method accuracy or a standard deviation large enough to cover the 99 percentile value, whichever was larger. The remainder of the data were treated as hard data, i.e. they were considered to be sufficiently accurate so that their measurement errors could be neglected compared to those below the detection limit or high outliers. When PM_{10} hard and soft data were used in previous BME studies, the BME method was found to be more accurate than the regression-based methods of classical Geostatistics that do not account for the uncertainty of soft data or the composite space/time variability (*14*).

Exploratory analysis indicated a high spatial and temporal variability in the PM_{10} field, as can be seen in the PM_{10} monitoring data shown on the maps and time series of Figure 2.2. Higher PM_{10} levels were observed in early mornings possibly due to more stable atmospheric conditions (Figure 2.2a). The morning atmosphere is more stable due to low temperature and less traffic which allows particles to settle down near the ground surface were they are collected by the measuring devices. We also note that PM_{10} levels vary considerably across the country. High values are found in the central areas while low values are observed in the south of Thailand. A seasonal effect can be seen in northern Thailand (Figure 2.2b) where temperatures are low in January and February. During these cold months, PM_{10} levels are found to be at elevated levels. These high PM_{10} levels could be due to two major causes. First, the atmosphere is more stable during the cold months, resulting in less horizontal and vertical mixing, which leads to a rise in the accumulated PM_{10}. Second, agricultural burning to prepare farm lands for the incoming planting season and forest fire are likely to happen during the cold season (*9*) preceding the warmer months. In addition some areas in the northern region of Thailand are surrounded by mountains, which provide a geography prone to the trapping and accumulation of air pollutants, thereby accentuating any

underlying seasonal effect. On the other hand stations located in the south do not exhibit the strong seasonal effect seen in the north (Figure 2.2b). Indeed the daily average temperature in this area is considerably more steady and higher with temperature greater than 30 °C recorded year-round. The PM_{10} concentration in the South is found to be low compared to other areas in the central or northern parts of Thailand. The south is surrounded with ocean and is under the influence of a strong ocean wind and heavy rain, which probably leads to a significant removal rate of PM_{10}. However the long-term temporal trend of PM_{10} in the South shows increasing levels since January 2002.

Space/time variability of PM_{10} field

The two data sets of PM_{10} daily average and daily maximum concentrations, represented by the S/TRF $Z(\mathbf{p})$, were log-transformed into $Y(\mathbf{p})=log(Z(\mathbf{p}))$, and then were further decomposed into a mean trend $m_Y(\mathbf{p})$ and a residual field $X(\mathbf{p})$, such that $Y(\mathbf{p}) = m_Y(\mathbf{p})+X(\mathbf{p})$. Results from some of the steps of this procedure are illustrated in Figure 2.3. The mean trend model $m_Y(\mathbf{p})$ was selected such the resulting mean trend removed log-transformed field $X(\mathbf{p})$ was homogenous over space and stationary over time, i.e. with a constant space/time mean (Figure 2.3c). Since the mean trend model is a deterministic function, the residual field $X(\mathbf{p})= Y(\mathbf{p})-m_Y(\mathbf{p})$ is a S/TRF with the same space/time variability and uncertainty as that associated with log-PM_{10} levels. The experimental covariance of $X(\mathbf{p})$ is computed for different classes of spatial and temporal lags using *BMElib* (*18*). Figure 2.4 shows the plot the experimental covariance obtained from the *X*-data. The top subplot shows the covariance as a function of spatial lag, while the bottom subplot shows the covariance as a function of temporal lag. Both subplots show an exponential behavior at the origin, meaning that the covariance for

log-PM_{10} decreases exponentially with spatial lag and temporal lag. Consequently the theoretical covariance model selected to fit these experimental covariance values is a nested model comprising four space/time separable exponential functions, as expressed mathematically by

$$c_X(r,\tau) = \mathrm{var}_X \left[\begin{array}{l} c_{01r}c_{01t}\ \exp(-\frac{3r}{a_{r1}})\exp(-\frac{3\tau}{a_{t1}}) + c_{02r}c_{02t}\ \exp(-\frac{3r}{a_{r2}})\exp(-\frac{3\tau}{a_{t2}}) \\ + c_{01r}c_{02t}\ \exp(-\frac{3r}{a_{r1}})\exp(-\frac{3\tau}{a_{t2}}) + c_{02r}c_{01t}\ \exp(-\frac{3r}{a_{r2}})\exp(-\frac{3\tau}{a_{t1}}) \end{array} \right] \quad (5)$$

The parameters of Eq. (5) are listed in Table 2.1 for both the daily mean as well as the daily maximum PM_{10} concentrations. As can be seen from this Table, the parameters are similar for the daily mean and daily maximum, emphasizing the physical connection between these two variables.

Most of the space/time variability of log-PM10 is explained by the first and the third components of theoretical covariance model of Eq. (5). As can be seen in Table 2.1, the first structure of the model indicates that about 47% of the variability in log-PM_{10} occurs over short distances (i.e. at a spatial range a_{r1} of 0.045 degree =5 Km) and over short time scale (i.e. at a temporal range a_{t1} of 4 to 6 days). We hypothesize that this variability at short spatial and temporal scales are due to local point sources similar to stack emissions of industrial emissions or crematorium burners lasting about 6 days before the atmosphere is cleaned by intermittent rain. The mortality rate in Thailand is about 1,000 deaths a day and most of these people are cremated at crematorium temples located in highly-populated areas. Thus crematorium sources are considered one of significant combustion sources in Thailand.

The third model structure explains about 43% of the variability of log-PM_{10} with again a short spatial range a_{r3} of about 5 Km, but a much longer temporal range a_{t3} of 180-210 days (about half year). Such variability can be explained by the combination of local point source emissions that contributes PM_{10} accumulation over whole dry seasons of 6-7 months and then being washed during the southwest monsoon lasting about 6 months. In the second model structure (5% of the variability) with long temporal range in large area, we describe this variability as related to natural windblown dust in large areas, for example in northeast area during the dry season. For the fourth structure in the covariance model contributing about 5% of variability, we hypothesize that this variability is due to re-suspended dust and traffic emission over large geographic areas with intermittent downpours cleaning the air. This type of the sophisticated space/time covariance model of 4 exponential components has never been investigated before in other PM_{10} data sets analyzed in earlier BME studies. The model helps us comprehend the new variation patterns described by the first and the third model structures, i.e. short in a_r - a_t and long in a_r - a_t.

BME estimation results

The knowledge of hard and soft data as well as the mean and covariance model of each data set were processed using the *BMElib* implementation of the BME method to produce the posterior PDF of the residual field $X(\boldsymbol{p})$ at mapping points $\boldsymbol{p_k}$ of interest. To characterize the BME mean and associated BME error variance of $Z(\boldsymbol{p})$, the BME posterior PDF of $X(\boldsymbol{p})$ is transformed back to that of $Z(\boldsymbol{p})$. Estimation was performed in two fashions, which were an estimation across the country on the most polluted day for each year of the 1998-2003 period, and an estimation across time at selected monitoring sites. In each case the analysis is

considered to be a space/time estimation because the hard and soft data used in the estimation are selected in a space/time neighborhood of the estimation point.

Figure 2.5 shows the temporal profiles of the BME mean estimates of the PM_{10} daily average and the PM_{10} daily maximum obtained at selected monitoring sites. The upper and lower bounds of the 68% confidence interval are shown in dotted lines, as well as the hard data depicted with circles. Stations 102 and 127 were selected because they are representative of stations having soft data and missing measurements. The shape of the upper and lower bounds of the 68% confidence interval are in good physical agreement with the fact that mapping uncertainty is zero at hard data points, and gradually increases in the time period between hard data measurements. The effect on the BME estimate profile of replacing hard data with soft data can be seen in Figure 2.5a and 5b where the BME estimate lines are different around day 1275. The same comparison is made between Figures 2.5c and 2.5d.

Using data collected on January 31st, 1998 as well as during the preceding days and following days, we calculated using *BMElib* the BME mean estimates for PM_{10} daily average and corresponding BME estimation variance across Thailand on January 31st, 1998. Figure 2.6a shows maps displaying the result of the analysis using either only hard data, or using both hard and soft data. The day of January 31st, 1998 was chosen because it experienced the highest PM_{10} daily average during the January 1998- June 2004 time period. Substantial spatial variability in BME estimates can be seen in both Figure 2.6a and 2.6b. Regardless of the type of analysis, the BME estimated values of daily average were clearly found to exceed 100 $\mu g/m^3$ in central Thailand, while the Thailand standard for the 24-hour average PM_{10} is 120 $\mu g/m^3$. In other word, it is likely that the population living in this area is exposed to high PM_{10} levels. In fact, BME estimation indicates that at a single mapping grid point the

estimated PM_{10} daily average is found to be as high as 293 $\mu g/m^3$. The estimated PM_{10} values were lower toward the north and the north east of the country where the population density is lower than in central Thailand. The estimated PM_{10} levels were lowest toward the south where the country is surrounded by the ocean. The associated normalized error variance is low at the data points and increases away from data points as can be seen in Figures 2.6a and 2.6b. In addition, larger polluted areas as well as higher BME estimates are observed when using both hard and soft data.

The BME mean estimates were calculated using both hard and soft data on the most polluted day in each year during 1998-2003. BME spatial maps were constructed to observe the temporal variation between these BME estimation maps. The most polluted day in each year is defined as the day having the highest spatially averaged value of PM_{10} daily average (see Figure 2.3b). The six BME spatial maps of PM_{10} daily average and PM_{10} daily maximum for 1998-2003 are depicted in Figure 2.7 and 2.8, respectively. As discussed earlier, the 1998 map in Figure 2.7a is the worst day of the 6 year period, while by contrast Figure 2.7d shows that the most polluted day in 2001 had much reduced PM_{10} levels. However as seen in the in the last map (Figure 2.7f), the most polluted day in 2003 increased over the levels seen in 2001. In the Bangkok area of central Thailand, the worst annual day is seen to have reducing PM_{10} levels from 1998 to 2001, resulting in a polluted area of diminishing size over these four years. However the polluted area seems to increase again for the last two years (2002 and 2003). There is some evidence of reducing PM_{10} daily average over six years period in the north regions where forest fires, traffic combustion, and agricultural open burning are important sources of PM_{10}. However, as a whole, the country is

experiencing an increase in the worst annual PM_{10} daily average for the 2001-2003 time period.

The daily maximum PM_{10} estimated on the worst day of each of the 1998-2003 time period are shown in Figure 2.8. These maps show a smoother spatial distribution than that seen in the daily average maps of Figure 2.7. In Figure 2.8, we can see higher daily maximum levels in the country main land (especially in the central region due to highly populated area and congested traffic), and lower daily maximum values in the south of the country due to ocean wind. Although the daily maximum hourly PM_{10} measurement is not yet regulated by the NAAQS, we observe that many spatial locations in the maps of Figure 2.8 are likely to experience hourly PM_{10} levels higher than 250 $\mu g/m^3$.

The BME posterior PDF is used to delineate non attainment areas that have a probability of PM_{10} being smaller than the standard (i.e. the probability of attaining the standard) is less than 0.68 (i.e. is not acceptable within a confidence level of 68%). Figures 2.9a-2.9f depict the areas that did not attain the NAAQS standard for daily PM_{10} within a confidence level of 68% on the worst day of each year (i.e. areas where the probability that PM_{10} daily average <120 $\mu g/m^3$ does not reach 68%). These figures show that the non attainment areas in the central region have continuously shrunk from 1998 to 2001 and then have increased for 2002-2003. The north shows much smaller size of the non-attainment areas than those in the central region. In addition, the north is free of non-attainment area for the last two years. Most areas in the south and northeast are attaining the NAAQS standard well with the confidence level of 68%.

Table 2.2 summarizes results obtained by utilizing Eq. (4), the calculated population error prediction indicator *I*, shown in the 5th column of this table. It is based on the linearly

interpolated population sizes for each district, and the BME normalized error variance estimated at district centroids on the worst day of 1998-2003. This permits the consideration at a scenario corresponding to an extremely polluted day. The calculated population error prediction indicator *I* identifies the districts with high BME normalized estimation error variance and high district population, which can be used to prioritize districts that should be targeted as sites for installing a new monitoring station. Figure 2.10 shows the locations of 5 districts suggested as target sites for new monitoring stations. Among these 5 districts, although district 51 located near Bangkok city ranks as the top priority, the northeast area seems to be the area where the need for new monitors is more pronounced. The indicator *I* should be recalculated when there is a modification in the monitoring network or as population size change due to rapid growth or to population migration from rural to urban areas.

Discussion

It is interesting to note that our findings about the space/time variability of PM_{10} across Thailand indicate that its spatiotemporal distribution is more distinct than that observed in the United States. As described by the coefficients of the space/time covariance model, about 47% of the variability occurs over small distances and short times, and 5% of the variability occurs over very large geographical areas and last for long time periods. This combination of spatial and temporal scales have not been reported in similar spatiotemporal BME mapping analysis of PM_{10} over other regions of the world, particularly in North Carolina and California (*14, 19*). These distinct combinations of the spatial and temporal scales of

variability of the PM_{10} field are due to characteristics of the topography, emission sources, and weather patterns that are specific to Thailand. For example it is hypothesized that the combination of natural emission sources acting over large geographic areas, such as re-suspended dust in the north east arid region, the sea spray in the southern region, and the biomass burning in large open spaces of the northern region, combine in a unique fashion with manmade point sources such industry emission stacks to create a spatial pattern of variability that is unique to Thailand. Similarly, it is hypothesized that these spatial patterns of variability interact with climatic weather patterns that are acting over large geographical areas and have intermittent events, such as the daily cycles of heavy downpours during the monsoon season, as well as almost dramatic seasonal events, such the change from very arid seasons to monsoon conditions. The combination of these factors makes the space/time variability the PM_{10} over Thailand unique.

BME framework rigorously characterizes the space/time distribution of PM_{10} across Thailand and provides informative BME space/time maps. These maps show that PM_{10} exhibits a considerable spatial and temporal variability. The most polluted days were found to be in December, January, and February. During these winter months, wind speed is usually low and the atmospheric mixing height is short (*20*). Such stable atmosphere and low mixing volume condition increase the chance for the accumulation of PM_{10}. Studies related to particulate matter in Thailand reported that PM_{10} levels were high in winters and low in summers (*9, 21*). The high PM_{10} value observed in the central area of the country are associated with the contribution of re-suspended road dust, industrial combustion, and heavily congested traffic, while the PM_{10} levels in the north region are related to biomass burning, vehicular emission, and forest fires (*1, 3, 9, 22-24*). The northeast area possibly

experiences more coarse particles than fine particles such as windblown dust or soil dust due to the long arid season. The southern area is relatively clean with comparatively lower PM_{10} levels because of the effect of the strong ocean winds, the northeast and southwest monsoon, and the high temperature prevalent year-round in this area that could cause the atmosphere to be dynamically unstable (*25*).

The estimation results obtained by analyzing only hard data and by analyzing both hard and soft data are not significantly different in this study. This is usually the case when most of data analyzed are hard data. Less than 4% of whole PM_{10} measured values showed high uncertainty due to measurement errors and were transformed to soft data in this study. The size of the non-attainment areas are diminishing over first 4 years and expanding in the last two years. This finding is consistent with the fossil fuel consumption and economic growth rate experienced by Thailand over the 1998-2003 time period. Therefore it confirms that the transportation and industry in the central region are important emission sources. On the other hand, the north region does not show any non-attainment area for the last two years, indicating that its main emission sources are not similar to those of the central region.

By way of summary, this work demonstrates the usefulness of the spatiotemporal BME approach to delineate non-attainment areas, which can be used by policy and decision makers. By taking into account the space/time variability of PM_{10} and the uncertainty in available measurements, the BME analysis provides accurate estimations of PM_{10} at any unsampled space/time locations. The BME posterior variance normalized by the prior variance is helpful in locating priority sites where new monitoring stations should be located in order to improve the current monitoring network. The maps of Figures 2.7-2.9 are based on an analysis using hard and soft data and account for the composite space/time variability

of PM_{10}. These maps demonstrate the feasibility and usefulness of the implementation of BME exposure mapping framework to analyze the spatiotemporal distribution of PM_{10} across Thailand. They illustrate how BME maps can provide invaluable information for health risk assessment, which will be considered in more details in the following Chapters.

Reference:

1. Thai Pollution Control Department. Thailand State of Environment: The Decade of 1990s (Thai version). Bangkok, Thailand: Ministry of Natural Resources and Environment, 2000.

2. Thai Pollution Control Department. State of Thailand's Pollution in Year 2002 (Thai version). Bangkok, Thailand: Ministry of Natural Resources and Environment, 2003.

3. Thai Pollution Control Department. State of Thailand's Pollution in Year 2003 (Thai version). Bangkok, Thailand: Ministry of Natural Resources and Environment, 2004.

4. Radian International LLC. PM abatement strategy for the Bangkok metropolitan area: final report. Austin, TX, 1998, 1998.

5. Jinsart W, Tamura K, Loetkamonwit S, Thepanondh S, Karita K, Yano E. Roadside particulate air pollution in Bangkok. J Air Waste Manag Assoc 52:1102-10(2002).

6. Ruchirawat M, Mahidol C, Tangjarukij C, Pui-ock S, Jensen O, Kampeerawipakorn O, Tuntaviroon J, Aramphongphan A, Autrup H. Exposure to genotoxins present in ambient air in Bangkok, Thailand -- particle associated polycyclic aromatic hydrocarbons and biomarkers. The Science of The Total Environment 287:121-132(2002).

7. Vajanapoom N, Shy CM, Neas LM, Loomis D. Associations of particulate matter and daily mortality in Bangkok, Thailand. Southeast Asian J Trop Med Public Health 33:389-99(2002).

8. Vichit-Vadakan N, Ostro BD, Chestnut LG, Mills DM, Aekplakorn W, Wangwongwatana S, Panich N. Air pollution and respiratory symptoms: results from three panel studies in Bangkok, Thailand. Environ Health Perspect 109 Suppl 3:381-7(2001).

9. Vinitketkumnuen U, Kalayanamitra K, Chewonarin T, Kamens R. Particulate matter, PM 10 & PM 2.5 levels, and airborne mutagenicity in Chiang Mai, Thailand. Mutation Research/Genetic Toxicology and Environmental Mutagenesis 519:121-131(2002).

10. Serre ML, Christakos G, Lee S-J. Soft Data Space/Time Mapping of Coarse Particulate Matter Annual Arithmetic Average over the U.S. In: geoENV IV 2004.

11. Serre ML, Carter G, Money E. Geostatistical space/time estimation of water quality along the Raritan river basin in New Jersey. In: Computational Methods in Water Resources 2004 International Conference 2004;1839-1852.

12. Christakos G, Kolovos A. A study of the spatiotemporal health impacts of ozone exposure. J Expo Anal Environ Epidemiol 9:322-35(1999).

13. Christakos G, Vyas VM. A composite space/time approach to studying ozone distribution over Eastern United States. Atmospheric Environment 32:2845-2857(1998).

14. Christakos G, Serre ML. BME analysis of spatiotemporal particulate matter distributions in North Carolina. Atmospheric Environment 34:3393-3406(2000).

15. Vyas VM, Christakos G. Spatiotemporal analysis and mapping of sulfate deposition data over Eastern U.S.A. Atmospheric Environment 31:3623-3633(1997).

16. Christakos G. Field Models in Earth Sciences. San Diego, CA:Academic Press, 1992.

17. Christakos G. Modern Spatiotemporal Geostatistics. New York, NY:Oxford University Press, 2000.

18. Christakos G, Bogaert P, Serre ML. Temporal GIS. New York, NY:Springer-Verlag, 2002.

19. Christakos G, Serre ML, Kovitz J. BME representation of particulate matter distributions in the state of California on the basis of uncertain measurements. Jour. of Geophysical Research 106:9717-9731(2001).

20. Khedari J, Sangprajak A, Hirunlabh J. Thailand climatic zones. Renewable Energy 25:267-280(2002).

21. Panther BC, Hooper MA, Tapper NJ. A comparison of air particulate matter and associated polycyclic aromatic hydrocarbons in some tropical and temperate urban environments*1. Atmospheric Environment 33:4087-4099(1999).

22. Chetwittayachan T, Shimazaki D, Yamamoto K. A comparison of temporal variation of particle-bound polycyclic aromatic hydrocarbons (pPAHs) concentration in different urban environments: Tokyo, Japan, and Bangkok, Thailand. Atmospheric Environment 36:2027-2037(2002).

23. Kim Oanh NT, Baetz Reutergardh L, Dung NT, Yu M-H, Yao W-X, Co HX. Polycyclic aromatic hydrocarbons in the airborne particulate matter at a location 40 km north of Bangkok, Thailand. Atmospheric Environment 34:4557-4563(2000).

24. Leong ST, Muttamara S, Laortanakul P. Influence of benzene emission from motorcycle on Bangkok air quality. Atmospheric Environment 36:651-661(2002).

25. Janjai S, Kumharn W, Laksanaboonsong J. Determination of Angstrom's turbidity coefficient over Thailand. Renewable Energy 28:1685-1700(2003).

Table 2.1 Covariance model coefficients, explaining the space/time variability of PM_{10} across Thailand from January 1998 to June 2004

Coefficients	Daily average	Daily maximum
Variance $(\mu g/m^3)^2$	0.628	0.782
C_{01r}	0.9	0.93
C_{02r}	0.1	0.07
C_{01t}	0.52	0.51
C_{02t}	0.48	0.49
a_{r1} (deg.)	0.045	0.045
a_{r2} (deg.)	2.5	1.4
a_{t1} (days)	6	4
a_{t2} (days)	210	180

Table 2.2 Districts prioritized to be the site of a new monitoring station

Districts	Region	Pop size *P*	BME normalized variance *V*	Station Indicator *I*	Priority
51	Bangkok vicinity	308346	0.9870	304338	1
198	North east	246200	0.9892	243541	2
380	North east	229892	0.9475	217823	5
355	North east	223706	0.9904	221558	3
93	Central	222419	0.9860	219305	4

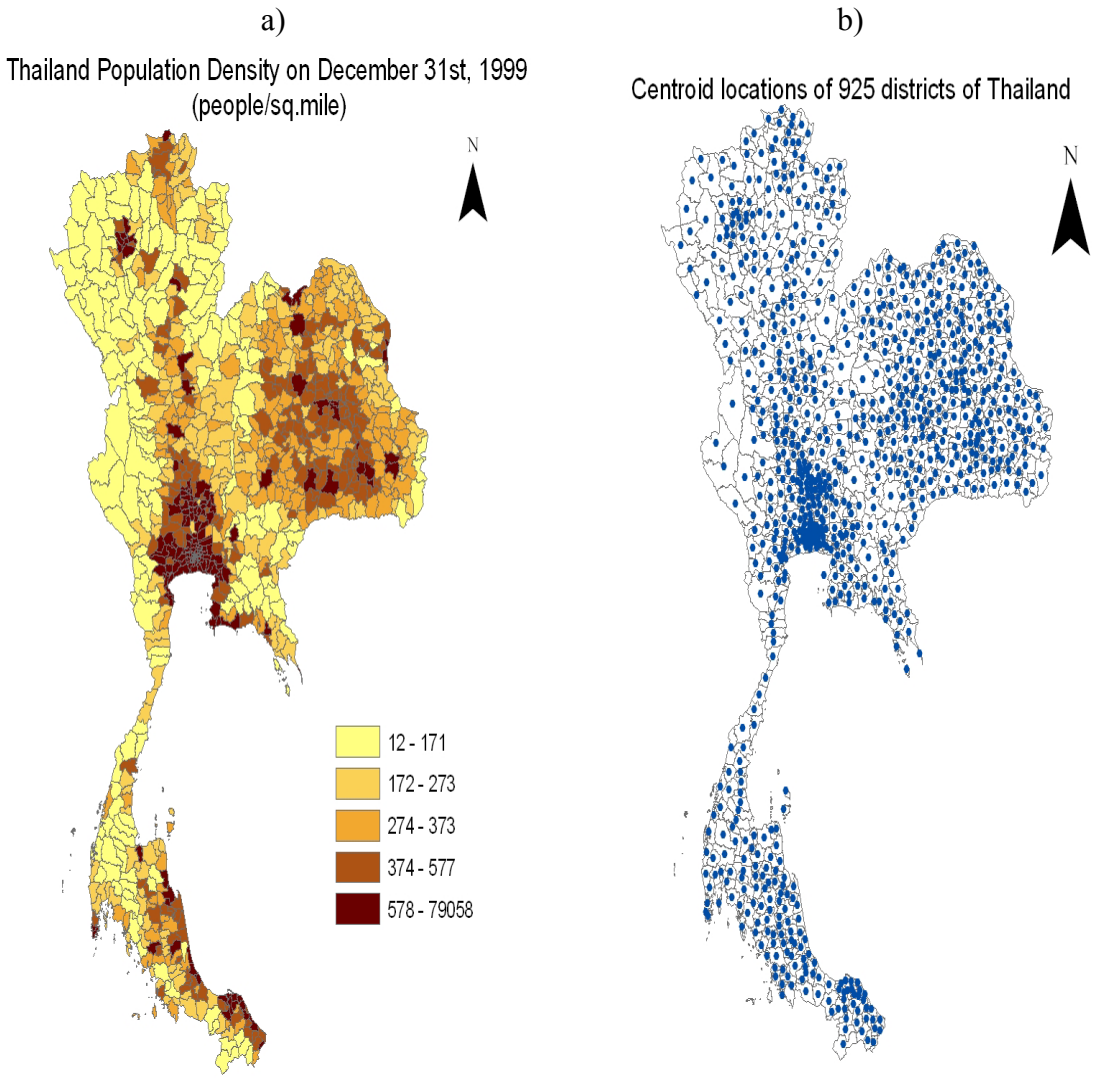

Figure 2.1 Spatial maps showing (a) the population density on December 31st, 1999 (people per sq.mile), and (b) the district centroids where daily population size and BME normalized estimation error variance were estimated.

a)

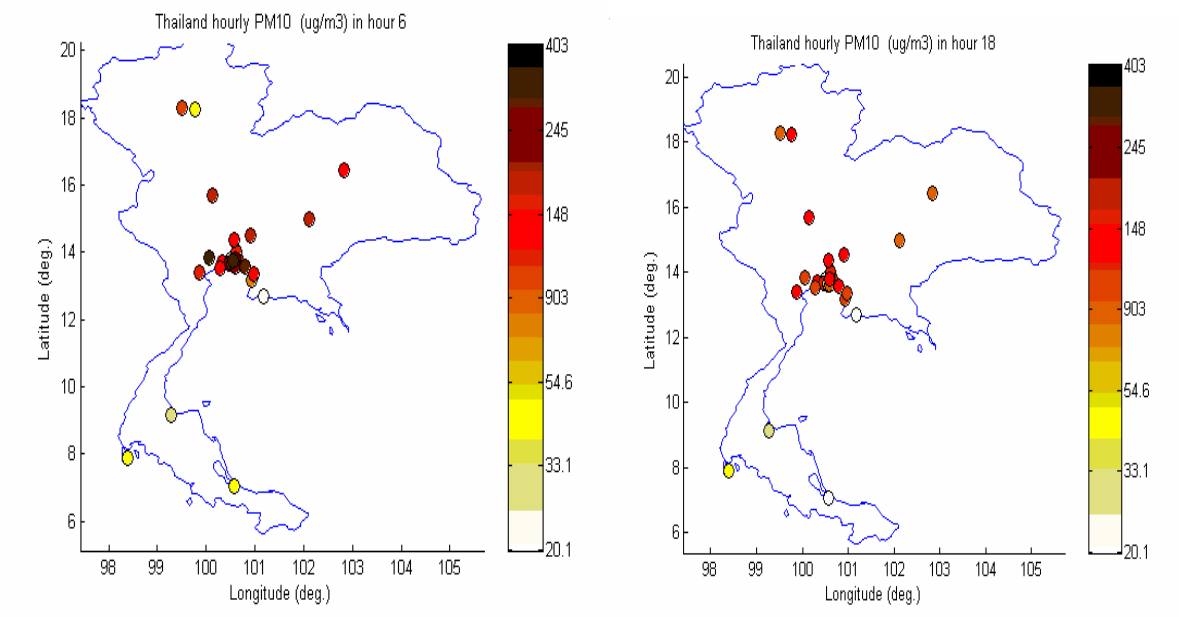

b)

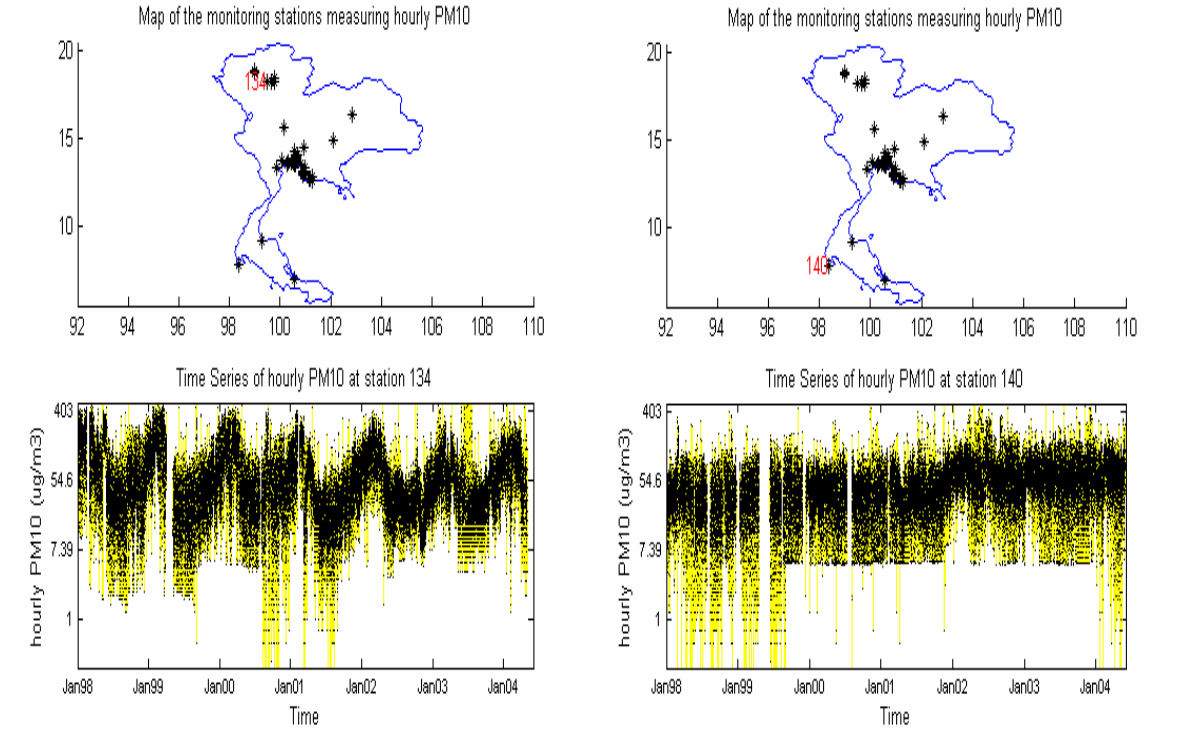

Figure 2.2 Exploratory analysis of hourly PM_{10} in Thailand showing (a) the color plot of hourly monitoring data at two hours on January, 1st 1998 (morning vs. evening), and (b) the time series of hourly data at two selected monitoring stations (north vs. south)

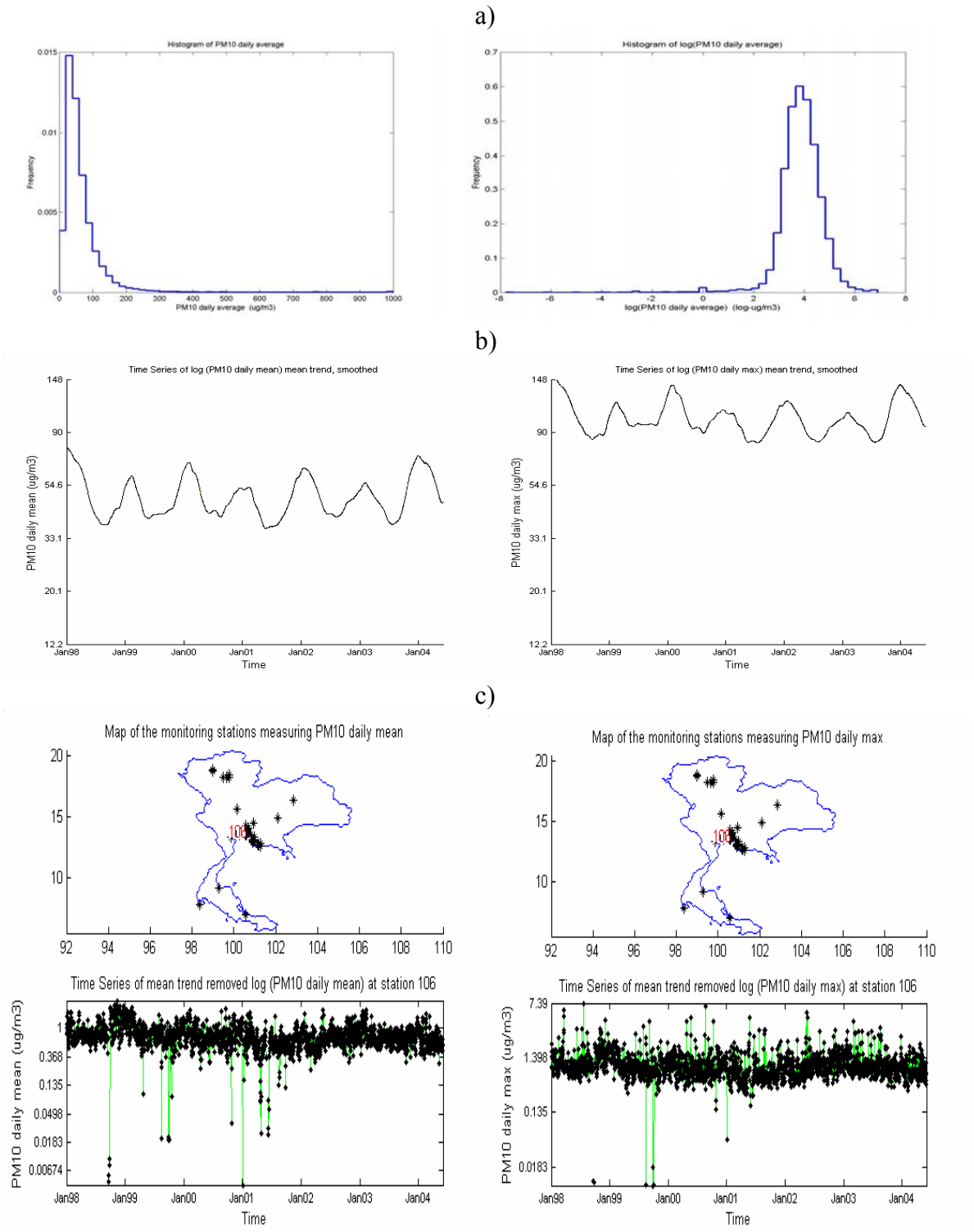

Figure 2.3 (a) histogram of hourly PM_{10} data (raw and log-transformed), (b) time series of the smoothed temporal mean trend (daily average PM_{10} and daily max PM_{10}), and (c) time series of the mean trend removed log-transformed PM_{10} data (daily average and daily max) at a selected station in Bangkok.

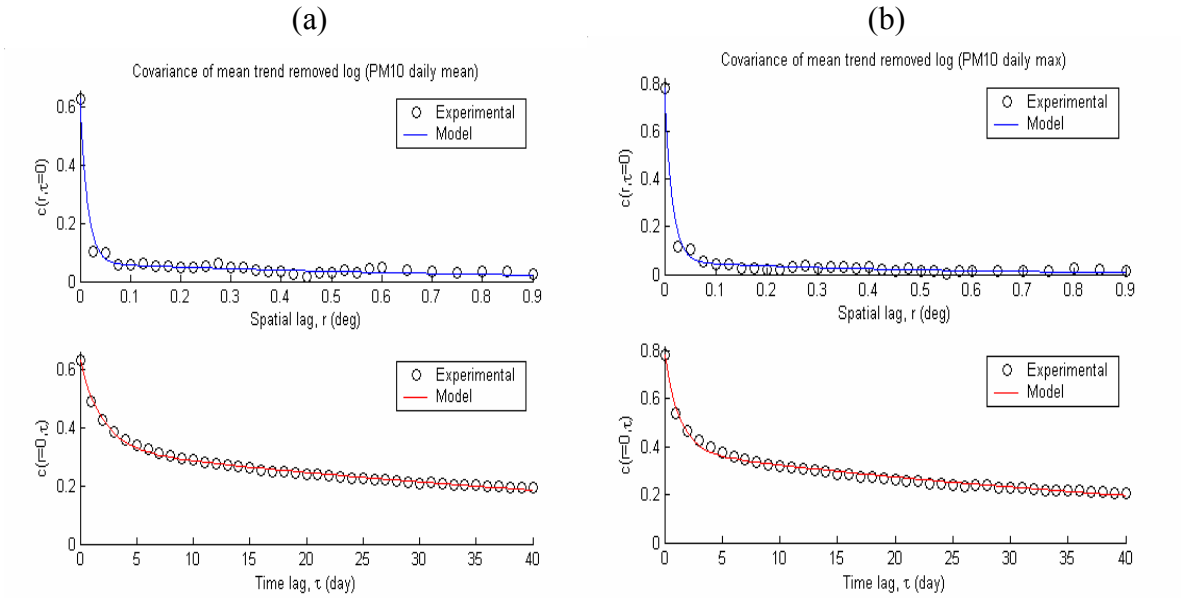

Figure 2.4 Covariance of the mean trend removed log-transformed PM_{10} for (a) daily average PM_{10} and (b) and daily maximum PM_{10} , shown as a function of spatial lag (top plots) and temporal lag (bottom plots)

a)

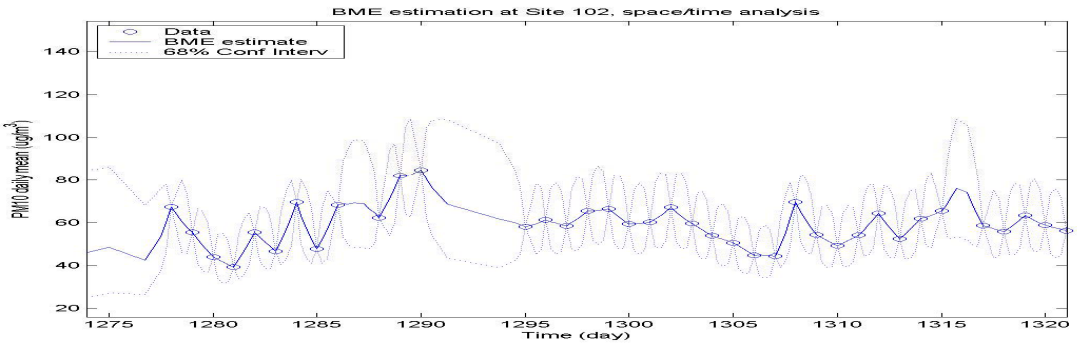

b)

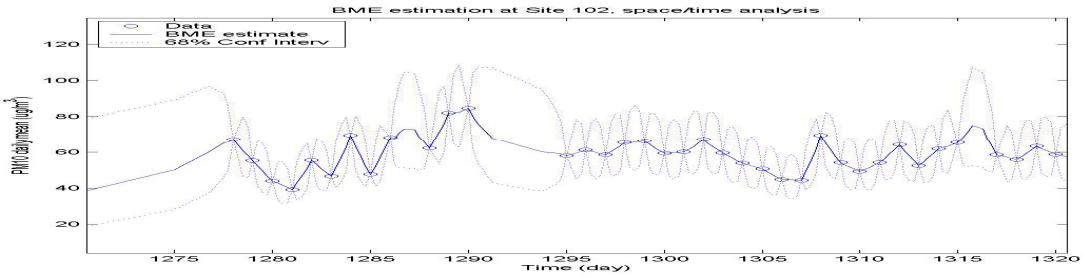

c)

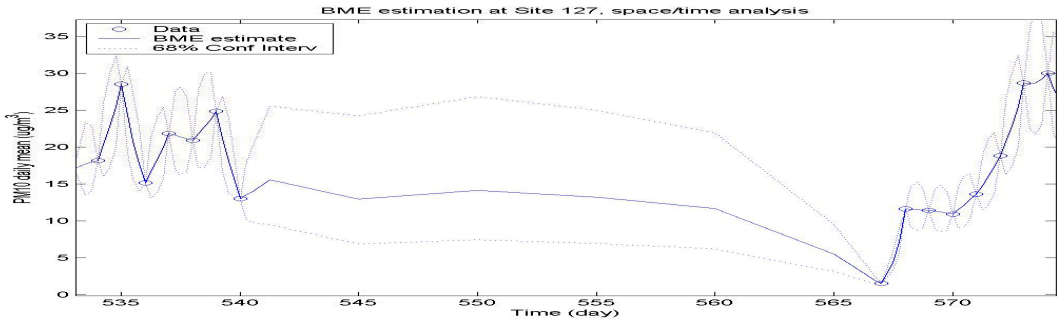

d)

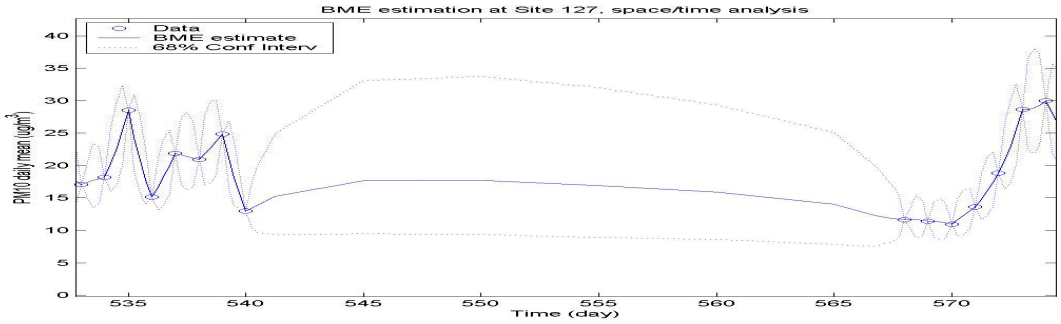

Figure 2.5 Time series of the BME mean estimate of daily average PM_{10} along with its 68% confidence interval obtained at station 102 using (a) only hard data, and (b) hard and soft data, and obtained at station 127 using (c) only hard data, and (d) hard and soft data.

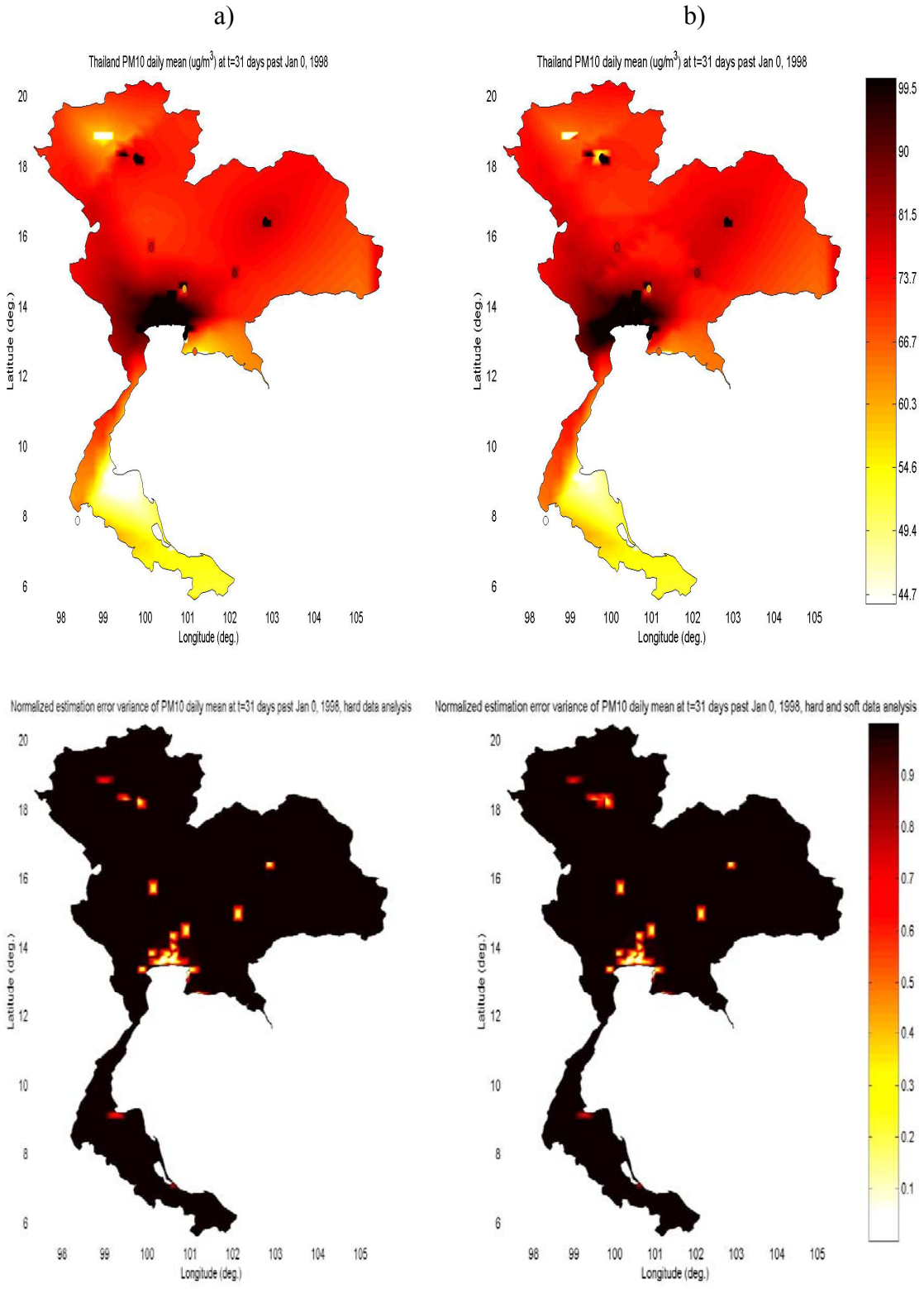

Figure 2.6 Maps of BME mean estimate (top) and normalized estimation error variance (bottom) of daily average PM_{10} obtained on the most polluted day in 1998 using (a) only hard data, and (b) hard and soft data.

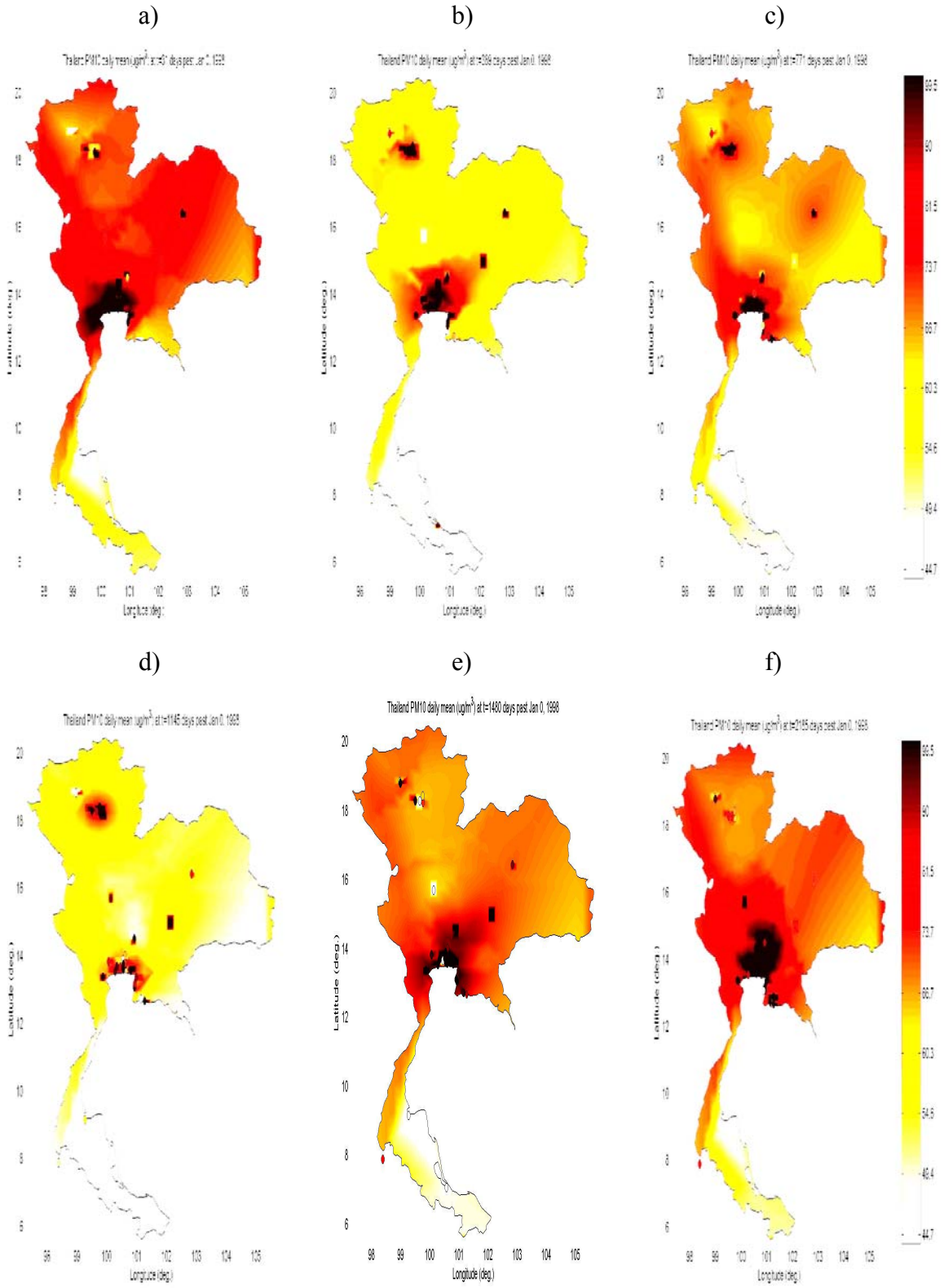

Figure 2.7 Maps of BME mean estimate of daily average PM_{10} obtained on the most polluted day of the year in (a) 1998, (b) 1999, (c) 2000, (d) 2001, (e) 2002, and (f) 2003 (analysis using hard and soft data).

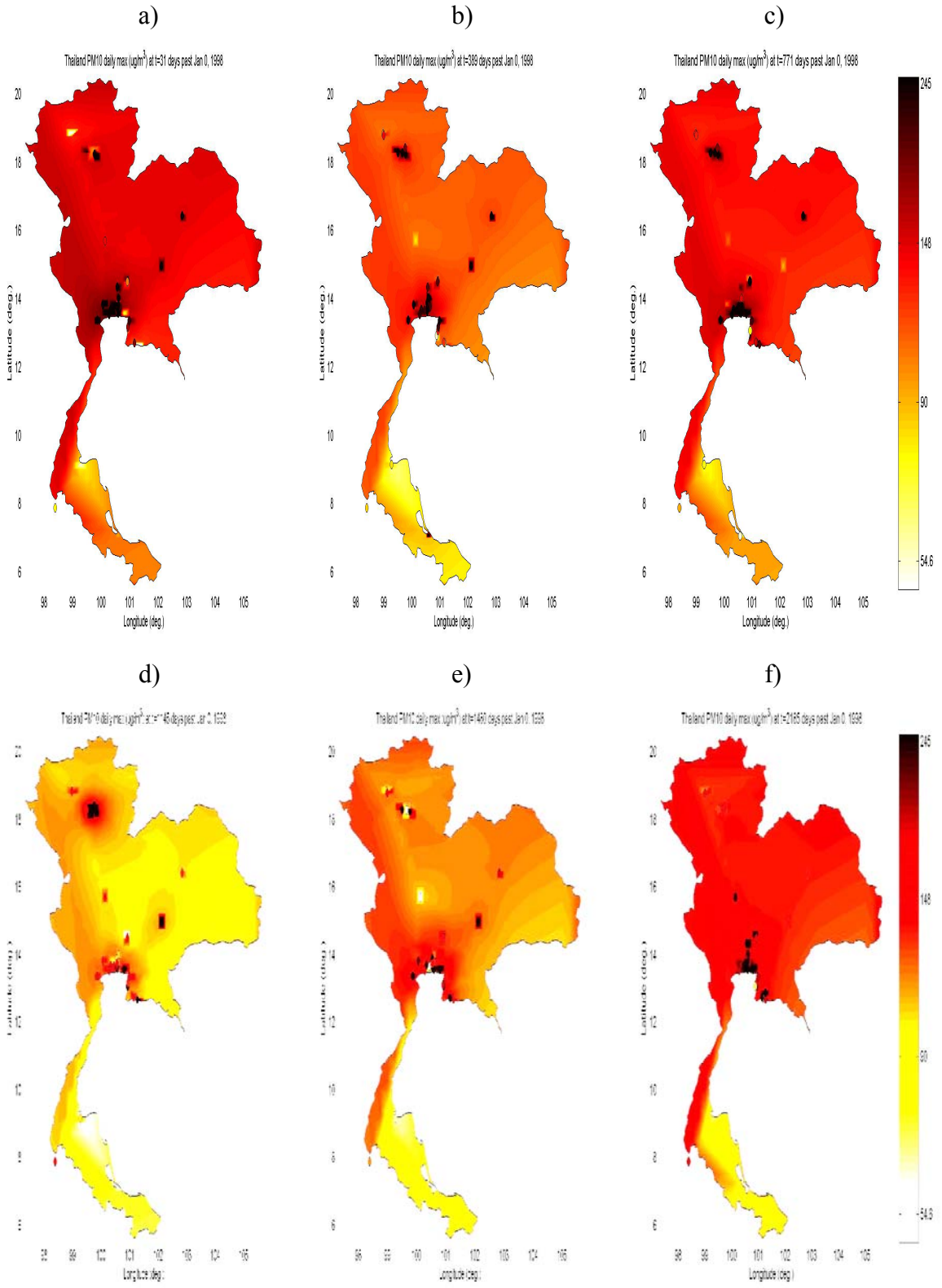

Figure 2.8 Maps of BME mean estimate of daily maximum PM_{10} obtained for the the most polluted day of the year in (a) 1998, (b) 1999, (c) 2000, (d) 2001, (e) 2002, and (f) 2003 (analysis using hard and soft data)

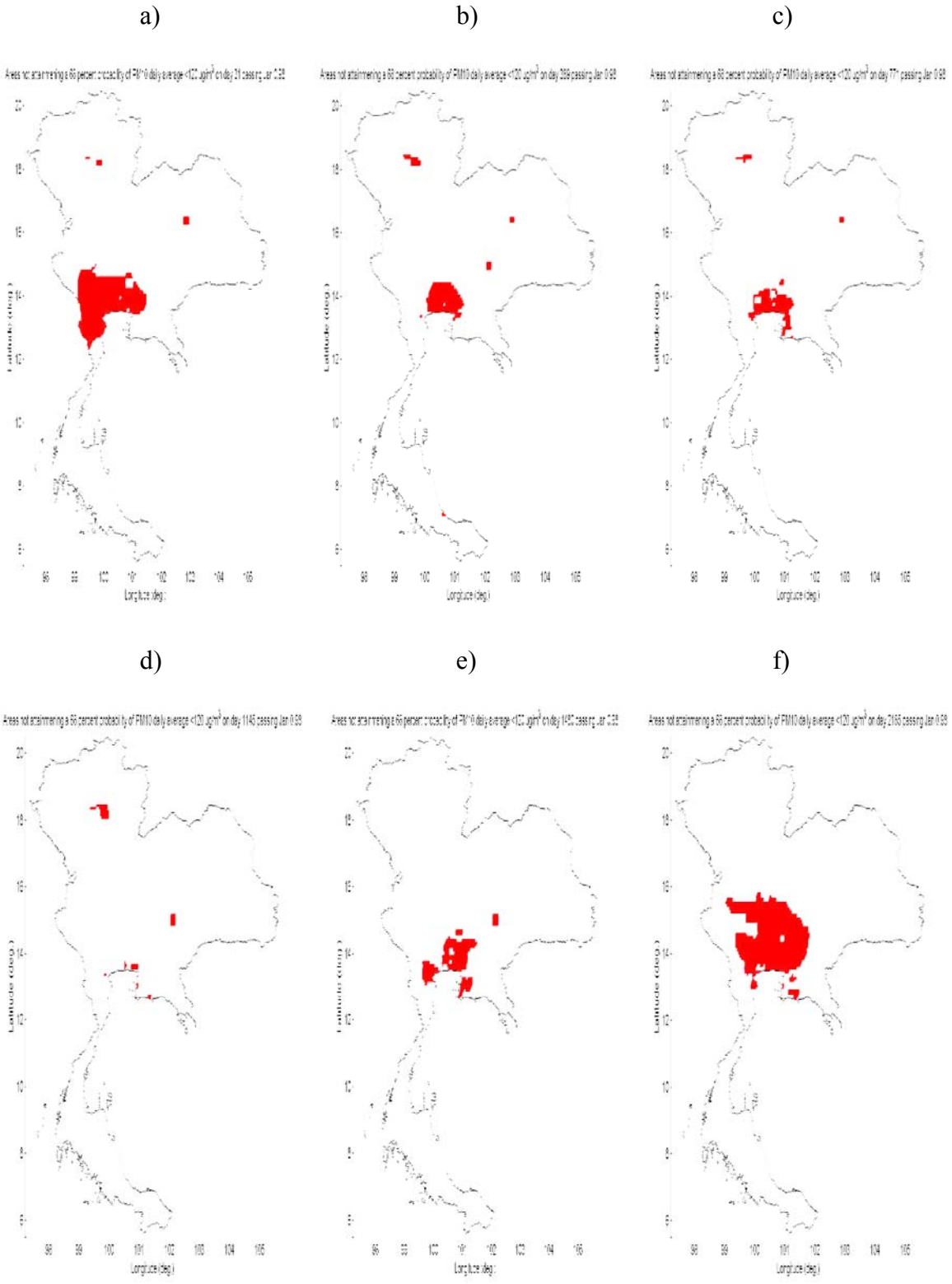

Figure 2.9 Maps of areas not attaining a 68% probability of PM_{10} daily average < 120 $\mu g/m^3$ on the most polluted day of the year in (a) 1998, (b) 1999, (c) 2000, (d) 2001, (e) 2002, and (f) 2003

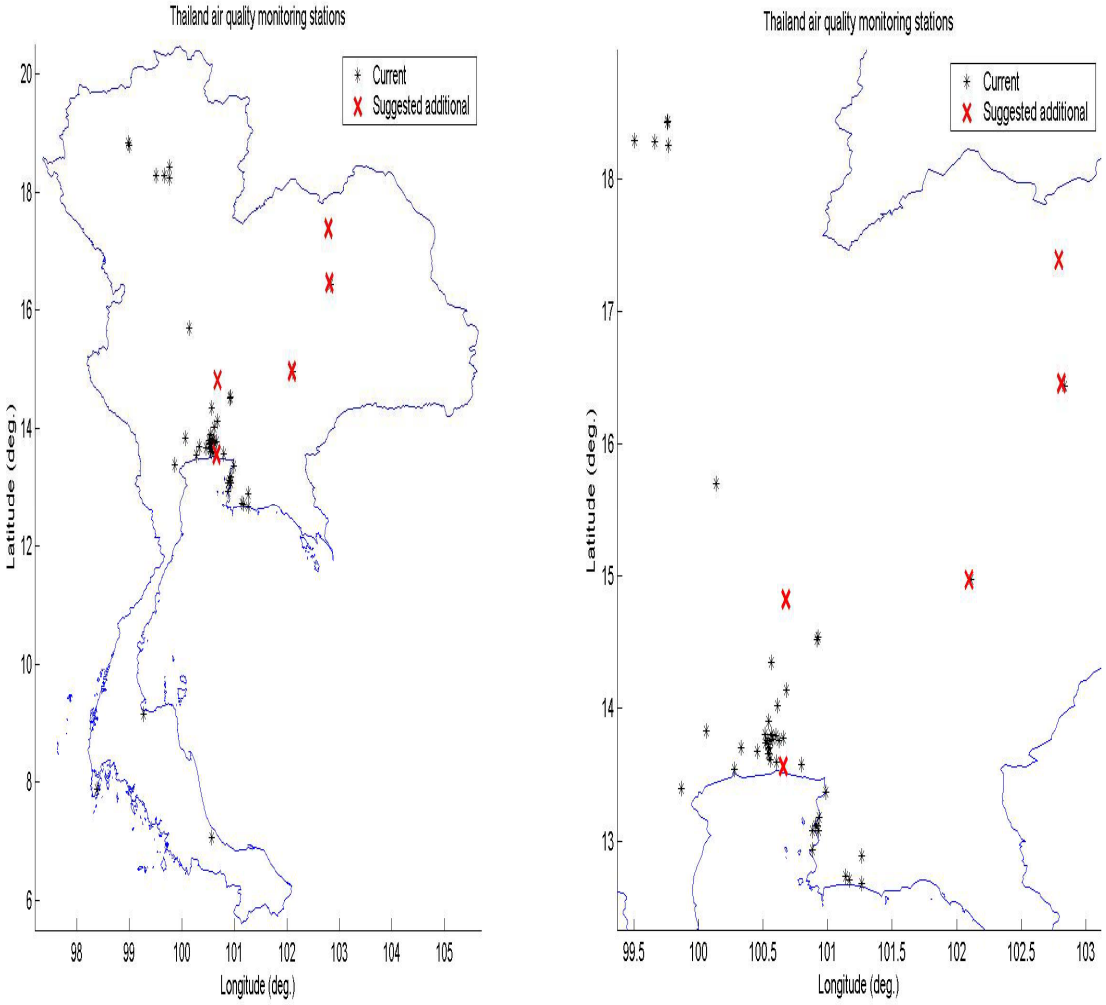

Figure 2.10 Locations of current monitoring stations shown with small star markers and suggested locations for new monitoring stations shown with large x markers.

III. MANUSCRIPT 2: REGIONAL ESTIMATES OF THE ASSOCIATION BETWEEN DAILY ATMOSPHERIC PARTICULATE MATTER AND CARDIOPULMONARY MORTALITY IN THAILAND

Abstract

Although previous studies have confirmed the association between short-term exposure to PM_{10} and the resulting increase in cardiopulmonary mortality in Thailand, such studies are not available for all five regions of Thailand, and there remain questions about the errors introduced by the interpolation techniques used to assess PM_{10} exposure, and the effect that these errors have in the estimated strength of the association. Indeed, obtaining a highly accurate estimation of ambient PM_{10} is vital when performing the analysis of the association between daily PM_{10} and mortality. Taking a spatial average of PM_{10} from neighboring monitoring stations or a temporal average of measurements at the closest station as an estimation of PM_{10} exposure does not account for the composite space/time variability of PM_{10} in the atmosphere. Unlike techniques used in previous studies, we use in this work the Bayesian Maximum Entropy (BME) mapping method of modern Spatiotemporal Geostatistics to construct accurate spatiotemporal maps of PM_{10} in Thailand. The BME framework rigorously takes in account the uncertainty associated with monitoring measurements as well as the natural space/time variability of PM_{10} in order to make the exposure estimation. We apply this framework to the analysis of all daily PM_{10} measurements collected from 1998 to 2003 across Thailand, and obtain the first BME assessment to date of the short term exposure to PM_{10} (daily concentration) for each death

(n=1.37 millions) geocoded in Thailand in that time period. We then use a case-crossover study design with a symmetric 7 day bidirectional selection of referent cases to estimate the strength of the association in several strata of the reported mortality cases, and we use a meta-analysis to aggregate results for these strata and obtain estimates of the strength of the association by cause of death (using ICD-10 classification) and for each of the 5 regions of Thailand, as well as a pooled estimate for the country. Pooled country estimates suggest a 10 $\mu g/m^3$ increase in PM_{10} is associated with increases of 0.85% (95% confidence interval, 0.15-1.36) in cardiovascular mortality and 0.53% (-0.95-2.03) in respiratory mortality.

Introduction

Many studies conducted in the North American and Western European countries have confirmed the relationship between fluctuations of daily PM_{10} (an ambient particulate matter in the air with an aerodynamic diameter < 10 μm) and cardiopulmonary mortality (*1-4*). In Bangkok, previous epidemiological studies have demonstrated that risks of cardiovascular and respiratory mortality associating with exposure to daily PM_{10} ambient levels were consistent with or slightly higher than those in US cities, although emission sources, weather patterns, and PM_{10} levels between the two countries are dramatically different (*5, 6*). They showed that the observed risk estimates associated with short-term exposure to PM_{10} were stronger for respiratory daily mortality than for cardiovascular daily mortality. Although previous studies have confirmed the association between short-term exposure to PM_{10} and the resulting increase in cardiopulmonary mortality in Thailand, such studies are not available for all 5 regions of Thailand, and there remain questions about the errors introduced by the interpolation techniques used to assess PM_{10} exposure, and the effect that these errors have in the estimated strength of the association.

In previous time-series studies of the association between PM_{10} and mortality, the PM_{10} exposure at various receptor locations is usually assumed to be equivalent to the PM_{10} concentration directly measured at a monitoring station in the proximity of the receptor, or to the linear interpolation of measurements in the space time neighborhood of the receptor. Due to the high natural spatial and temporal variability of PM_{10} (*7, 8*), the accuracy of linear interpolation or the direct use of observed values at the closest monitoring site are questionable. To overcome this discrepancy, in this study we propose to use the Bayesian Maximum Entropy (BME) estimation method of modern spatiotemporal Geostatistics to treat

PM_{10} outlier measurements as soft data with high uncertainty, and then obtain BME estimated values of PM_{10} by rigorously accounting for their composite space/time variability. Previous work has shown that the reported risk could be biased in a single city study (*9*). Therefore, the PM_{10}-cardiovascualar and respiratory mortality associations reported in previous studies and the corresponding estimated risk in Bangkok need to be reinvestigated and extended to the whole country using the proposed stochastic BME exposure mapping analysis. In air pollution epidemiology studies of short-term effect, two study designs are commonly used: time-series and case-crossover. Traditional time-series design applies Poisson regression with smooth functions or regression splines to model seasonal variations and indirectly account for confounding factors. On the other hand, it has been demonstrated that the case-crossover design directly controls for confounding factors associated with case characteristics while also offering the flexibility to control for some time trend effects (*10, 11*). This advantage of the case-crossover design to directly control for case characteristics is quite attractive and makes the framework an alternative to Poisson regression.

The case-crossover design has been extensively used in epidemiologic studies and recently adopted as a viable approach to estimate the strength of associations between short-term exposure to ambient particulate matter and acute health end points (*12-18*). The case-crossover study design is an adaptation of matched case-control analysis in which case and control (referent) are the same subject. This study design compares the exposure level at an index time (exposure time) just before the event when the subject experienced an acute health event (i.e. death) with exposure at one or more referent times when the subject did not experience that health event (*19*). A conditional logistic regression analysis is conducted to

model the linear dependence of the logit transform of the probability of the health event (i.e. probability of death) with PM_{10} exposure, as expressed by the following model

$$\text{Logit}\left(Prob.[Death] \right) = \beta_0 + \beta_{PM}\ PM_{10} \qquad (1)$$

where *Prob.*[ ] is the probability operator, β_0 and β_{PM} are the regression coefficients and PM_{10} is the daily average concentration of PM_{10}. The coefficient β_{PM} provides a measure of relative risk as it is directly related to the odds ratio (OR) (i.e. the ratio of the odds of death for a 1μg/m^3 increase in daily PM_{10}) by the following equation (*20*)

$$\text{Odds ratio (OR)} = \exp(\beta_{PM}), \qquad (2)$$

By contrasting the exposure for the same subject, say subject *i*, between the day of the health event (i.e. when *Prob*(Subject *i*, Death)=1) with adjacent control days when the health event did not occur (i.e. when *Prob*(Subject *i*, Death)=0), time-independent confounders such as health behavior or health status are automatically controlled for because they remain unchanged, while time-dependent confounders such as exposure trend or day of week and seasonal effects are controlled by time matching. Hence these confounders are controlled by design instead of being controlled through smooth functions or regression spline with somewhat arbitrary smoothing parameters as is the case for other time-series approaches.

Previous work has investigated in detail different referent sampling schemes (i.e. the scheme used to select the control days) and their associated bias (*21*). Typical referent sampling selection schemes include unidirectional, bidirectional, and time stratified referent

selection schemes. The unidirectional referent selection scheme uses referents only at times *before* the index time, and leads to a significant bias if there exists a long time trend in the exposure time series (*22*). The bidirectional referent selection scheme on the other hand requires selecting referents at times *before* and *after* index time (*23*), which removes the bias seen with the unidirectional referent selection scheme in the presence of long time trend in the exposure time series. Furthermore by restricting the selection of referent times in multiples of seven days, one can control for 'day-of-the-week' effects, while at the same time removing issues of PM_{10} autocorrelation between case and control as long as the temporal range of auto correlation is less then 7 days. Similar strategies can be used to control for seasonal effects. A limitation of the unidirectional and bidirectional referent selection schemes is that the selected referent days may be considered to be in non-localizable windows, in that the referent days may fall into different months, seasons, or years than the day of death. This leads to an overlap in the selected strata, which may invalidate the independent sampling inherent to conditional likelihood, resulting in an overlap bias. However the overlap bias reported in bidirectional referent sampling is very small (*24, 25*). Nevertheless, the overlap bias can be altogether eliminated by dividing the study period into fixed strata, and then restricting the selection of referent days within each strata. The referent times are then in localizable windows within pre-specified strata that are fixed and disjointed, thereby eliminating the overlap bias. This selection scheme requires larger dataset and is known as the time stratified referent selection scheme.

The goal of this study is to obtain regional estimates of the association between daily atmospheric particulate matter and cardiopulmonary mortality in Thailand. The two main objectives to meet that goal are (1) the use of BME estimates of daily PM_{10} concentrations

across Thailand between 1998 and 2003 to obtain a BME assessment of the short term exposure to PM_{10} for each death reported across Thailand in that time period, and (2) the use of a case-crossover study design with conditional logistic regression to obtain regional estimates of the strength of the association between short term PM_{10} exposure and cardiovascular as well as respiratory mortality in the five regions of Thailand, as well as pooled estimates of the strength of the association for the whole country.

Methods

PM_{10} data

Currently the Thai PCD maintains a nation wide air monitoring network comprising 51 stations with equipment using the PM_{10} automatic beta-gauge method. The monitoring stations maintained by the PCD are located on curbsides of major roads and in residential areas. As can be seen from Figure 3.1, most of these stations are clustered around the capital city, Bangkok, while few additional stations are located in the other five regions of Thailand. We obtained from the PCD approximately 1.9 million measurements of hourly PM_{10} concentration collected at these stations during 1998-2003, and we averaged these values every 24 hours to obtain approximately 79 thousands measurements of daily PM_{10} concentration across Thailand during 1998-2003.

Mortality Data

We obtained from the Bureau of Policy and Strategy (BPS) of the Thai Ministry of Public Health a comprehensive dataset containing all records of death from natural causes that

occurred between January 1998 and December 2003 in Thailand. This mortality dataset was made up of information from death certificates for about 1.93 million Thai residents, with reported location at the time of death corresponding to one of 2,087 primary or secondary administrative districts in Thailand. Because geographic locations for the secondary administrative districts were not available, we eliminated deaths reported at secondary administrative districts, resulting in approximately 1.37 million records of death from natural cause reported to any of the 925 primary districts that makes up Thailand (Figure 3.2b). We will hereafter refer to these deaths from natural causes as the total mortality. For illustration purposes, we show in Figure 3.2a a map showing the spatial distribution of total mortality for January 31st, 1998. The centroid for each of the district is shown in Figure 3.2b. In this work we will investigate specific causes of deaths as classified according to the International Classification of Diseases, 10th Revision (ICD-10) (World Health Organization 1993). Our six year dataset includes 213,736 neoplasm deaths (ICD-10 codes C00-D48), 137,019 cardiovascular deaths (ICD-10 codes I00-I99), 82,934 respiratory deaths (ICD-10 codes J00-J99), 36,015 genitourinary deaths (ICD-10 codes N00-N99), 35,329 digestive deaths (ICD-10 codes K00-K93), and 30,859 endocrine, nutritional, and metabolic deaths (ICD-10 codes E00-E90).

BME mapping framework

In environmental exposure studies, the distribution of an exposure variables X of interest such as PM_{10} can be represented in terms of a Space/Time Random Field (S/TRF) $X(\boldsymbol{p})$, where the vector $\boldsymbol{p} = (\boldsymbol{s}, t)$ defines a space/time point at the spatial location $\boldsymbol{s} = (s_1, s_2)$ and time t (*26*). The randomness and natural space/time variability of the S/TRF $X(\boldsymbol{p})$ are

represented as a collection of realizations (possibilities) of the $X(\boldsymbol{p})$ field over its space/time domain. The BME mapping approach rigorously incorporates two types of knowledge bases of the S/TRF $X(\boldsymbol{p})$, which are the general and site-specific knowledge bases. The general knowledge may include the spatiotemporal mean trend and covariance structures of the S/TRF $X(\boldsymbol{p})$ (*27*). The mean function describes the spatiotemporal trend of $X(\boldsymbol{p})$ while the covariance function characterizes spatiotemporal correlation between pairs of points $\boldsymbol{p}$ and $\boldsymbol{p'}$. The site-specific knowledge refers to hard data (accurate reading values from monitoring instrument) or soft data (readings with associated uncertainty, such as readings below the detection limit corresponding to soft data of interval types with a lower bound of 0 and an upper bound equal to the detection limit, or high outlier values that can be treated as soft data of a probabilistic type having a large uncertainty due to measurement error). When hard and soft data are both used in the BME analysis, the BME method is found to be more accurate than the linear regression methods of classical Geostatistics which do not rigorously account for soft data with non-Gaussian distributions and the composite space/time variability of PM_{10} fields (*7*).

The mathematically rigorous knowledge processing rules of the BME method allow one to process the general and site-specific knowledge bases available, and produce a posterior probability density function (PDF) characterizing the $X(\boldsymbol{p})$ at each mapping grid point of interest. The posterior PDFs offer a complete stochastic description of the S/TRF $X(\boldsymbol{p})$ at the estimation points, and are used to construct the BME spatiotemporal maps. Knowing the posterior PDF of PM_{10} permits any predictors such as the BME mean, the BME mode, or the BME median, as well as any confidence intervals for the estimated value (*27*). The *BMElib* software (*28*) written in the MATLAB platform provides an efficient

computational implementation of the BME method. BME analysis has also been used in other human exposure studies by investigating stochastic exposure-health effect associations and determining population health risks (*29-31*).

In this analysis the estimation points $\boldsymbol{p_k}$ are located at the centroid of each district polygon. The BME mapping method establishes a prior PDF corresponding to the general knowledge consisting in the spatiotemporal mean trend and covariance functions of the S/TRF $X(\boldsymbol{p})$ representing PM_{10}, and then restricts this posterior PDF using the data collected everyday at all available ambient air monitoring sites. The magnitude of estimation errors depends on the proximity of the monitoring data in the neighborhood of the estimation district centroid, and the uncertainty associated with these data. Results of the BME mapping analysis of PM_{10} in Thailand were presented in the previous chapter of this dissertation and include: 1) the mean trend model for the log-transformed PM_{10} field; 2) the covariance model for the mean trend removed log-transformed PM_{10} field; and 3) BME spatiotemporal maps which show the temporal evolution of the spatial distribution of PM_{10} daily average across Thailand. For illustration purposes BME map in Figure 3.2c shows the spatial distribution across Thailand of the daily average concentration of PM_{10}. Figure 3.2a on the same date shows the total mortality for January 31st, 1998.

Referent and lag selection

While a time stratified case-crossover study design offers a selection of referents that prevents the overlap bias, the symmetric bidirectional case-crossover study design has been more extensively used in air pollution epidemiologic studies since 1999 (*21*). In this work, the short-term effect of PM_{10} is estimated using a mortality database that includes most of the

deaths reported from 1998 to 2003 in Thailand. Performing a conditional logistic regression for such a large dataset will have a high numerical complexity resulting in large computing times (see next section on *computation demand*). To lower the numerical complexity so as to obtain results within a manageable computational time, it was preferred to lower the number of referent days used as controls for each death. This was achieved by using the 7 day symmetric bidirectional scheme to obtain the referent days used as control for each death (see Figure 3.3) (*11*). By restricting the referents days to be 7 days prior and after the index time, we narrow the number of controls used for each death to only two referent days, which reduces considerably numerical cost, as desired in this study. The 7 day bidirectional scheme has the obvious advantage of automatically eliminating the day-of-the-week confounding effect because a case and its controls are by design on the same day of the week. Furthermore a 7 day time difference is short enough that a case and its controls are usually always in the same season, while at the same time is long enough so that the PM_{10} level between a case and its controls can be considered to be un-correlated. Indeed, the autocorrelation of PM_{10} in Thailand lasts up to about 6 days (see results section of the previous chapter), which is less than the 7 days time difference between a case and its controls.

Up to this point the scheme used to select the referent days relative to the index time has been discussed. In Fig. 3.3(a) we show how this scheme looks when the index day (day of exposure) is the same as the day of death. This corresponds to a lag of 0 days between exposure and effect. It is easy to modify the selection scheme to consider a 1 day lag between exposure (index day) and effect (day of death), as is shown in Fig. 3.3(b). Other lags can easily be considered as well, by setting a lag between the index day and death day,

while keeping the two referent days used as crossover controls to be 7 days prior and 7 days after the index day, respectively. In this work lags up to 10 days were considered along with the calculated slope β_{PM} (Eq. 2) that corresponds to each of these lags.

This study divided Thailand into 5 regions which were: Bangkok and its vicinity, the central region around Bangkok, the northern region, the southern region, and the northeast region. Districts located in Bangkok and its vicinity were excluded from the central region, so that the regions were mutually exclusive (i.e. no overlap existed between regions).

Computational demand

The conditional logistic regression model (Eq. 2) was implemented using the *Logistic* procedure in SAS® (version 9.1) and matching each case and its two cross-over controls to a single individual (strata) within the conditional likelihood function. Hence, if n is the number of death cases in a subset of the overall dataset, then the number of observations is $N=3n$ (two cross over controls for each death case) corresponding to n distinct strata. The computation was run on a high performance computer system available on the University of North Carolina at Chapel Hill campus (UNC) (hereafter referred to as the UNC *STATapps* computer system) comprised of 20 processors (of type 1.05 GHz Sun E15K) and with access to 40 Giga Bytes of Random Access Memory. In order to assess the computational work involved, a test case was run consisting of N= 85,000 observations, and found that the computing time required was 45 hours. Because of the long computation time corresponding to this rather small number of death cases ($n=N/3$=17,000 death cases), the weather variables of daily interpolated humidity and temperature were not included in this analysis, as well as the atmospheric co-pollutants to PM_{10}, because these variables would have considerably

increased the number of observations N for the same n, resulting in much longer computation times (or put in other words, their inclusion would have come at the expense of reducing the number of death cases n considered for the same computation time T). In order to assess how the computation time T scales with the number of observations N, we run test cases with smaller number of observations, and we show in Figure 3.4 a plot of computational times obtained for each number of observations considered. It is clear from this log-linear plot that for the range of computation time T investigated, the computation time scales as a function of N according to the log-linear equation $\log T = \log T_0 + \alpha N$, where T_0 is a start up time and α is a log-linear slope. Using that equation we find that the computation time that would be required for a number of observations N, corresponding to the whole dataset of geocoded deaths from natural causes in Thailand from 1998 to 2003 (i.e N= 1.37 million death cases + 2.74 million crossover referents) would be approximately $T = 2.25 \times 10^{31}$ years. Clearly this estimate might be a gross over-estimation of the time it would take, or it might only reflect the fact that the numerical implementation we have chosen may not be the most efficient, but nonetheless this enormous computation time suggests that an efficient strategy is to divide the overall dataset into logical subsets using some sensible stratification of the death cases, obtain the association between PM_{10} and death for each subset, and then perform a meta-analysis of these associations to calculate the association for some aggregate of the sub-datasets. For example if we divided the overall dataset into 180 equal sized sub-datasets, then the corresponding computation time would be $T = 180[T_0 \exp(\alpha N/180)]$, corresponding to an estimated computation time of approximately 8.3 days. We implemented this approach by stratifying the dataset according to the 5 regions of Thailand described earlier, 6 specific causes of deaths, and the 5 years of the 1998-2003 time period, leading to 180 sub-datasets of

slightly different sizes (due to the uneven distribution of deaths between specific cause, etc.), and we considered 11 lags for each of these sub-dataset (0 day lag to 10 days lag), leading to the calculation of 180*11=1,980 β_{PM} coefficients. The calculation of these 1,980 β_{PM} coefficients consumed 91days of computing time on the UNC *STATapps* computer system.

Pooled estimates of the PM_{10}–mortality association by regions and for the country

A meta-analysis of the 1,980 β_{PM} estimated coefficients was performed to obtain pooled estimates by region and for the country of the association between PM_{10} and cause specific deaths for each of the 11 time lags considered. The pooled estimate of the association for a region for a specific cause of death and time lag was obtained by pooling the 6 β_{PM} coefficients estimated in that region for each of the 6 different years (1998 to 2003), while the pooled estimate of the association for the country for a specific cause of death and time lag was obtained by pooling the 30 β_{PM} coefficients estimated for each of the 5 different regions of Thailand and 6 different years of the 1998-2003 time period. The meta-analysis that we utilized to calculate a given pooled estimate used either a fixed-effect model or a random-effect model depending on a Chi-square statistical test. The null hypothesis of that test is that the β_{PM} coefficients for each lag being pooled are homogeneous. When the Chi square test rejected that hypothesis with p-value <0.01 (significant heterogeneity among the β_{PM} coefficients being pooled) we reported the pooled estimate obtained using the random-effect model, otherwise we reported the pooled estimate obtained using the fixed-effect model. In the case of the regional estimates of the association this procedure lead to only reporting pooled estimates obtained using a meta-analysis with the random-effect model, while in the case of the country estimates of the association, this procedure lead to reporting

pooled estimates calculated sometimes with the fixed-effect model, and sometimes with the random-effect model, depending on the case by case result of the Chi-square.

Results

Meta-analysis pooled estimates of the regional and country-wide ORs (i.e. the ratios of the odds of death for a 1$\mu g/m^3$ increase in daily PM_{10}, see Eq. 2) and their 95% confidence intervals are shown in Figures 3.5-3.8 as a function of the time lag (in days) between exposure to PM_{10} and resulting mortality from specific causes of death. Country-wide pooled OR estimates for cause-specific mortality are plotted in Figure 3.5a. This figure indicates that country –wide ORs in cardiovascular and respiratory deaths were higher than those related to other causes of death. In addition, the results suggest that the pattern of delayed effect between exposure and death was seen only for cardiovascular and respiratory mortality, i.e. their ORs remained positive for some continuous lags. These findings are in agreement with previous studies supporting that there is a causal association between short term exposure to PM_{10} and cardiopulmonary mortality. Graphs of the ORs for neoplasm, endocrine gland, digestive and genitourinary mortality are also Fig. 3.5a. These graphs exhibits randomly fluctuating ORs as a function of lag, and in general showed negative associations. We therefore eliminated results of these four causes of death and in Fig. 3.5b we focus on the ORs for cardiovascular and respiratory mortality. The association between PM_{10} exposure and mortality is found to be strongest at a lag of 1 day and 3 days for cardiovascular and respiratory mortality, respectively. Furthermore, the association between PM_{10} and cardiovascular mortality was found to be statistically significant for a time lag

between exposure and effect of 1 day as well as 2 days. The delay between exposure to PM_{10} and its effect was found to be longer for pulmonary mortality, with positive PM_{10}-pulmonary mortality associations found for lags of 2, 3, 4, 5 and 6 days.

The regional pooled OR estimates for cardiovascular and respiratory mortality are plotted in Figure 3.6 and 3.7. These figures also show the country-wide pooled OR estimate of Fig. 3.5 for comparison purposes. In Fig. 3.6a we show the regional estimates of the OR for cardiovascular mortality in all 5 regions of Thailand (i.e. the Bangkok area, the central region excluding Bangkok, the Northern region, the Southern region, and the Northeastern region). The curves depicting how the OR changes with delay between exposure and effect are consistent for Bangkok, the central region, and the Northern region. These curves show delayed effects with positive associations that remain positive for lags of 0, 1, and 2 days. On the other hand, the same curves for the Southern and Northeastern regions show fluctuating estimates with large confidence intervals. We will discuss the OR curves for these two regions in the next section, and for now we remove them so as to focus in Figure 3.6b on the OR curves obtained for the remaining 3 regions. This figure indicates that the strongest PM_{10}-cardiovascular mortality association is detected in the Northern region for a lag of 2 days between exposure and effect. In Bangkok and the central region, the strongest association is attained at a lag of 1 day between exposure and effect. The positive association is found to be statistically significant in Bangkok and the central region, while this is not the case for the Northern region.

Fig. 3.7a shows the regional OR curves for respiratory mortality. These curves have similar profiles as that of Fig. 3.6 for cardiovascular mortality, i.e. there is a positive association with delayed effects over continuous time lags in Bangkok and in the central and

Northern regions. These results are not observed in the Southern and Northeastern regions, where high uncertainty in the results exists. Figure 3.7b focuses on the OR curves obtained for Bangkok and the central and Northern regions. The strongest PM_{10}-pulmonary mortality association is detected in the Northern region for a lag of 2 days between exposure and effect. In Bangkok, statistically significant positive associations between PM_{10} and pulmonary mortality are observed for lags of 3 days to 5 days between exposure and effect, while in the central region the PM_{10}-pulmonary mortality association is positive for lags of 2 days to 7 days, but not statistically significant. Figures 3.6b and 3.7b show that the regional association between PM_{10} and cardiopulmonary mortality observed in the Northern region is distinct of that observed in Bangkok and the central region.

Figure 3.8 compares the PM_{10}-cardiovascular mortality association with the PM_{10}-respiratory mortality association in three regions of Thailand, as well as for the whole country. Results show that association is stronger for respiratory effects in each region (Fig. 3.8a-c), but that this reverses when considering the country as a whole (Fig. 3.8d). The country pooled respiratory odds ratios were lower as they were affected by results in the Southern and Northeastern regions that have extreme uncertainty and strong negative associations. The association observed in Bangkok and in the central region are very similar and with narrow confidence intervals as seen in Figures 3.8a and 3.8b. More uncertainty in the results is suggested by length of the confidence intervals observed in the Northern region (Fig. 3.8c), where the pattern of the OR curves was not consistent with that of other figures in terms of delayed effects and lag with the strongest association. Finally this figure clearly shows that the strength of the association for both cardiovascular and respiratory mortality is found to be the strongest in the Northern region.

To summarize the effect of PM_{10} on cardiovascular and respiratory mortality, we tabulate in Table 3.1 all the meta-analysis results of odds ratios shown in Figures 3.5-3.8. This table includes the regional estimates of the PM_{10}-cardiopulmonary mortality association for Bangkok, the central and Northern regions, and the pooled estimates for the whole country.

The concentration-response curves of Figures 3.9 and 3.10 show the percent increase in cardiovascular and respiratory mortality caused by a ΔPM_{10} increase in PM_{10} concentration in the air. The percent change in Mortality = $100*[\exp(\beta_{PM}\Delta PM_{10})-1]$ where β_{PM} is the estimate of the logistic regression coefficient (see Eq. 1), and ΔPM_{10} is the increase in daily PM_{10} concentration. These curves and their 95 % confidence bounds appear linear rather than exponential in the plotted ranges of $\Delta PM_{10} = 0$ to 100 $\mu g/m^3$ because the magnitude of the β_{PM} coefficients is very small. These concentration-response curves are useful in health risk assessment. Figure 3.9 shows the percent change in cardiovascular mortality as a function of increase in PM_{10} for a lag of 1 day for in Bangkok, the central region, and the whole county, and a lag of 2 days in the Northern region. The lower bound of these curves is generally positive (Figures 3.9a, 3.9b, and 3.9d) except in Northern region. This means that although the same increase in PM_{10} leads to a sharper increase in cardiovascular mortality in the Northern region, as seen in Figure 3.9c, the corresponding confidence interval is noticeably wider. Figure 3.10 shows the concentration –response curves for respiratory mortality. The curve in each region was calculated by using a lag corresponding to the strongest association between PM_{10} and respiratory mortality for that region. Hence this lag varies from 2 days in the Northern region (shortest delay between exposure and effect) to 4 days in the central region (longest delay). Bangkok is the only area

of Thailand with a lower bound of the risk estimate that is greater than zero. Figures 3.10a and 3.10b suggests the same rate in risk increase in Bangkok and the central region as their curves are approximately parallel. The concentration-response curves of the Northern region and the country (Figures 3.10c and 3.10d) have wider CI bounds. In general, the concentration-response curves are steeper for respiratory mortality than for cardiovascular mortality in all regions of Thailand, while this is not true when considering the country-wide concentration-response curve.

Table 3.2 and Table 3.3 summarize the percent change in daily cardiovascular and respiratory mortality, respectively, corresponding to a 10 $\mu g/m^3$ increase in PM_{10} and to the lag (delay between exposure and effect) for which the strongest association was observed. The tables indicate the lag in the second columns, and the 95% CI in the fourth columns. These tables are useful for discussing our results obtained in Thailand and comparing these results in the next section with previously published single-location and multi-location studies.

Discussion

This work uses a case-crossover study design followed by a meta-analysis of conditional logistic regression coefficients to obtain regional estimates of the association between PM_{10} and cardiovascular and respiratory mortality in Thailand using a comprehensive dataset of PM_{10} monitoring data obtained daily at 51 monitoring stations throughout the country between 1998 and 2003, and of 1.37 million reports of death from natural causes geocoded at the centroid of the 925 primary districts of the country. A positive association between short-

term exposure to PM_{10} and daily cardiovascular and respiratory mortality was detected in several regions of Thailand. In the Bangkok metropolitan area, the positive association was found to be statistically significant for both cardiovascular and respiratory mortality, with greater association strength observed in the case of respiratory mortality. In the central region, the positive association was statistically significant for cardiovascular mortality. In the Northern region, the strength of the association was greatly elevated but the positive association was not statistically significant due to the large uncertainty in the odds ratio estimates. When considering the whole country, although the negative and highly fluctuating associations of the Southern and Northeast regions were pooled in the meta-analysis of the country wide odds ratio, we found that an increase in PM_{10} results in a statistically significant increase in the country-wide cardiovascular mortality, while a positive but not statistically significant association is observed between PM_{10} and country wide respiratory mortality.

The results we obtain for Bangkok can be compared with results of several previously published single-city time-series studies. A study conducted in Vancouver, Canada reported high increased risk in cardiovascular death (5.4% per 10 $\mu g/m^3$ increase in PM_{10}: 95% CI, 1.0-9.8) but did not find association with respiratory mortality (*4*). In Coachella Valley, USA, a cardiovascular mortality study reported a statistically significant increased risk of 1.0% (95% CI, 0.5-2.0) per 10 $\mu g/m^3$ PM_{10} (*32, 33*). A study in Phoenix, AZ, reported that an increase of 10 $\mu g/m^3$ in PM_{10} was estimated to result in a 1.98% risk increase (95% CI, 0-3.52) in cardiovascular mortality in the elderly population (*34*). In another time series study using data from 3 counties, an increase of 10 $\mu g/m^3$ in PM_{10} was associated with an increase in daily cardiovascular mortality of 0.44% (95% CI, 0.07-0.80) in Cook county, IL, of 0.87% (95% CI, 0.32-1.43) in LA county, CA, and of 1.71% (95% CI, 0.51-2.88) in Maricopa

county, AZ (*35*). In agreement with the results of our study, results in two earlier Bangkok studies by Ostro *et al*. and Vajanapoom *et al*. found stronger positive associations of PM_{10} with respiratory mortality than with cardiovascular mortality (*5, 6*). The first study used only one PM_{10} station, and detected statistically significant increases in cardiovascular mortality (1.62% per 10 $\mu g/m^3$ PM_{10}: 95% CI, 0.63-2.36) and in respiratory mortality (6.19% per 10 $\mu g/m^3$ PM_{10}: 95% CI, 2.08-10.41) while the latter study, which used PM_{10} levels from three PM_{10} monitoring sites, reported an increase of 0.26% in cardiovascular mortality (95% CI, -0.3, 0.79) per 10 $\mu g/m^3$ increase in PM_{10}, and an increase of 1.67% in respiratory mortality (95% CI, 0.20-3.10) per 10 $\mu g/m^3$ increase in PM_{10}. Our Bangkok estimates (see Tables 3.2 and 3.3) of increased mortality risk of 0.92% (cardiovascular)and 1.25% (respiratory) per 10 $\mu g/m^3$ increase in PM_{10} are in the ranges or slightly above the lower end of the findings from the previous studies mentioned above.

Our country wide pooled estimate of increased risk in cardiovascular mortality (0.85%) and respiratory mortality (0.53%) per 10 $\mu g/m^3$ increase in PM_{10} in Thailand are slightly higher than those previously reported in other multi-location studies. The Health Effects Institute had called for the re-analysis of some earlier PM_{10}-mortality time-series studies (*36*) because inappropriate default convergence criteria in the generalized additive model (*37*) had lead to over-estimates of the strength of the association. The estimated increased risk for combined cardiopulmonary mortality reported in the re-analysis of the National Morbidity, Mortality and Air Pollution Study (NMMAPS) using data from the 90 largest US cities was 0.31% (95% CI, 0.22-0.40) per 10 $\mu g/m^3$ increase in PM_{10} (*37*). In the time-series analysis of the 20 largest US cities, the authors reported the reanalyzed national average estimate for increase in cardiopulmonary mortality at 0.30% (95% CI, 0.18-0.51) per

10 μg/m^3 increase in PM_{10} (*38*). The Netherlands time-series study using deaths for the whole country reported a reanalyzed estimate of the increased risk in cardiovascular mortality of 0.18% (95% CI, -0.16-0.53) per 10 μg/m^3 increase in PM_{10} (*3*). In a study applying a moving total mortality count in the cities in NMMAPS, a 10 μg/m^3 increase in PM_{10} was associated with a 0.17% increase in combined cardiopulmonary mortality (*39*). Lastly, mortality data from 29 European cities were analyzed and the authors reported that a 10 μg/m^3 increase in PM_{10} was associated with increases of 0.76% (95% CI, 0.47-1.05) in cardiovascular mortality and 0.58% (95% CI, 0.21-0.95) in respiratory mortality (*1*).

In this study, our single-city estimates of increased mortality risk for Bangkok are higher than the pooled country-wide estimates, which is in agreement with previously reported results. Our regional estimates in Bangkok metropolitan area and in the central and Northern regions indicate a stronger association between PM_{10} and respiratory mortality and a more delayed effect than that observed for cardiovascular mortality, which is again consistent with the previous studies. However some of our estimates of the strength of the association between PM_{10} and cardiovascular or respiratory mortality are higher than those reported in earlier studies. Some explanations for these higher estimated risks can be addressed here. First, most PM_{10} monitoring stations in Thailand are located on the curbsides of roads with heavy traffic and in dense residential areas close to major emission sources. Since the monitoring stations are preferentially located at polluted sites in Thailand, it results that the BME estimates in districts away from these sites may over estimate PM_{10} levels, resulting in an under estimation of the strength of the association (because the same increase in mortality is, in fact, caused by a smaller increase in PM_{10} than that estimated). However this under estimation is probably inconsequential when comparing our odds ratio estimates in

Thailand with that estimated elsewhere since the same argument for under estimation of the strength of the association can arguably be made for a number of monitoring networks, hence we still need to explain why several of the odds ratios we are finding in Thailand are higher than that reported elsewhere. We turn to our second explanation, which deals with how people in Thailand get exposed to outdoor air pollution. Meteorological conditions in Thailand allow people to spend more time outside of their houses, and to likely have their windows open year-round. Previous study showed that PM_{10} monitoring stations in Bangkok could capture daily variations of indoor PM level or even personal exposure (*40*). As a result, it may be that the same increase in outdoor PM_{10} recorded by the monitoring stations corresponds in fact to a greater increase in personal exposure than that in other countries where people are more sheltered from the outdoor air, resulting in a higher increase in mortality. These two first explanations deal with flaws in assessing what people exposures really are, and lead to effects (under and over estimation of odds ratio, respectively) that may cancel each other out. We then finally turn to the last explanation, which deals with the specific conditions encountered in Thailand. Emission sources of particulate matter, toxic components in PM_{10}, and the weather (particularly extremes in temperature and humidity) in Thailand are dramatically different from those in North American and Western European cities. Furthermore the exposed population in Thailand may have ethnic groups, age distribution, diet, pre-existing risk factors, etc. such that their susceptibility to adverse health responses from exposure to air pollution may be different than that seen in other countries. These country specific factors may result in higher strength of the association between PM_{10} and cardiovascular or respiratory mortality in Thailand than some reported in other countries. Investigating these country specific factors provide ground for future work.

Difference or similarity between regional estimates of the PM_{10}-mortality association among the 5 regions of Thailand could be discussed using information in Table 3.4. Although a positive association was found for some lags in the Southern and Northeastern regions, overall the association estimates show considerable uncertainty for these two regions. This uncertainty is most likely due to the insufficient number of PM_{10} monitoring stations in these regions, leading to poor PM_{10} exposure estimates. Indeed the combined area of the Southern and Northeastern regions is about half of Thailand, while these two regions only have 5 PM_{10} monitoring stations out of the 51 installed in the country. By contrast, the Bangkok metropolitan area is comparatively very small (about 2% of the country area) but it has 21 PM_{10} monitoring stations. Positive associations may really exist in the Southern and the Northeast areas, but many more PM_{10} monitoring stations will be needed to detect these associations. However the high uncertainty and negative association observed for some lags could also reasonably be explained by the fact that these regions may have more natural sources emitting particulate matter in the air. Natural sea spray due to strong ocean wind and monsoon in the Southern region, and natural windblown dust occurring during the 6 month of dry season in arid parts of the Northeastern regions are natural source of particulate matter measured by the PM_{10} monitoring stations. Previous findings reported insignificant associations between coarse windblown dust and cardiovascular and respiratory mortality (*41, 42*). These natural components of PM_{10} in the Southern and Northeastern regions would explain a weaker strength of the association than observed in the other regions of Thailand.

Even though the Bangkok metropolitan area and the central region did not overlap in our study, we find very similar PM_{10}-mortality associations in these two regions. This makes sense because they share the same airshed, with similar emissions of fine particles related to

vehicular and industrial combustions and coarse particles from construction, as well as similar populations. As can be seen in Table 3.4, about 91,000 deaths from cardiopulmonary causes were reported in the Bangkok metropolitan area and the central region, while these two regions combine to have 41 PM_{10} monitoring stations. These data lead to PM_{10} and mortality dataset with higher statistical power than that in other regions, leading to narrow confidence intervals and statistically significant estimates.

The PM_{10} associations with both cardiovascular and respiratory mortality were the strongest in the Northern region. Some hypotheses explaining this unique finding relates to the unique geographic topography and differences in emission sources between the Northern region and other parts of Thailand. Burning of household garbage and biomass burning of agricultural waste, wood, or dried grass in open space as well as forest fire are prevalent in the Northern region, while strong traffic emissions were observed in Chiang Mai, the second largest city in Thailand (*43, 44*). Many populated parts of the Northern region are surrounded by mountain ranges on its eastern, northern and western sides. A landscape made of valleys has the potential to trap and accumulate particulate matter during atmospheric event with low winds and high atmospheric stability during the winter months. These specific sources of PM_{10} combined with the potential for their being trapped in the air breathed by the population in the Northern regions could be factors in the high strength in the PM_{10} - mortality association observed, and merit further investigation. Additionally the effect of PM_{10} is much stronger for respiratory mortality than for cardiovascular mortality in the Northern region, which could provide a useful clue for future work in unraveling the etiology of the health impact of PM_{10} in that region. However, the uncertainty associated with the estimates of the strength of the association in that region is high. This high uncertainty is due

in large part to the relative small number of monitoring stations operating in the Northern region (6 stations covering approximately 33% of the country area). Future work in that region would therefore be greatly improved by increasing its number of monitoring stations.

The statistical significance of the positive association between PM_{10} and cardiovascular mortality is found to be more pronounced than that for respiratory mortality, which can be explained due to the larger incidence in deaths from cardiovascular causes resulting in increased statistical power. This higher incidence is in part due to the fact that when there are complications of chronic respiratory diseases combined with cardiovascular conditions, the reported cause of death tends to be cardiovascular.

Most of the findings from previous studies discussed above, and results of this study were not adjusted for effects of gaseous co-pollutants. However, the US Environmental Protection Agency has periodically reviewed health effects due to PM_{10} exposure to revise PM_{10} ambient standards, and they recently reported that controlling for effect of gaseous co-pollutants through regression did not meaningfully affect short-term PM_{10} effect estimates in cardiovascular and respiratory morbidity and mortality (*45*).

In conclusion, this analysis reports evidence of significant increased risk of cardiovascular and respiratory mortality associated with short-term exposure to PM_{10} in different regions of Thailand. In addition, it utilized the BME framework to rigorously model the spatiotemporal distribution of PM_{10} across Thailand and provide an assessment of the short term exposure to PM_{10} for each reported death case. This analysis is considered to be the first multi-location case-crossover study investigating cardiovascular and respiratory cause-specific mortality.

Reference:

1. Analitis A, Katsouyanni K, Dimakopoulou K, Samoli E, Nikoloulopoulos AK, Petasakis Y, Touloumi G, Schwartz J, Anderson HR, Cambra K, Forastiere F, Zmirou D, Vonk JM, Clancy L, Kriz B, Bobvos J, Pekkanen J. Short-term effects of ambient particles on cardiovascular and respiratory mortality. Epidemiology 17:230-3(2006).

2. Dominici F, McDermott A, Daniels M, Zeger SL, Samet JM. Revised analyses of the National Morbidity, Mortality, and Air Pollution Study: mortality among residents of 90 cities. J Toxicol Environ Health A 68:1071-92(2005).

3. Hoek G. Daily Mortality and Air Pollution in The Netherlands. In: Revised Analyses of Time-Series Studies of Air Pollution and Health. Special Report. Boston:Health Effects Institute, 2003;133-142.

4. Villeneuve PJ, Burnett RT, Shi Y, Krewski D, Goldberg MS, Hertzman C, Chen Y, Brook J. A time-series study of air pollution, socioeconomic status, and mortality in Vancouver, Canada. J Expo Anal Environ Epidemiol 13:427-35(2003).

5. Ostro BD, Chestnut LG, Vichit-Vadakan N, Laixuthai A. The impact of particulate matter on daily mortality in Bangkok, Thailand. Journal of The Air & Waste Management Association 49:100-107(1999).

6. Vajanapoom N, Shy CM, Neas LM, Loomis D. Associations of particulate matter and daily mortality in Bangkok, Thailand. Southeast Asian J Trop Med Public Health 33:389-99(2002).

7. Christakos G, Serre ML. BME analysis of spatiotemporal particulate matter distributions in North Carolina. Atmospheric Environment 34:3393-3406(2000).

8. Serre ML, Christakos G, Lee S-J. Soft Data Space/Time Mapping of Coarse Particulate Matter Annual Arithmetic Average over the U.S. In: geoENV IV 2004.

9. Anderson HR, Atkinson RW, Peacock JL, Sweeting MJ, Marston L. Ambient particulate matter and health effects: publication bias in studies of short-term associations. Epidemiology 16:155-63(2005).

10. Bateson TF, Schwartz J. Control for seasonal variation and time trend in case-crossover studies of acute effects of environmental exposures. Epidemiology 10:539-44(1999).

11. Bateson TF, Schwartz J. Selection bias and confounding in case-crossover analyses of environmental time-series data. Epidemiology 12:654-61(2001).

12. Zanobetti A, Schwartz J. The effect of particulate air pollution on emergency admissions for myocardial infarction: a multicity case-crossover analysis. Environ Health Perspect 113:978-82(2005).

13. Lin M, Stieb DM, Chen Y. Coarse particulate matter and hospitalization for respiratory infections in children younger than 15 years in Toronto: a case-crossover analysis. Pediatrics 116:e235-40(2005).

14. Kunzli N, Schindler C. A call for reporting the relevant exposure term in air pollution case-crossover studies. J Epidemiol Community Health 59:527-30(2005).

15. Forastiere F, Stafoggia M, Picciotto S, Bellander T, D'Ippoliti D, Lanki T, von Klot S, Nyberg F, Paatero P, Peters A, Pekkanen J, Sunyer J, Perucci CA. A Case-crossover Analysis of Out-of-Hospital Coronary Deaths and Air pollution in Rome, Italy. Am J Respir Crit Care Med(2005).

16. Barnett AG, Williams GM, Schwartz J, Neller AH, Best TL, Petroeschevsky AL, Simpson RW. Air pollution and child respiratory health: a case-crossover study in Australia and New Zealand. Am J Respir Crit Care Med 171:1272-8(2005).

17. Schwartz J. Is the association of airborne particles with daily deaths confounded by gaseous air pollutants? An approach to control by matching. Environ Health Perspect 112:557-61(2004).

18. Schwartz J. The effects of particulate air pollution on daily deaths: a multi-city case crossover analysis. Occup Environ Med 61:956-61(2004).

19. Jaakkola JJ. Case-crossover design in air pollution epidemiology. Eur Respir J Suppl 40:81s-85s(2003).

20. Kleinbaum GK, Kupper LL, Muller KE, Nizam A. Applied regression analysis and other multivariable methods. Pacific Grove, CA:Duxbury Press, 1998.

21. Janes H, Sheppard L, Lumley T. Case-crossover analyses of air pollution exposure data: referent selection strategies and their implications for bias. Epidemiology 16:717-26(2005).

22. Navidi W. Bidirectional case-crossover designs for exposures with time trends. Biometrics 54:596-605(1998).

23. Greenland S. Confounding and exposure trends in case-crossover and case-time-control designs. Epidemiology 7:231-9(1996).

24. Janes H, Sheppard L, Lumley T. Overlap bias in the case-crossover design, with application to air pollution exposures. Stat Med 24:285-300(2005).

25. Lumley T, Levy D. Bias in the case-crossover design: implications for studies of air polltion. Environmetrics:689-704(2000).

26. Christakos G. Field Models in Earth Sciences. San Diego, CA:Academic Press, 1992.

27. Christakos G. Modern Spatiotemporal Geostatistics. New York, NY:Oxford University Press, 2000.

28. Christakos G, Bogaert P, Serre ML. Temporal GIS. New York, NY:Springer-Verlag, 2002.

29. Serre ML, Kolovos A, Christakos G, Modis K. An application of the holistochastic human exposure methodology to naturally occurring arsenic in Bangladesh drinking water. Risk Anal 23:515-28(2003).

30. Christakos G, Kolovos A. A study of the spatiotemporal health impacts of ozone exposure. J Expo Anal Environ Epidemiol 9:322-35(1999).

31. Christakos G, Serre ML. Spatiotemporal analysis of environmental exposure-health effect associations. J Expo Anal Environ Epidemiol 10:168-87(2000).

32. Ostro B, Broadwin R, Lipsett M. Coarse and fine particles and daily mortality in the Coachella Valley, California. In: Health Effects Institue, Special Report. Revised analyses of time-series studies of air pollution and health, 2003;199-204.

33. Ostro BD, Broadwin R, Lipsett MJ. Coarse and fine particles and daily mortality in the Coachella Valley, California: a follow-up study. J Expo Anal Environ Epidemiol 10:412-9(2000).

34. Mar TF, Norris GA, Koenig JQ, Larson TV. Associations between air pollution and mortality in Phoenix, 1995-1997. Environ Health Perspect 108:347-53(2000).

35. Moolgavkar SH. Air pollution and daily mortality in three U.S. counties. Environ Health Perspect 108:777-84(2000).

36. Health Effects Institue. Revised analyses of the National Morbidity, Mortality, and Air Pollution Study (NMMAPS), Part II. In: Revised Analyses of Time-Seires Studies of Air Pollution and Health. Special Report. Boston:Health Effects Institute, 2003;9-72.

37. Dominici F, Daggett DA, McDermott A, Zeger SL, Samet JM. Shape of the expsure-response relaton and mortality displacement in the NMMAPS database. In: Revised Analyses of Time-Series Studies of Air Pollution and Health. Special Report. Boston:Health Effects Institute, 2003;91-96.

38. Daniels MJ, Dominici F, Zeger SL, Samet JM. The National Morbidity, Mortality, and Air Pollution Study. Part III: PM10 concentration-response curves and thresholds for the 20 largest US cities. Res Rep Health Eff Inst:1-21; discussion 23-30(2004).

39. Roberts S, Martin MA. Applying a moving total mortality count to the cities in the NMMAPS database to estimate the mortality effects of particulate matter air pollution. Occup Environ Med 63:193-7(2006).

40. Tsai FC, Smith KR, Vichit-Vadakan N, Ostro BD, Chestnut LG, Kungskulniti N. Indoor/outdoor PM10 and PM2.5 in Bangkok, Thailand. J Expo Anal Environ Epidemiol 10:15-26(2000).

41. Chen YS, Sheen PC, Chen ER, Liu YK, Wu TN, Yang CY. Effects of Asian dust storm events on daily mortality in Taipei, Taiwan. Environ Res 95:151-5(2004).

42. Wong TW, Tam WS, Yu TS, Wong AH. Associations between daily mortalities from respiratory and cardiovascular diseases and air pollution in Hong Kong, China. Occup Environ Med 59:30-5(2002).

43. Thai Pollution Control Department. State of Thailand's Pollution in Year 2002 (Thai version). Bangkok, Thailand: Ministry of Natural Resources and Environment, 2003.

44. Vinitketkumnuen U, Kalayanamitra K, Chewonarin T, Kamens R. Particulate matter, PM 10 & PM 2.5 levels, and airborne mutagenicity in Chiang Mai, Thailand. Mutation Research/Genetic Toxicology and Environmental Mutagenesis 519:121-131(2002).

45. US.EPA. Air Quality Criteria for Particulate Matter. Washington, DC:U.S. Environmental Protection Agency, 2004.

Table 3.1 The meta-analysis results of odds ratios and 95% CI for associations between PM_{10} and cardiovascular and respiratory mortality in selected regions

Areas, lag	Cardiovascular mortality		Respiratory mortality	
Bangkok vicinity*				
0	1.0003	(0.9995, 1.0011)	0.9999	(0.9988, 1.0010)
1	1.0009	(1.0001, 1.0017)	1.0001	(0.9990, 1.0011)
2	1.0008	(1.0000, 1.0016)	1.0006	(0.9995, 1.0016)
3	1.0000	(0.9992, 1.0008)	1.0012	(1.0002, 1.0023)
4	0.9995	(0.9987, 1.0003)	1.0012	(1.0001, 1.0022)
5	0.9995	(0.9987, 1.0003)	1.0011	(1.0001, 1.0022)
6	0.9997	(0.9989, 1.0005)	1.0005	(0.9994, 1.0015)
7	0.9999	(0.9991, 1.0007)	1.0003	(0.9993, 1.0014)
8	0.9995	(0.9987, 1.0002)	0.9997	(0.9987, 1.0008)
9	0.9996	(0.9988, 1.0004)	1.0000	(0.9990, 1.0010)
10	0.9998	(0.9990, 1.0006)	0.9997	(0.9986, 1.0007)
Central*				
0	1.0002	(0.9995, 1.0010)	0.9997	(0.9987, 1.0007)
1	1.0008	(1.0001, 1.0016)	0.9998	(0.9988, 1.0008)
2	1.0008	(1.0000, 1.0015)	1.0003	(0.9993, 1.0014)
3	0.9998	(0.9991, 1.0006)	1.0009	(0.9999, 1.0020)
4	0.9994	(0.9986, 1.0001)	1.0010	(1.0000, 1.0021)
5	0.9996	(0.9988, 1.0003)	1.0009	(0.9999, 1.0019)
6	0.9998	(0.9990, 1.0006)	1.0003	(0.9993, 1.0013)
7	0.9999	(0.9992, 1.0007)	1.0003	(0.9993, 1.0013)
8	0.9995	(0.9988, 1.0003)	0.9998	(0.9988, 1.0008)
9	0.9996	(0.9989, 1.0004)	1.0001	(0.9991, 1.0010)
10	0.9999	(0.9992, 1.0007)	0.9997	(0.9988, 1.0007)
North*				
0	1.0004	(0.9973, 1.0034)	1.0008	(0.9973, 1.0044)
1	1.0011	(0.9980, 1.0041)	1.0022	(0.9986, 1.0057)
2	1.0015	(0.9985, 1.0046)	1.0029	(0.9994, 1.0064)
3	1.0006	(0.9976, 1.0037)	1.0017	(0.9982, 1.0053)
4	0.9985	(0.9955, 1.0015)	1.0007	(0.9973, 1.0042)
5	0.9995	(0.9965, 1.0026)	0.9996	(0.9961, 1.0030)
6	0.9982	(0.9951, 1.0012)	1.0010	(0.9975, 1.0045)
7	0.9995	(0.9965, 1.0025)	0.9997	(0.9962, 1.0032)
8	1.0001	(0.9972, 1.0030)	0.9989	(0.9956, 1.0023)
9	1.0002	(0.9974, 1.0031)	0.9974	(0.9941, 1.0007)
10	0.9992	(0.9965, 1.0020)	0.9981	(0.9949, 1.0013)
Country[$]				
0	1.0002	(0.9997, 1.0008)	0.9998	(0.9991, 1.0006)
1	1.0009	(1.0003, 1.0014)	1.0000	(0.9993, 1.0007)
2	1.0008	(1.0003, 1.0013)	1.0005	(0.9997, 1.0012)
3	0.9999	(0.9994, 1.0004)	1.0005	(0.9990, 1.0020)
4	0.9994	(0.9989, 0.9999)	1.0003	(0.9987, 1.0020)
5	0.9995	(0.9990, 1.0001)	1.0004	(0.9990, 1.0018)
6	0.9997	(0.9991, 1.0002)	1.0004	(0.9997, 1.0011)
7	0.9999	(0.9994, 1.0004)	0.9996	(0.9978, 1.0013)
8	0.9995	(0.9990, 1.0001)	0.9997	(0.9990, 1.0004)
9	0.9999	(0.9984, 1.0014)	0.9993	(0.9977, 1.0009)
10	1.0003	(0.9985, 1.0021)	0.9995	(0.9981, 1.0009)

*Pooled region-specific results based on meta-analyses using a fix-effect model

[$]Pooled country results based on using either a fix-effect model or a random-effect model depending on heterogeneity test result for each lag.

Table 3.2 Percent change in daily cardiovascular mortality and 95% CIs per 10 μg/m^3 increment in PM_{10}

Regions	Lag (days)	Percent Increased Risk (per 10 μg/m^3)	95% CI
Bangkok	1	0.92	(0.12,1.73)
Central	1	0.84	(0.07,1.62)
North	2	1.52	(-1.51,4.65)
Thailand	1	0.85	(0.31,1.40)

Table 3.3 Percent change in daily respiratory mortality and 95% CIs per 10 μg/m^3 increment in PM_{10}

Regions	Lag (days)	Percent Increased Risk (per 10 μg/m^3)	95% CI
Bangkok	3	1.25	(0.17,2.35)
Central	4	1.02	(-0.01,2.07)
North	2	2.92	(-0.65,6.62)
Thailand	3	0.53	(-0.95,2.03)

Table 3.4 Number of PM_{10} monitors, emission sources, death counts, and area size by region

Regions	PM_{10} stations	Emissions	Cardio. deaths	Resp. deaths	Area (sq.mile)
Bangkok	21	heavy traffic, industry, construction	36,941(27%)	21,155(25%)	2,990(2%)
Central	20	traffic, industry, biomass burning	21,797(16%)	11,561(14%)	32,220(16%)
North	6	biomass burning, traffic, forest fire	30,346(22%)	23,039(28%)	66,890(33%)
South	3	natural sea spray, high removal rate	13,555(10%)	8,082(10%)	30,320(15%)
Northeast	2	natural windblown dust, residence	34,380(25%)	19,097(23%)	67,590(34%)

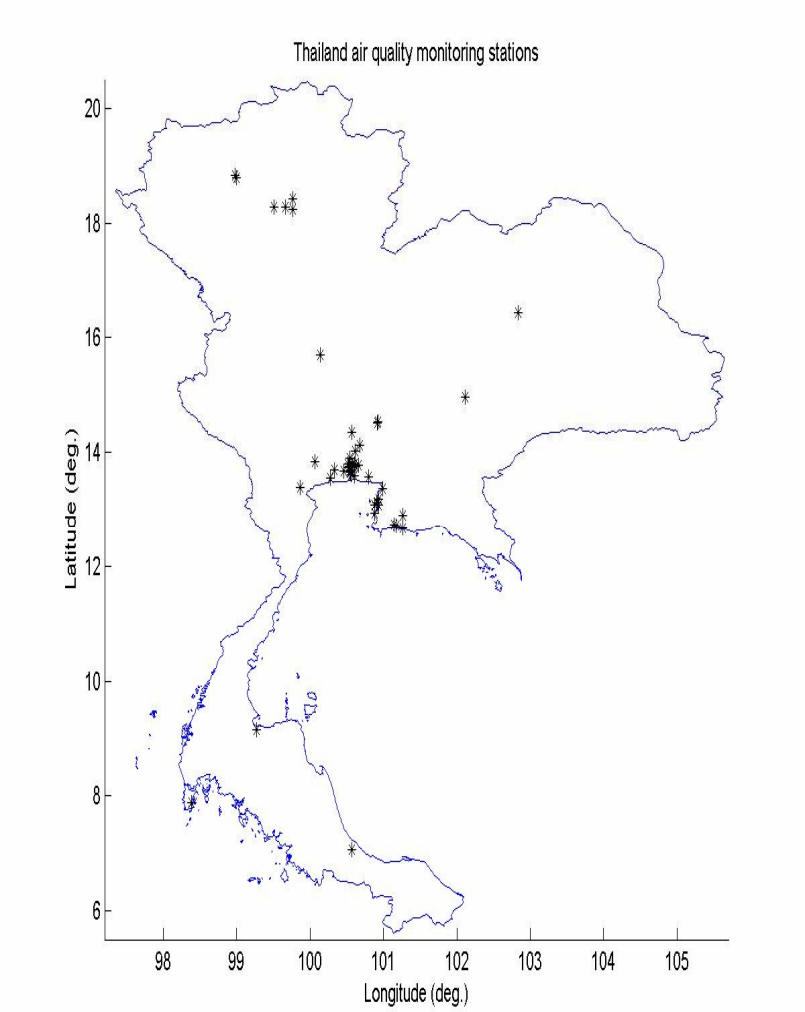

Figure 3.1 Locations of 51 air quality monitoring stations in Thailand

(a) (b) (c)

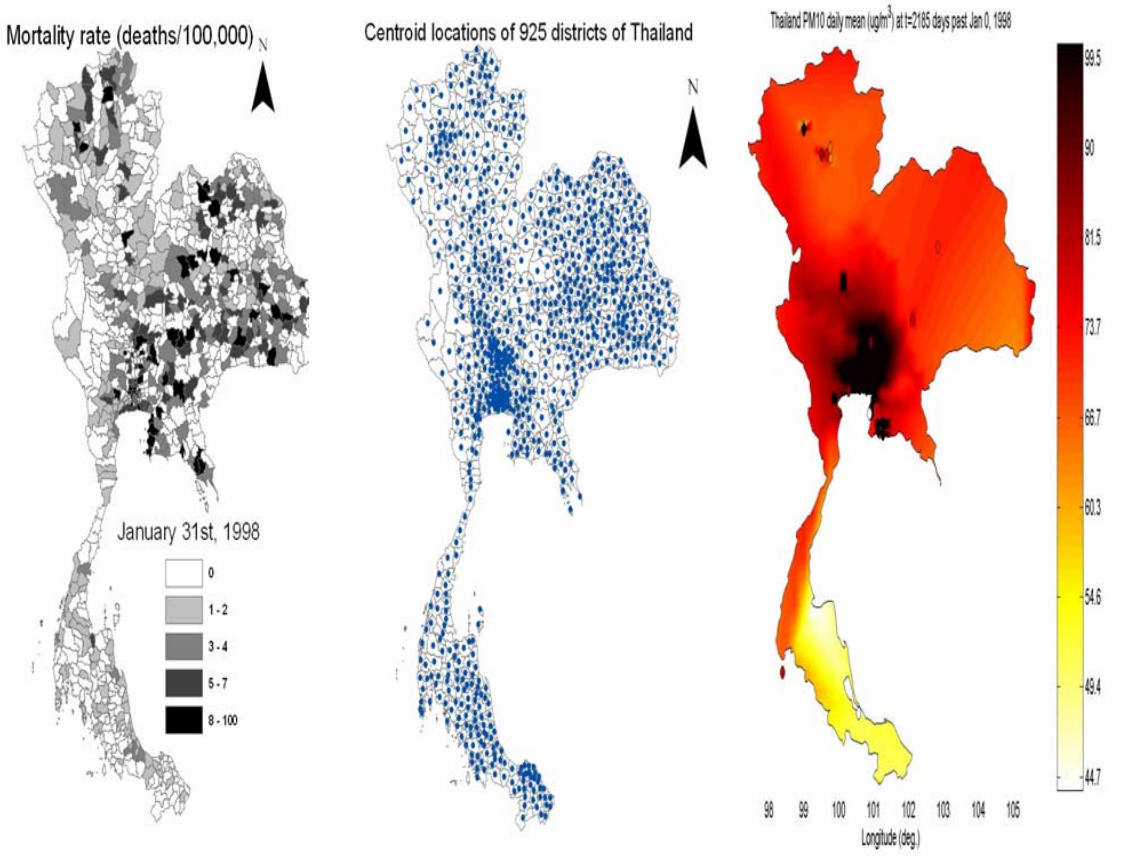

Figure 3.2 Maps of Thailand showing (a) the mortality rate for each of 925 primary districts on January 31, 1998, (b) the centroid of each of these districts, and (c) the PM_{10} map obtained on the basis of the BME estimate of daily concentration at each district centroid

(a)

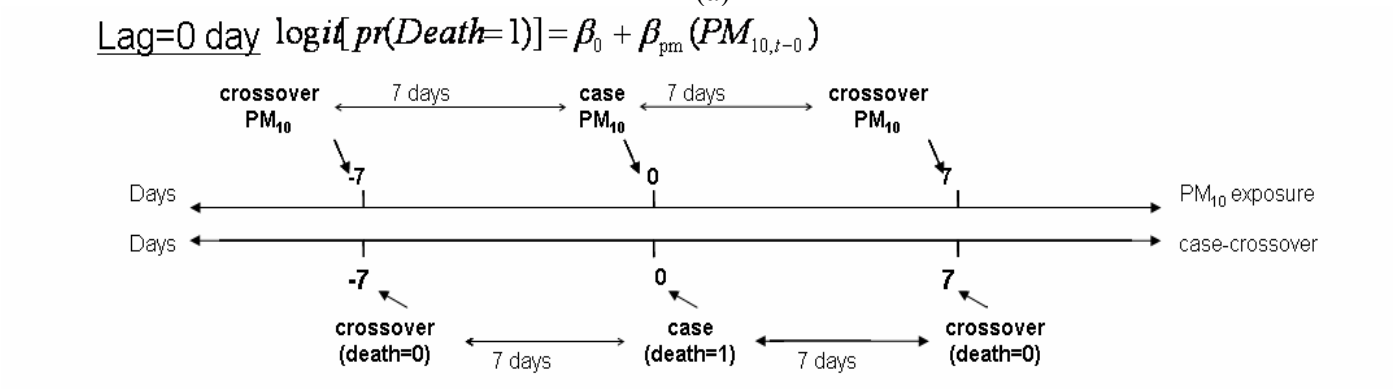

a) Lag 0 exposure, case and referent were assigned same day PM_{10} concentration

(b)

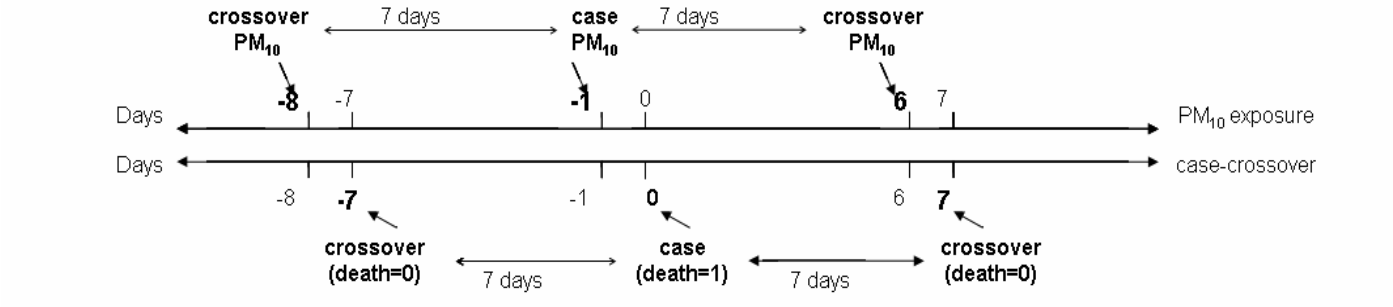

b) Lag 1 exposure, case and referent were assigned previous day PM_{10} concentration

Figure 3.3 Depiction of the 7 day symmetric bidirectional scheme to obtain the crossover referent days used as controls for a death case for (a) a 0-day, and (b) a 1 day lag between exposure (daily average PM_{10} concentration) and effect (death case).

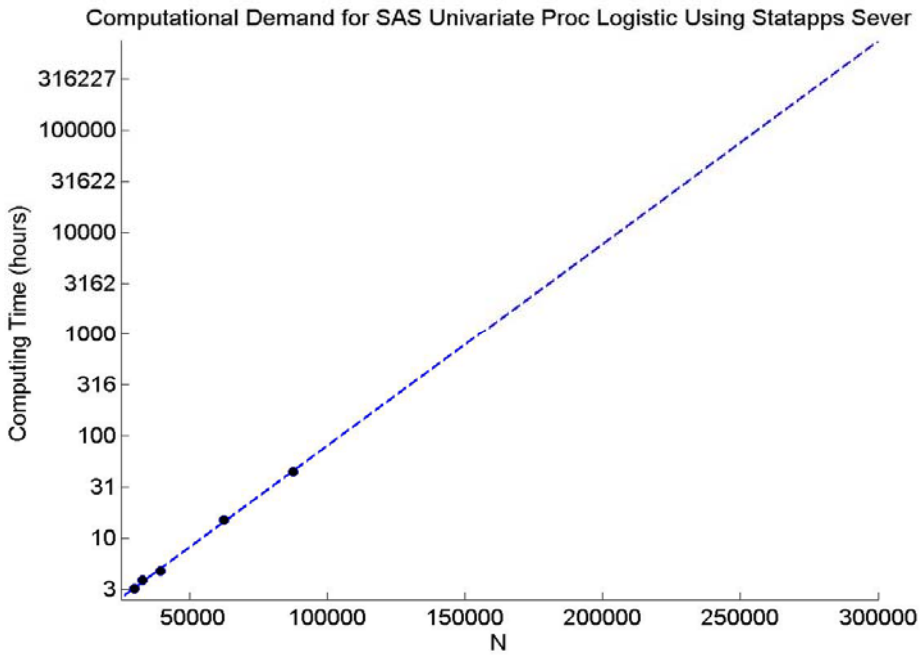

Figure 3.4 Computing time *T* on the UNC *STATapps* computer system when solving the univariate conditional logistic model for *N* observations using the *Logistic* procedure in SAS®.

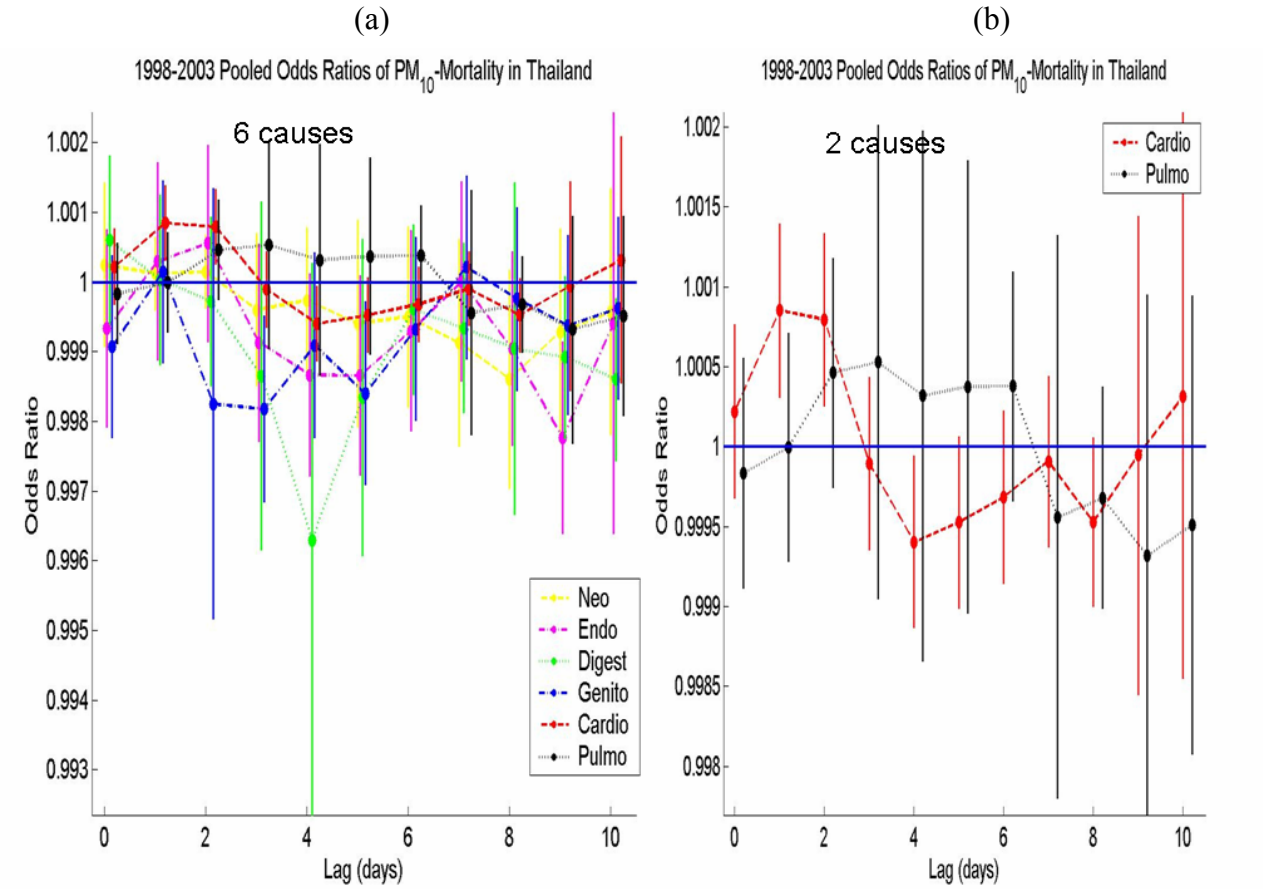

Figure 3.5 Graphs of the country wide pooled estimates of odds ratios (i.e. ratio of the odds of death for a 1μg/m^3 increase in daily PM_{10} in Thailand) showing results for (a) all 6 causes of death, and for (b) only 2 selected causes of death.

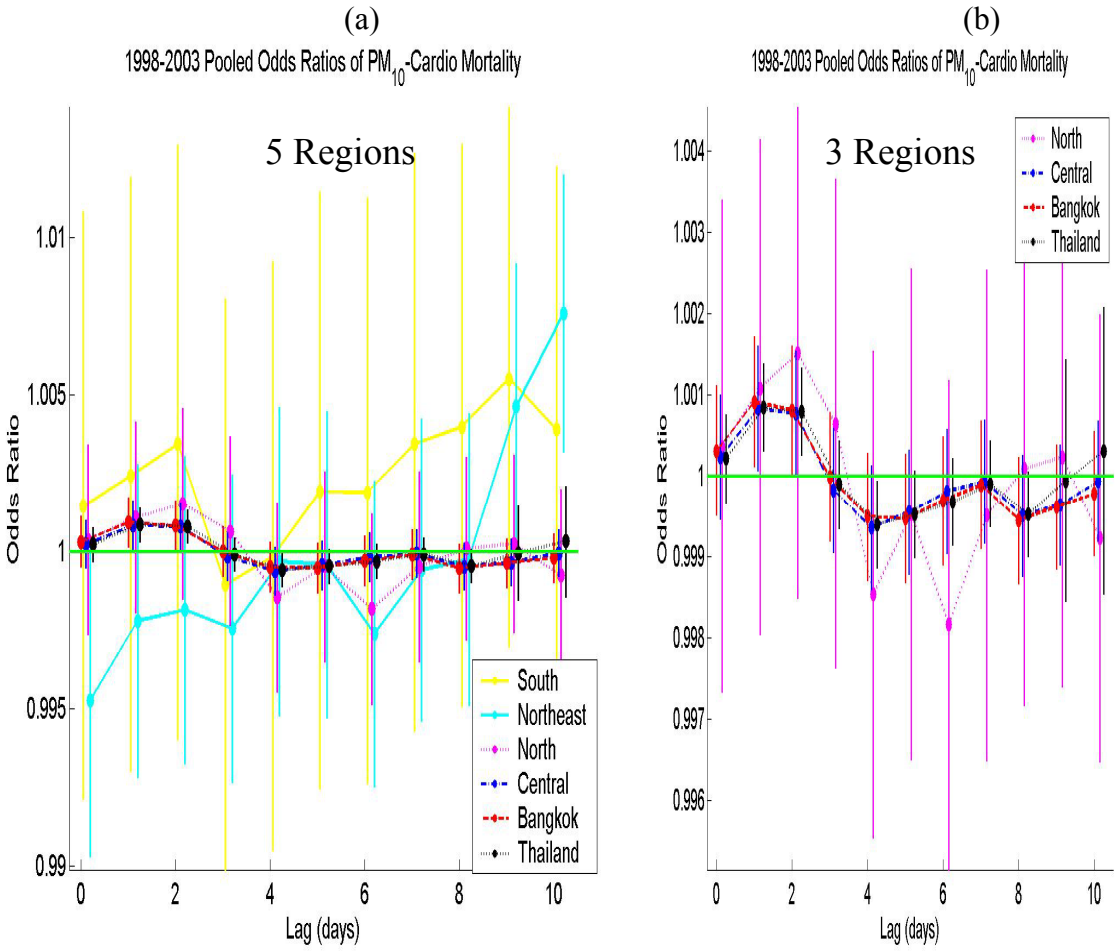

Figure 3.6 Graphs of the regional and country-wide pooled estimates of the odds ratios for cardiovascular mortality showing results for (a) all 5 regions, and (b) only 3 selected regions.

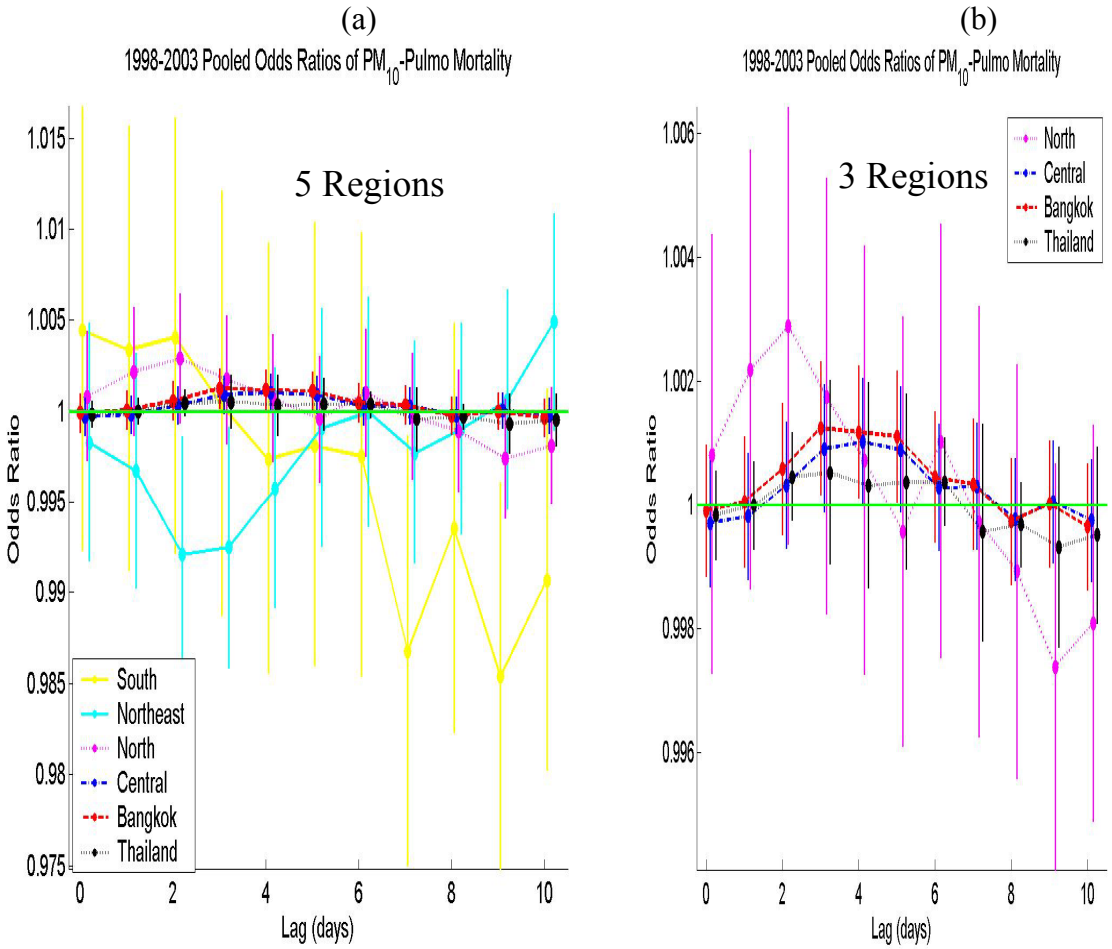

Figure 3.7 Graphs of the regional and country-wide pooled estimates of the odds ratios for pulmonary mortality showing results for (a) all 5 regions, and (b) only 3 selected regions.

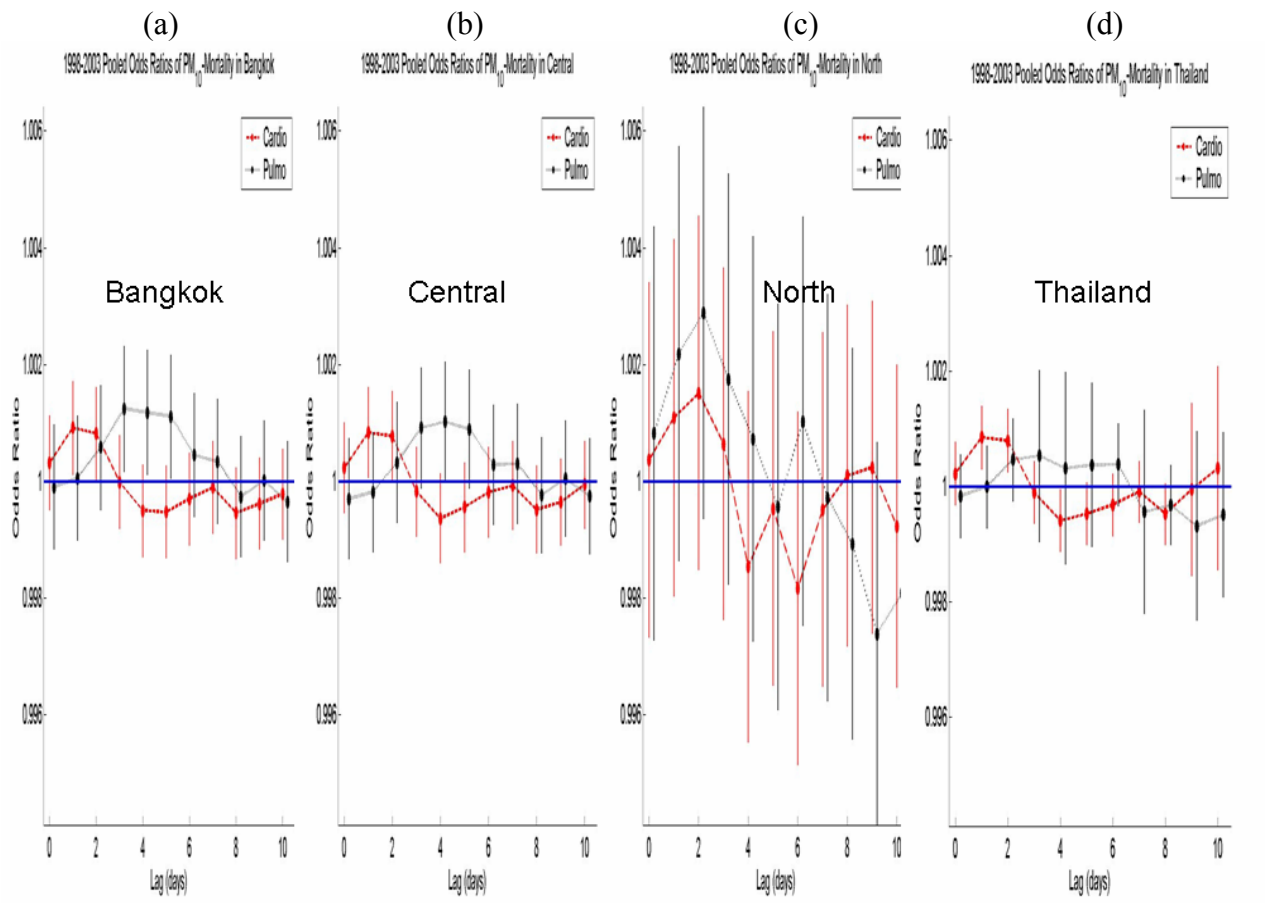

Figure 3.8 Graphs of the odds ratios for cardiovascular and pulmonary mortality showing pooled estimates obtained for (a) Bangkok, (b) the central region, (c) the Northern region, and (d) for Thailand.

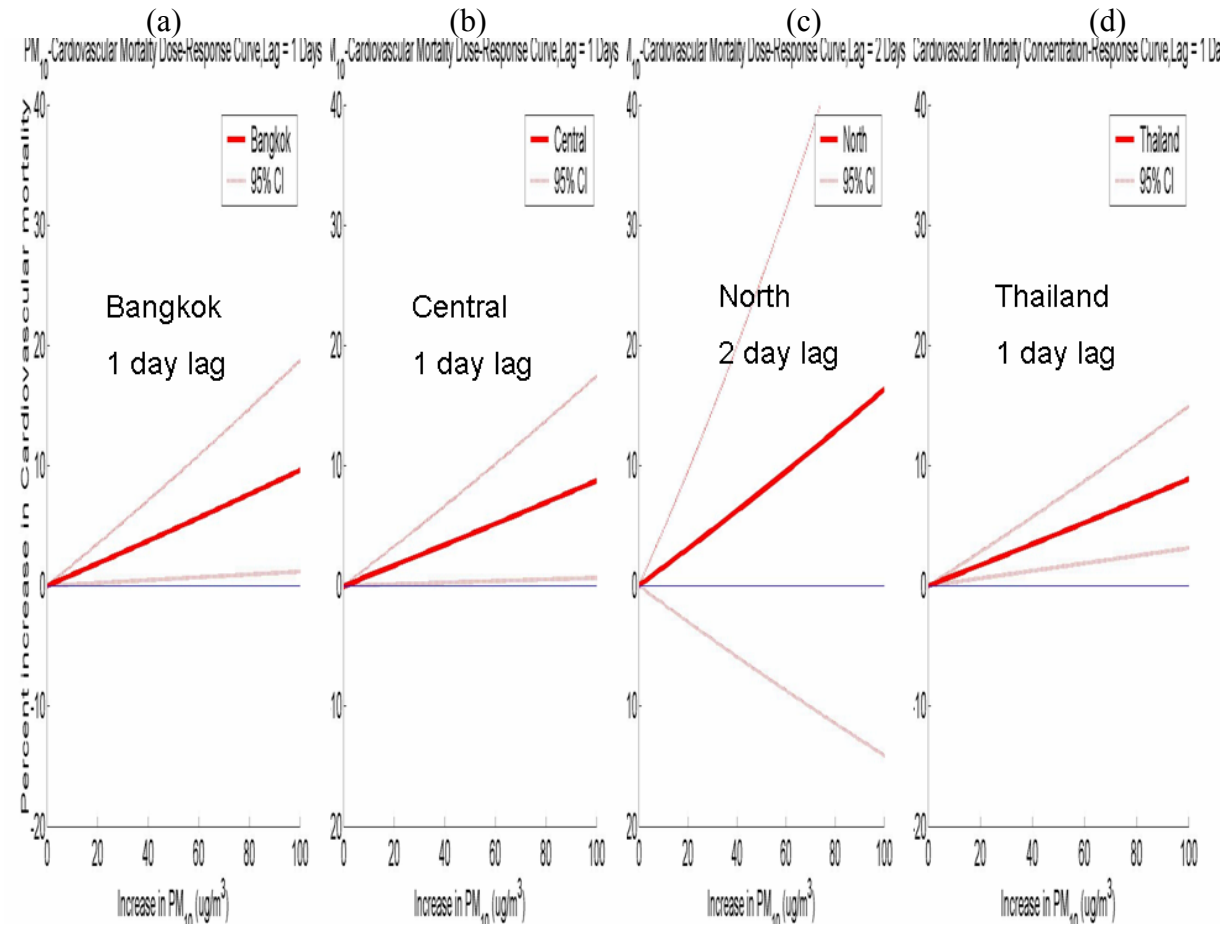

Figure 3.9 Percent change in cardiovascular mortality as a function of increase in PM_{10} ($\mu g/m^3$) in (a) Bangkok, (b) the central region, (c) the Northern region, and (d) for Thailand.

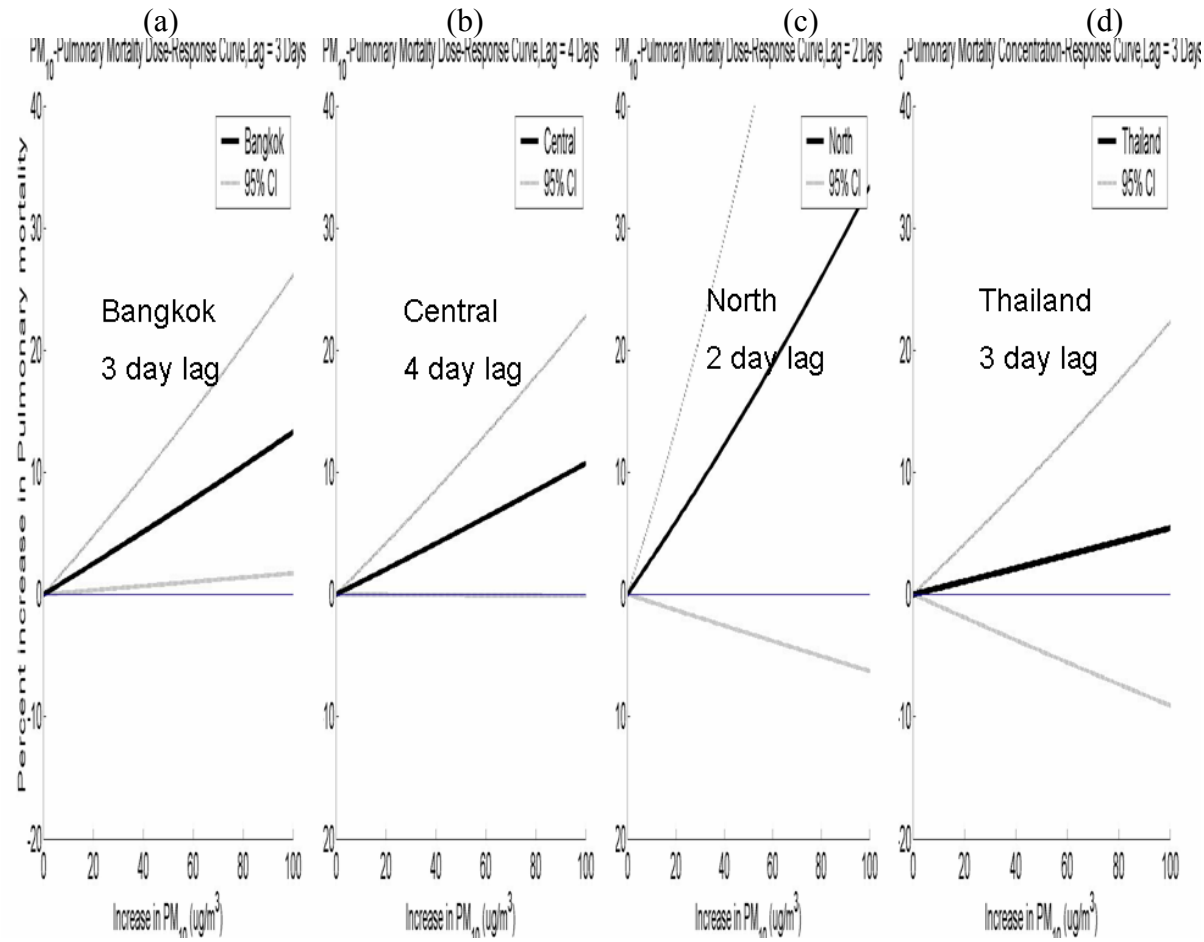

Figure 3.10 Percent change in pulmonary mortality as a function of increase in PM_{10} ($\mu g/m^3$) in (a) Bangkok, (b) the central region, (c) the Northern region, and (d) for Thailand.

IV. MANUSCRIPT 3: A Comprehensive Space/Time Assessment of Cardiovascular and Respiratory Mortality Risk associated with Short Term Exposure to PM_{10} in Thailand

Abstract

A comprehensive space/time framework for cardiovascular and respiratory mortality risk assessment is proposed for use in different regions of Thailand by adapting the holistochastic human exposure approach presented in previous works. This framework integrates the BME estimation method as a central component to rigorously process the available knowledge base about PM_{10}. Using the BME estimation method and other information processing rules, the proposed framework incorporates the various kinds of knowledge available for risk assessment, including physical knowledge of the PM_{10} field, epidemiological relationships, and demographics. Each step of the proposed framework generates maps that allow a better assessment of the excess mortality risk induced by increases in daily PM_{10} in defined space/time domains, providing crucial information for public health interactions in Thailand. The applied holistochastic approach also appropriately quantifies and integrates the uncertainties in each step of the analysis. These accumulated uncertainties yield the best-case and the worst-case scenarios corresponding to predicted lower and upper bounds of total count of premature cardiovascular and respiratory mortality across Thailand in 2004. Uncertainty quantification using the elasticity approach demonstrates how to improve future mortality risk assessments at regional scale.

Introduction

The rapid growth of population and industrial activities in all regions of Thailand and the ensuing heavy traffic congestion have resulted in a polluted environment and health problems. Particulate matter from combustion during traffic jam and biomass burning in open space is discharged into the air stream along traffic roads and agricultural fields and then disperses to densely populated residential areas. Poor air quality due to suspended particulate matter has been linked to various cardiopulmonary health problems (*1-4*) as well as premature deaths (*5-8*). Exposure to air pollution in Bangkok has been estimated to cause thousands of premature death and several million cases of sickness every year (*9*). A previous study in Bangkok showed that the observed associations between daily PM_{10} and daily mortality were stronger for respiratory mortality than for cardiovascular mortality (*10*). An increase of about 3-6% in respiratory mortality and 1-2% in cardiovascular mortality were reported when PM_{10} levels in Bangkok were raised by 10 $\mu g/m^3$ (*11*). However the assessment of the excess number of cardiovascular and respiratory death counts due to short-term exposure to PM_{10} over different regions of Thailand has never been done.

In this analysis, cardiovascular and respiratory mortality risk associated with population exposure to PM_{10} is evaluated in defined space/time domains. The best-case and worst-case scenarios of the total cardiovascular and respiratory deaths caused by exposure to PM_{10} in Thailand in 2004 are presented. The best-case and worst-case scenarios are directly related to the lower and upper bounds, respectively, of the confidence interval for the estimated total death count. Such interval provides vital information about the uncertainty associated with the mortality risk assessment, which is

critical for public health policy and decision makers. Hence the framework proposed attempts to propagate the uncertainty associated in the steps of the analysis leading to the risk assessment. The proposed space/time risk assessment approach presented in Figure 4.1 is an adaptation of the so-called holistochastic framework (*12*) used to predict population-level bladder cancer risk in Bangladesh due to exposure to arsenic in the drinking water (*13*). The framework consists of three main steps, which are: 1) to use the space/time BME mapping method to obtain exposure maps of PM_{10} in Thailand; 2) to apply the epidemiological PM_{10}-mortality relationship developed from the case-crossover analysis from Chapter 3 to estimate the mortality risk increase; and 3) to incorporate demographic information to obtain space/time maps of the expected mortality density loss and related population health impact measures.

The two main research questions addressed in this analysis are how many premature cardiovascular and respiratory deaths are likely to result from increase in daily PM_{10} across Thailand in 2004; and what are the best-case and worst-case scenarios of the effect of daily PM_{10} exposure which provides a confidence interval for total cardiovascular and respiratory death count describing the uncertainty associated with risk assessment. The objective for this study is to assess the cardiovascular and respiratory mortality risk resulting from increase in daily PM_{10} across Thailand in 2004 by applying the holistochastic population exposure framework and BME mapping method.

Methods

PM_{10} data

The PM_{10} data used in this study consisted of all the daily PM_{10} concentration collected in 2004 by the Thai Pollution Control Department (PCD). As described in Chapter 2 and 3, the PCD maintains a nation wide air monitoring network comprising 51 stations with equipment using the PM_{10} automatic beta-gauge method with a detection limit of 2 $\mu g/m^3$ and a relative error of 8%. The monitoring stations maintained by the PCD are located on curbsides of major roads and in residential areas. Most of these stations are clustered around the capital city, Bangkok, while few additional stations are located in the other four regions of Thailand. We obtained from the PCD approximately 300 thousands measurements of hourly PM_{10} concentration collected at these stations during 2004, and we averaged these values every 24 hours to obtain approximately 13 thousands measurements of daily PM_{10} concentration across Thailand during 2004.

Space/time risk assessment framework

In step 1 of the space/time risk assessment framework, the BME estimation method is used to process the PM_{10} monitoring data available for 2004, and construct maps showing the spatiotemporal distribution of daily average PM_{10} concentration across Thailand and for each day of 2004. The BME estimation method has been used in previous studies to model the spatiotemporal distribution of several environmental contaminants, including subsurface arsenic, surface water quality parameters, ambient ozone, and PM_{10} (*13-16*). The BME approach starts by modeling the mean trend and space/time covariance of the PM_{10} Space/Time Random Field (S/TRF) describing the consistent patterns and systematic dependencies of the distribution of PM_{10} across space and time. These mean trend and covariance models constitute the general knowledge base G-KB processed at

the prior stage of the BME analysis using the epistemic knowledge processing rule of entropy maximization. Then, at the meta-prior stage of the BME analysis, the site specific data of daily PM_{10} measurements collected in 2004 and the associated measurement errors are assessed and properly modeled by means of hard and soft data, and log-transformed if needed. For example high outlier measurements may be deemed uncertain and therefore represented by means of probabilistic soft data with Gaussian distributions having a high measurement error variance. These hard and soft data constitute the site specific knowledge base, S-KB, which is processed together with G-KB at the integration stage of the BME analysis using an operational Bayesian conditionalization knowledge processing rule, to obtain the estimated daily PM_{10} exposure level $E(\boldsymbol{p}_k)$ at estimation point $\boldsymbol{p}_k$ i.e. we have

$$(G,S) \rightarrow E(\boldsymbol{p}_k) \qquad (1)$$

where $\boldsymbol{p}_k = (\boldsymbol{s},t)$ is the space/time location for any administrative district in Thailand and any day of interest in 2004.

In step 2 of the proposed space/time risk assessment framework we will use the epidemiological PM_{10}-mortality relationships developed in the case-crossover analysis presented in Chapter 3 of the association between PM_{10} and cardiovascular and respiratory mortality for different regions of Thailand. As explained earlier, this analysis provided regional estimates and corresponding CI for the coefficient β_{PM} of the logistic regression equation Logit $\left(Prob.[Death] \right) = \beta_0 + \beta_{PM}\, PM_{10}.$, it follows immediately from this logistic regression equation that the predicted percent change in mortality at

some estimation point $\boldsymbol{p}_k$ caused by a $\Delta PM_{10}(\boldsymbol{p}_k)$ increase of daily PM_{10} above background level can be estimated using the following equation:

$$\text{Percent change in mortality at } \boldsymbol{p}_k = 100\left[\exp(\beta_{PM}\Delta PM_{10}(\boldsymbol{p}_k))-1\right] \qquad (2)$$

where $\Delta PM_{10}(\boldsymbol{p}_k)$ can be obtained by subtracting the regional background PM_{10} concentration from the BME maps of daily PM_{10} concentration obtained in step 1. Causality of the association between PM_{10} and cardiovascular and respiratory mortality is supported by the literature of possible biological mechanisms suggesting that short term exposure to PM_{10} is a possible causal factor for increased cardiopulmonary mortality in the following one to four days. Therefore the use of the PM_{10}-mortality relationships obtained from epidemiologic studies analyzing the strength of the PM_{10}-mortality association is appropriate in risk assessment to estimate the health impact of PM_{10} pollution. Alternative approaches to obtain this relationship would be by applying a toxicokinetic modeling approach, or to use dose-response relationship models obtained in other studies. Hence we generalize the relationship by denoting it as $H = g_H(E)$, where the *health* effect H obtained through Equation (2) is the expected percent change in mortality resulting from an *exposure E* corresponding the increase of daily PM_{10} above background level, and $g_H(.)$ is an exposure-health response relationship. In the space/time domain, we write this step as:

$$E(\boldsymbol{p}_k) \xrightarrow{gH(.)} H(\boldsymbol{p}_k) \qquad (3)$$

Furthermore, in the proposed space/time risk assessment framework, we propagate the uncertainty coming both from the exposure field E as well as the exposure-health response relationship $g_H(.)$ in order to assess the uncertainty associated with the resulting health risk estimate H. For example the uncertainty could be propagated using a probabilistic approach. In this work, the uncertainty in the exposure field E is expressed in terms of the variance σ_E^2 of the BME posterior PDF for PM_{10} obtained in step 1, while the uncertainty in the relationship $g_H(.)$ is encapsulated by the estimation variance of the regression coefficient $\beta_{PM.}$.

In step 3 of the proposed space/time risk assessment framework, we assess the expected mortality density loss L (deaths per mile^2) resulting from the population exposure to PM_{10}. This step integrates demographic information with the mortality risk increase predicted in step 2. Such mortality risk density are simply calculated as a product of the predicted percent change in mortality, the baseline daily mortality rate, and daily interpolated population density. In the space/time domain we write this step of the analysis as:

$$H(\boldsymbol{p}_k) \xrightarrow{gL(.)} L(\boldsymbol{p}_k) \tag{4}$$

where $gL(.)$ is a demographic transfer function, and $L(\boldsymbol{p}_k)$ is the resulting mortality density loss at point $\boldsymbol{p}_k$. The propagation of uncertainties will lead to the estimation of lower and upper bounds for the mortality density field $L(\boldsymbol{p}_k)$.

Results and Discussion

PM_{10} exposure mapping

We used the BME mapping framework to assess the daily fluctuating PM_{10} levels that Thai people were exposed to in 2004. The PM_{10} data were found to be log-normally distributed, so we carried out the BME analysis on the log-transformed PM_{10} data. The exploratory analysis detected the presence of a non-homogeneous/non stationary mean trend in the log-PM_{10} data, so we modeled this mean trend and removed it from the log-PM_{10} data to obtain mean-trend removed log-PM_{10} data that were modeled as a homogeneous/stationary residual space/time random field. We then modeled the covariance of this residual field, which was processed in the BME analysis together with the log-transformed mean trend removed hard and soft PM_{10} data to obtain BME estimates of the residual field. By adding back the mean trend model and back log-transforming, we obtained the BME estimate and association estimation variance of PM_{10} at the centroid of the 925 primary districts making up Thailand for each day in 2004.

We obtained the ΔPM_{10} increase of daily PM_{10} above background by subtracting from the BME estimate of PM_{10} a background assumed equivalent to the 5^{th} percentile of monitoring data collected in each region during 1998-2003. The regional background levels thus obtained were 3.02 $\mu g/m^3$ in Bangkok and the central region, 7.42 $\mu g/m^3$ in the Northern region, 12.33 $\mu g/m^3$ in the Southern region, and 7.65 $\mu g/m^3$ in the Northeastern region. We also assumed that the uncertainty of the background level was small enough so that the uncertainty associated with the ΔPM_{10} increase of daily PM_{10} above background was the same as that of the BME estimate of PM_{10}.

We show in Fig. 4.2a the map of ΔPM_{10} obtained for day 286 in 2004 (September 13th, 2004). This day provides result of the typical spatial distribution across Thailand of the increase in PM_{10} above background. For the district locations with negative increases in PM_{10} (i.e. for districts with a BME estimate of PM_{10} calculated to be on day 286 below the 5th percentile of the monitoring data collected during 1998-2003 in that district's region) no risk in cardiovascular and respiratory mortality is associated with short term exposure to PM_{10} that day, and we therefore assign a zero value to ΔPM_{10}. As can be seen in Fig. 4.2a, the graduated scale for ΔPM_{10} on day 286 is truncated at 62 $\mu g/m^3$ to make the map more readable, however ΔPM_{10} reaches a maximum of 88 $\mu g/m^3$ at the most polluted district on that day, and the maximum of ΔPM_{10} obtained across all districts of Thailand throughout 2004 is 255 $\mu g/m^3$. For each map of estimated ΔPM_{10}, the BME analysis provides the map of the associated uncertainty as characterized by the BME posterior variance (σ_E^2), which provides an assessment of the mapping uncertainty due to the natural space/time variability of the air pollutant, the sparse nature of the collected monitoring data, and the uncertainty associated with the measurement error and outliers in the data. This uncertainty is taken into account in the next step of the risk assessment framework when predicting the excess mortality risk resulting from exposure to PM_{10}. The standard deviation (σ_E) is smaller at districts closer to monitoring sites and larger at locations away from these sites.

We show in Fig. 4.2b the map of the relative error σ_E/E corresponding to the ratio of the standard deviation σ_E divided by the BME estimate of PM_{10}. Say that this map is very useful as it captures the environmental uncertainty in that it quantifies our lack of knowledge of the true environmental exposure to PM10. High environmental uncertainty

is found in the south area and low environmental uncertainty is observed in Bangkok and central areas where the monitoring sites are clustered.

Health risk mapping of cardiovascular and respiratory mortality

After we obtaining the ΔPM_{10} increase in PM_{10} above background and the associated relative error σ_E/E describing environmental uncertainty, in step 2 we made use of the epidemiologic knowledge from Chapter 3 to determine the cardiovascular and mortality risk increase at all space/time district points $\boldsymbol{p}_k$ in 2004. The percent change in mortality due to increase in PM_{10} was estimated using Equation (2). However the β_{PM} estimates for the Southern and Northeastern region as previously reported in Chapter 3 are not quite acceptable for risk assessment because of their high uncertainty due to the lack of sufficient monitoring stations to properly assess the strength of the PM_{10}-mortality associations in these regions. Therefore we propose to use the pooled β_{PM} country estimates as a substitution for the regional β_{PM} estimates in these two regions. Although the β_{PM} estimates of regional PM_{10} effects in Bangkok and the central and Northern regions suggest stronger association with respiratory mortality than cardiovascular mortality, the country pooled effects reported in Chapter 3 show the reverse, which is undesirable. To improve the β_{PM} pooled country estimate for respiratory mortality, we re-run its meta-analysis by pooling the β_{PM} obtained in each region at the lag corresponding to the highest strength of PM_{10}-mortality association. This lead to pooling the regional β_{PM} obtained at a lag of 0 day instead of a lag of 3 days in the Southern region and Northeastern regions together with the regional β_{PM} in other regions to yield a country pooled estimate for β_{PM} of 0.00085 (instead of the 0.00053 value obtained in Chapter 3),

which was then substituted as the regional estimate of β_{PM} for respiratory mortality in the Southern and Northeastern regions. The regional estimates of β_{PM} summarized in Table 4.1 include this re-analyzed value for pulmonary mortality.

Because of the small magnitude in the regional β_{PM} values, Eq. (2) for the percent change in mortality is quasi linear in the range of PM_{10} concentration observed in Thailand. Thus a good approximation for the health effect relationship is provided by the following linear relationship

$$H(\boldsymbol{p}_k) = B\, E(\boldsymbol{p}_k), \tag{5}$$

where the health effect $H(\boldsymbol{p}_k)$ is the estimated mortality increase at district location $\boldsymbol{p}_k$, B is a regional linear coefficient corresponding to the β_{PM} logistic regression coefficient listed in Table 4.1 and expressed in the proper unit (e.g. increased fraction of mortality per an increase of 1 $\mu g/m^3$ in PM_{10}), and $E(\boldsymbol{p}_k)$ is equivalent to ΔPM_{10} at space/time point $\boldsymbol{p}_k$. To propagate uncertainties in B and E through the estimated H, we assumed that B and E were normally distributed with means, m_B and m_E, respectively, and variances σ_B^2 and σ_E^2, respectively, i.e. $E \sim N(m_E, \sigma_E^2)$ and $B \sim N(m_B, \sigma_B^2)$. We know that for any random variables such as B and E their covariance is defined as $\mathrm{cov}(B,E) = \overline{(B - m_B)(E - m_E)} = \overline{BE} - m_B m_E$. From this relationship, we obtain $\overline{BE} = \mathrm{Cov}(B,E) + m_B m_E$. Therefore the mean of $H=BE$ can be obtained by the following equation:

$$m_H = m_B m_E + \mathrm{cov}(B,E). \qquad (6)$$

We also know that the variance of *H* can be written as:

$$\sigma_H^2 = \overline{(H-m_H)^2} = \overline{H^2 - 2Hm_H + m_H^2} = \overline{H^2} - 2\overline{H}m_H + m_H^2 = \overline{H^2} - 2m_H m_H + m_H^2 \qquad (7)$$

which can be reduced to

$$\sigma_H^2 = \overline{H^2} - m_H^2 = \overline{B^2E^2} - m_H^2. \qquad (8)$$

In order to simplify further these equations, we need to consider the independence between the mortality slope *B* obtained in the epidemiologic study, and the exposure *E*. Since the mortality slope *B* was obtained from an epidemiologic study performed using only PM_{10} and mortality data from 1998-2003, and the exposure field *E* is obtained using a discontiguous dataset consisting in the PM_{10} collected only in 2004, it is reasonable to assume that *B* and *E* are independent. As a result we have cov(B, E) = 0, and therefore Equation (6) reduces to

$$m_H = m_B m_E. \qquad (9)$$

Furthermore independence of *B* and *E* means that $\overline{B^2E^2} = \overline{B^2}\,\overline{E^2}$, and as a result Equation (8) becomes:

$$\sigma_{\mathrm{H}}^{\ 2} = \overline{\mathrm{B}^2}\,\overline{\mathrm{E}^2} - \mathrm{m}_{\mathrm{H}}^{\ 2} = (\sigma_{\mathrm{B}}^{\ 2} + \mathrm{m}_{\mathrm{B}}^{\ 2})(\sigma_{\mathrm{E}}^{\ 2} + \mathrm{m}_{\mathrm{E}}^{\ 2}) - \mathrm{m}_{\mathrm{B}}^{\ 2}\,\mathrm{m}_{\mathrm{E}}^{\ 2} \qquad (10)$$

which can further be simplified as

$$\sigma_{\mathrm{H}}^{\ 2} = \sigma_{\mathrm{B}}^{\ 2}\sigma_{\mathrm{E}}^{\ 2} + \sigma_{\mathrm{B}}^{\ 2}\mathrm{m}_{\mathrm{E}}^{\ 2} + \sigma_{\mathrm{E}}^{\ 2}\mathrm{m}_{\mathrm{B}}^{\ 2}. \qquad (11)$$

Equation (11) combines the environmental uncertainty σ_E^2 with the epidemiological uncertainty $\sigma_B{}^2$. This equation propagates these two main sources of uncertainty to obtain the combined uncertainty σ_H^2 in the health risk estimate H. The variance σ_H^2 is meaningful in regional and national public health planning as it can be used to determine the upper and lower bounds of the health effect H and provide the worst and best cases scenario of percent change in mortality risk due to increase in short-term exposure to PM_{10} at any district space/time point $\boldsymbol{p}_{\mathrm{k}}$.

The maps of estimation percent excess mortality risk H on day 286 of 2004 and its associated relative error σ_H/H are shown in Figures 4.3 and 4.4 for cardiovascular and respiratory mortality, respectively. Fig. 4.3a shows that on that day the highest increase in cardiovascular mortality caused by short term exposure to PM_{10} was in the Northern region (where the increase of cardiovascular mortality caused by PM_{10} was up to 9.5%) followed by the Bangkok metropolitan area. Actually, over the whole 2004 year, the increase in daily cardiovascular mortality caused by PM_{10} reached as much as 34.6% in the Northern region. This result is due to the high levels of air pollution observed in the Northern region combined with the high strength of the association between PM_{10} and cardiovascular mortality in that region. The associated relative error map depicted in Fig.

4.3b for day 286 of 2004 shows that the uncertainty associated with the cardiovascular mortality risk assessment is highest in the Northern region, followed by the Southern region. The high cardiovascular risk uncertainty in the Northern region is likely due to the high epidemiologic uncertainty (i.e. high σ_B/B) in that region, while in the Southern region the main contribution to high cardiovascular risk uncertainty is likely the high environmental uncertainty (i.e. high σ_E/E).

As can be seen in Fig. 4.4a, the highest increase in respiratory mortality due to short term exposure to PM_{10} is also in the Northern region, where it reached a maximum of 18.2% for the most polluted district on day 286 of 2004, and as much as 47.1% over the whole year. Such high respiratory mortality excess risks in the Northern region are likely to be due to the particularly high strength of the PM_{10} association with respiratory mortality in that region, which is almost three times higher than that of other regions of Thailand (Table 4.1). Interestingly, the associated relative error map depicted in Fig. 4.4b for day 286 of 2004 shows that the uncertainty associated with the respiratory mortality risk assessment is highest in the Southern and Northeastern regions, instead of the Northern region. This shift of uncertainty towards these two regions is likely due to the fact that we had to use the country pooled estimate for B in theses regions because of the lack of sufficient epidemiologic data (table 4.1), and as a result the propagated uncertainty for pulmonary mortality excess risk is highest in these two regions than for the other regions where more reliable estimate of the strength of the association between PM_{10} and respiratory mortality exist. Furthermore the Southern and Northeastern regions have the highest environmental uncertainty (i.e. highest σ_E/E) due to sparse monitoring

networks in these two regions, which further explains the high relative error σ_H / H for the respiratory health risk H in these two regions.

Population health impact

In step 3 of the space/time risk assessment framework, we calculate the health effect at the population level in terms of the space/time population mortality loss L defined as the daily mortality density, corresponding to the number of lives per square miles and per day that were shortened due to death caused by an acute health response to PM_{10}. This is a useful measure that allows public health policy makers to assess where and when the short term population health impact of PM_{10} is strongest in Thailand. In this step of the analysis, we integrate information about the percent change H in mortality rate (obtained in previous step of the analysis for any space/time point $\boldsymbol{p}_k$ corresponding to a district of Thailand and a day in 2004), the baseline cardiovascular or respiratory mortality rate R, the number of people P living in the district at $\boldsymbol{p}_k$, and the area A of that district. The product $(H(\boldsymbol{p}_k)R)$ is the fraction of people dying over one day due to exposure to PM_{10} at district and day $\boldsymbol{p}_k$, so that $(H(\boldsymbol{p}_k)R)\, P(\boldsymbol{p}_k)$ is the number of death per day caused by PM_{10} at district and day $\boldsymbol{p}_k$, and therefore the population mortality loss L at $\boldsymbol{p}_k$ is simply the daily mortality density calculated as

$$L(\boldsymbol{p}_k) = \left[(H(\boldsymbol{p}_k)R)\, P(\boldsymbol{p}_k) \right] / A. \qquad (12)$$

Since the baseline mortality R for a district is unknown, we used the assumption that is it not significantly different from the observed daily mortality rate during the 1998-2003

time period preceding 2004. Hence, for each district, the baseline rate R was obtained by averaging the daily mortality rate observed from 1998 to 2003, and this rate was considered constant throughout 2004. On the other hand the number of people P living in a district at some day in 2004 was obtained by linear interpolation of the census data available for the end of 2003 and 2004.

While the daily maps of $L(\boldsymbol{p}_k)$ provide a description of the spatial distribution of the daily mortality density (number of death per square miles and per day) caused by PM_{10} for any day of 2004, it is useful to aggregate these maps over the year to obtain the yearly mortality density (number of death per square miles for 2004) caused by PM_{10} over the whole year. Hence we show the map we obtained for cardiovascular yearly mortality density in Fig. 4.5a, and the map of respiratory yearly mortality density in Fig. 4.5b. While the cardiovascular yearly mortality density map (Fig. 4.5a) has a graduated scale truncated at $0.16*10^{-3}$ deaths per square mile (so that comparisons can be made between regions), the maximum cardiovascular mortality density observed across Thailand is actually much higher, reaching a value of as high as 15 cardiovascular deaths caused by PM_{10} per square mile in a densely populated district of Bangkok. Similarly, while the graduated scale for the respiratory yearly mortality density map is truncated at $0.13*10^{-3}$ deaths per square mile (Fig. 4.5b), this map has values as high as 11 respiratory deaths per square miles caused in 2004 by PM_{10}.

We can see from Figures 4.5a and 4.5b that the density of cardiovascular mortality is more evenly distributed throughout the country than that of respiratory mortality. Fig. 4.5b clearly shows that PM_{10} air pollution has a high impact on respiratory mortality in the Northern region. The Northeastern region, which is the

largest region of Thailand, exhibits sporadic areas with medium cardiovascular excess mortality caused by PM_{10}, while the Southern region, a lightly populated area of Thailand, seems to be the least affected by PM_{10} air pollution, consistent with the maps of mortality risk increase H presented earlier. These maps of population damage L (expressed in death per square miles caused by PM_{10}) can be useful to target areas where PM_{10} abatement strategies are needed either at the local or regional scale.

Regional population mortality health impact

The lower and upper bounds of the confidence intervals characterizing the uncertainty associated with estimates of the population health impact of PM_{10} play an important role in terms of revising regulations and standards, and planning environmental sampling and health budgets. Accounting for the main sources of uncertainty and properly propagating them throughout the steps of the risk assessment analysis is vital in obtaining the lower and upper bounds of confidence intervals. At the first step of the space/time risk assessment framework, the BME estimation method processes the uncertainty due to the sparse nature of the monitoring network, the space/time variability of PM_{10}, and the measurement errors of monitoring data, and characterizes this uncertainty in terms of the BME map of the relative error σ_E/E. This map characterizes the environmental uncertainty (i.e. the uncertainty associated with estimating environmental exposures) which is then merged with the epidemiological uncertainty σ_B^2 through Equation (11) to obtain the combined variance $\sigma_H^2$of the health effect field of interest, i.e. cardiovascular and respiratory mortality in our case. Using the estimated health risk H and its standard deviation σ_H we derive the lower and upper bound of its 68% CI, which after using Eq.

(12) provides us with the lower and upper bounds of the 68% CI of the mortality density loss L.

While the daily mortality density $L(\boldsymbol{p}_k)$ provides an assessment of health impact of PM_{10} at space/time location $\boldsymbol{p}_k = (\boldsymbol{s}_k, t_k)$ where $\boldsymbol{s}_k$ is the spatial location and t_k time, it is sometimes useful to assess the aggregated effect of PM_{10} over some geographical region A and over some time T. We define such aggregated health effect as the regional population damage indicator η given by the equation

$$\eta = \int_A d\boldsymbol{s}_k \int_T dt_k L(\boldsymbol{s}_k, t_k) \tag{13}$$

where A is one of the 5 regions of Thailand considered in the work, the time period T corresponds to the year 2004, and η is simply the number of cardiovascular or respiratory deaths caused by PM_{10} in 2004 for the region of interest. The estimated value for η is obtained by integrating the estimated field $L(\boldsymbol{p}_k)$, while the lower and upper bounds of its 68% CI are obtained by integrating in Eq. (13) the corresponding bounds of 68% CI for the $L(\boldsymbol{p}_k)$ field. The death count η and the lower and upper bounds of its 68% CI obtained using Eq. (13) for each region of Thailand are shown in Table 4.2 for cardiovascular mortality and for respiratory mortality. By summing up the death counts in each region, we obtain the total death count for Thailand shown in the last row of table 4.2, which tells that across Thailand there were, in 2004, 1,251 deaths from cardiovascular causes and 1,121 deaths for respiratory cause that we expect were the result of acute health response to exposure to PM_{10} in the air of Thailand.

We can see from Table 4.2 that the death counts for cardiovascular mortality are usually higher than those of respiratory mortality in all regions of Thailand except for the Northern region. In addition we see that the Northern region experiences the highest death counts in both cardiovascular and respiratory mortality. Even though it covers only a small area of Thailand, the Bangkok metropolitan area experienced as much as 22 % of the country wide excess mortality in both causes of death in 2004 while it comprises of about 10% of the Thai population. These findings will be very important to Thailand health authorities in efficiently designing and targeting their strategies, especially in these two areas.

Elasticity analysis of uncertainty sources

Understanding the contribution of different uncertainty sources to the cumulated uncertainty of risk estimates is critical for policy makers and planners to better allocate existing resources to reduce uncertainty in risk assessment, which will lead to better information in designing future policies. Here, we focus on assessing the respective uncertainty contribution of the exposure field E and the strength of the exposure-mortality association B to the uncertainty of the health effect H. The uncertainty associated with the exposure field E is characterized by its mapping standard deviation σ_E. We refer to σ_E as the 'environmental' uncertainty to emphasize that the source of this uncertainty is the environmental monitoring network and its ability in properly assess exposure to PM_{10} at any space/time point $\boldsymbol{p}_k$. The uncertainty associated with B is characterized by its regression standard deviation σ_B, and we refer to it as the 'epidemiologic' uncertainty to emphasize that its source in the epidemiologic study and

the statistical power of the available PM_{10} and mortality data used in the regression analysis to obtain the strength of association *B*.

A useful metric used to assess the contribution of different inputs to an output variable is the elasticity ρ. Simply put, the elasticity is a measure of the responsiveness of one variable to another. Hence the elasticity provides a tool to quantify to responsiveness of σ_H to changes in either σ_E or σ_B, or in other words, the respective contribution of environmental uncertainty and epidemiologic uncertainty to the risk assessment uncertainty. For instance, the elasticity of σ_H with respect to σ_E, which we denote as $\rho_{\sigma_H}^{\sigma_E}$, is the responsiveness of σ_H to changes in σ_E, and it is calculated as the percentage change in σ_H divided by the corresponding percent change in σ_E as follow

$$\rho_{\sigma_H}^{\sigma_E} = \frac{(\sigma'_H - \sigma_H)/(0.5[\sigma'_H + \sigma_H])}{(\sigma'_E - \sigma_E)/(0.5[\sigma'_E + \sigma_E])} \tag{14}$$

where σ'_E corresponds to a 1% increase over σ_E, and σ'_H is the corresponding standard deviation calculated using Equation (11). Similarly we denote as $\rho_{\sigma_H}^{\sigma_B}$ the elasticity of σ_H with respect to σ_B, calculated as follow

$$\rho_{\sigma_H}^{\sigma_B} = \frac{(\sigma'_H - \sigma_H)/(0.5[\sigma'_H + \sigma_H])}{(\sigma'_B - \sigma_B)/(0.5[\sigma'_B + \sigma_B])} \tag{15}$$

where σ'_B corresponds to a 1% increase over σ_B, and σ'_H is the corresponding standard deviation calculated using Equation (11).

Maps of the elasticity's $\rho_{\sigma_H}^{\sigma_E}$ and $\rho_{\sigma_H}^{\sigma_B}$ obtained for day 286 in 2004 are shown in Figures 4.6 and 4.7, respectively. These maps are useful in assessing how responsive is σ_H over space and time to a 1% change in σ_E and σ_B, respectively. Turning to the maps of $\rho_{\sigma_H}^{\sigma_E}$ (Fig. 4.6) we see that in the case of cardiovascular mortality (Fig. 4.6a) the elasticity is highest in the Southern and Northeastern region. This means that improvements in the PM_{10} monitoring network in these two regions will have the most effect in improving cardiovascular mortality risk assessment. However in the case of respiratory mortality (Fig. 4.6b), we see that the elasticity $\rho_{\sigma_H}^{\sigma_E}$ is highest in the central region. Hence improvement in the PM_{10} monitoring network in the central region will improve the assessment of the respiratory health effect caused by PM_{10} in that region. However overall, the spread of $\rho_{\sigma_H}^{\sigma_E}$ elasticity across the country is small, so that any improvement of the PM_{10} monitoring network anywhere in the country will help improve PM_{10} health risk assessment.

Turning to the maps of $\rho_{\sigma_H}^{\sigma_B}$ (Fig. 4.7) we see that in that case, the elasticity varies substantially across the country (by a factor of over 3 fold). This indicates the needs for regional epidemiologic studies. In the case of cardiovascular mortality (Fig. 4.7a) the elasticity is highest in the Northern region. This means that further epidemiologic studies on the association between PM_{10} and cardiovascular mortality are needed in the Northern region, and such studies would have a much larger impact at improving our assessment of the overall impact of PM_{10} on cardiopulmonary mortality in Thailand than similar studies in other regions of Thailand. In the case of pulmonary mortality (Fig. 4.7b) the elasticity is highest in the Southern and Northeastern regions. This finding points to the fact that

due to the lack of adequate epidemiologic studies on the association between PM_{10} and respiratory mortality in these two regions, further epidemiologic studies in these regions would have the largest impact in reducing the uncertainty in our assessment of the overall impact of PM_{10} on respiratory mortality in Thailand.

The next question might be how can we improve epidemiologic studies in the Northern region (focusing on cardiovascular mortality), and in the Southern and Northeastern regions (focusing on respiratory mortality)? A clue might be provided by examining the ratio r_ρ of elasticity defined as

$$r_\rho = \frac{\rho_{\sigma_H}^{\sigma_B}}{\rho_{\sigma_H}^{\sigma_E}} . \qquad (16)$$

This ratio compares the relative effectiveness of epidemiologic uncertainty and environmental uncertainty to reducing risk assessment uncertainty. A ratio smaller than 1 means that reducing risk assessment uncertainty is more efficiently achieved by reducing environmental uncertainty than it is by reducing epidemiologic uncertainty. We show in Fig. 4.8a and 4.8b the elasticity ratio obtained on day 286 in 2004 for cardiovascular mortality and respiratory mortality, respectively. As can be seen from these maps, the elasticity ratio is consistently less than 1 throughout Thailand on day 286 in 2004. This finding is useful is suggesting how to improve regional epidemiologic studies in areas where they are needed. It suggests that in these areas, one should improve the PM_{10} monitoring network, which will improve epidemiologic studies by providing better exposure estimates, and also will have the greatest impact in reducing the uncertainty in

any risk assessment analysis needed by Thai policy makers and public health officials. Hence these findings suggest that future work should focus in improving the PM_{10} monitoring network in the Southern and Northeastern regions, where very few stations are located, as well as in the Northern region, where the network is still sparse, and that the resulting PM_{10} exposure maps be used to improve PM_{10}-mortality epidemiologic studies focusing on cardiovascular health endpoints in the Northern region and respiratory health endpoints in the Southern and Northeastern regions.

Conclusion

In this study, we examined excess risk of cardiovascular and respiratory mortality at 925 districts of Thailand for 366 days in 2004, i.e. at 338,550 space/time points. This study consists of the application of a space/time risk assessment framework to asses the cardiovascular and respiratory mortality risk increase resulting from the population exposure to PM_{10} across Thailand in 2004. The BME method is an important component of this proposed framework, as it allows quantifying the exposure estimation uncertainty associated with the mapping analysis of PM_{10} across space/time domain of Thailand. This mapping uncertainty is propagated along with the uncertainty associated with the PM_{10}-mortality epidemiologic relationship to obtain the best-case and worst-case scenario of the total death count due to increase in daily PM_{10} in Thailand.

Reference:

1. Zanobetti A, Canner MJ, Stone PH, Schwartz J, Sher D, Eagan-Bengston E, Gates KA, Hartley LH, Suh H, Gold DR. Ambient pollution and blood pressure in cardiac rehabilitation patients. Circulation 110:2184-9(2004).

2. Zanobetti A, Schwartz J. Cardiovascular damage by airborne particles: are diabetics more susceptible? Epidemiology 13:588-92(2002).

3. Baldacci S, Viegi G. Respiratory effects of environmental pollution: epidemiological data. Monaldi Arch Chest Dis 57:156-60(2002).

4. Penttinen P, Timonen KL, Tiittanen P, Mirme A, Ruuskanen J, Pekkanen J. Ultrafine particles in urban air and respiratory health among adult asthmatics. Eur Respir J 17:428-35(2001).

5. Analitis A, Katsouyanni K, Dimakopoulou K, Samoli E, Nikoloulopoulos AK, Petasakis Y, Touloumi G, Schwartz J, Anderson HR, Cambra K, Forastiere F, Zmirou D, Vonk JM, Clancy L, Kriz B, Bobvos J, Pekkanen J. Short-term effects of ambient particles on cardiovascular and respiratory mortality. Epidemiology 17:230-3(2006).

6. Dominici F, McDermott A, Daniels M, Zeger SL, Samet JM. Revised analyses of the National Morbidity, Mortality, and Air Pollution Study: mortality among residents of 90 cities. J Toxicol Environ Health A 68:1071-92(2005).

7. Hoek G. Daily Mortality and Air Pollution in The Netherlands. In: Revised Analyses of Time-Series Studies of Air Pollution and Health. Special Report. Boston:Health Effects Institute, 2003;133-142.

8. Villeneuve PJ, Burnett RT, Shi Y, Krewski D, Goldberg MS, Hertzman C, Chen Y, Brook J. A time-series study of air pollution, socioeconomic status, and mortality in Vancouver, Canada. J Expo Anal Environ Epidemiol 13:427-35(2003).

9. Radian International LLC. PM abatement strategy for the Bangkok metropolitan area: final report. Austin, TX, 1998, 1998.

10. Vajanapoom N, Shy CM, Neas LM, Loomis D. Associations of particulate matter and daily mortality in Bangkok, Thailand. Southeast Asian J Trop Med Public Health 33:389-99(2002).

11. Ostro BD, Chestnut LG, Vichit-Vadakan N, Laixuthai A. The impact of particulate matter on daily mortality in Bangkok, Thailand. Journal of The Air & Waste Management Association 49:100-107(1999).

12. Christakos G, Hristopulos DT. Spatiotemporal environmental health modelling: A tractatus stochasticus. Boston, MA:Kluwer Academic Publishers, 1998.

13. Serre ML, Kolovos A, Christakos G, Modis K. An application of the holistochastic human exposure methodology to naturally occurring arsenic in Bangladesh drinking water. Risk Anal 23:515-28(2003).

14. Christakos G, Serre ML. BME analysis of spatiotemporal particulate matter distributions in North Carolina. Atmospheric Environment 34:3393-3406(2000).

15. Christakos G, Vyas VM. A composite space/time approach to studying ozone distribution over Eastern United States. Atmospheric Environment 32:2845-2857(1998).

16. Serre ML, Carter G, Money E. Geostatistical space/time estimation of water quality along the Raritan river basin in New Jersey. In: Computational Methods in Water Resources 2004 International Conference 2004;1839-1852.

Table 4.1 β_{PM} and 95% standard error (SE) estimates obtained from conditional logistic regression model for the lag corresponding to the highest strength of the PM_{10}-mortality association

	Cardiovascular Mortality			Respiratory Mortality		
Areas	β_{PM}[1]	SE[1]	lag	β_{PM}[1]	SE[1]	lag
Bangkok vicinity	0.00092	0.00041	1	0.00125	0.00055	3
Central	0.00084	0.00039	1	0.00102	0.00053	4
North	0.00151	0.00155	2	0.00288	0.00180	2
Country	0.00085	0.00028	1	0.00085	0.00069	0,3[2]

[1]Estimated using data sets from 1998-2003

[2] lag 0 was used in the south and north east areas and lag 3 was used in Bangkok, central, and north areas in this re-analysis

Table 4.2 Estimated counts of deaths caused in 2004 by short term exposure to daily PM_{10}

	Cardiovascular Mortality		Respiratory Mortality	
Areas	Counts[1,2]	Bounds[3]	Counts[1,2]	Bounds[3]
Bangkok vicinity	326	[117, 573]	255	[91, 440]
Central	190	[78, 271]	125	[46, 181]
North	389	[0, 837]	550	[173, 932]
South	87	[47, 129]	51	[5, 98]
Northeast	258	[156, 368]	140	[20, 258]
Total	1,250	[398, 2,178]	1,121	[335, 1,909]

[1]Sum of daily counts over district locations in each region

[2]Estimated using daily density loss at each district

[3]Estimated using yearly density loss directly calculated from yearly average of PM_{10} increase in each region

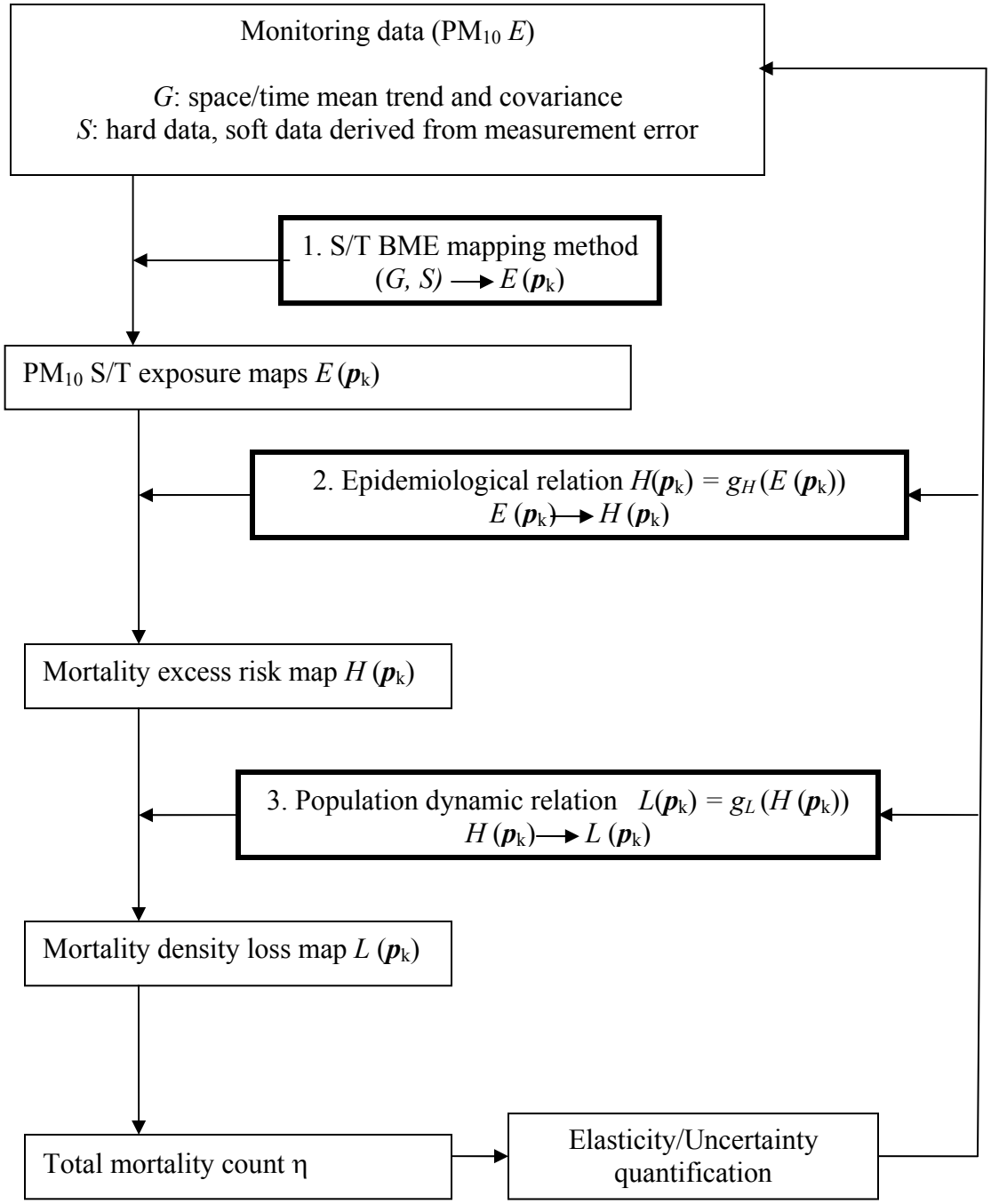

Figure 4.1 Space/time risk assessment framework to assess cardiovascular and respiratory mortality risk due to increase in daily PM_{10}

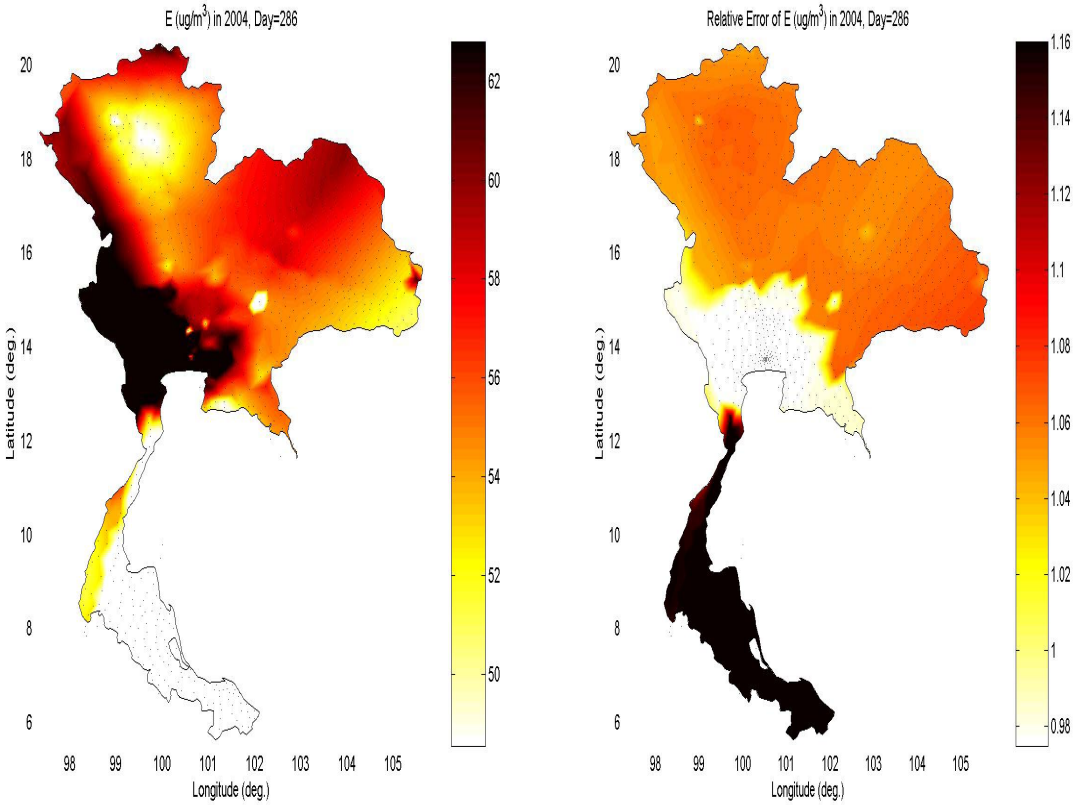

a) Increase in PM_{10} ($\mu g/m^3$) above background b) Relative error σ_E/E

Figure 4.2 Maps of (a) the ΔPM_{10} ($\mu g/m^3$) increase in PM_{10} above background, and (b) the corresponding relative error σ_E/E on day 286 in 2004.

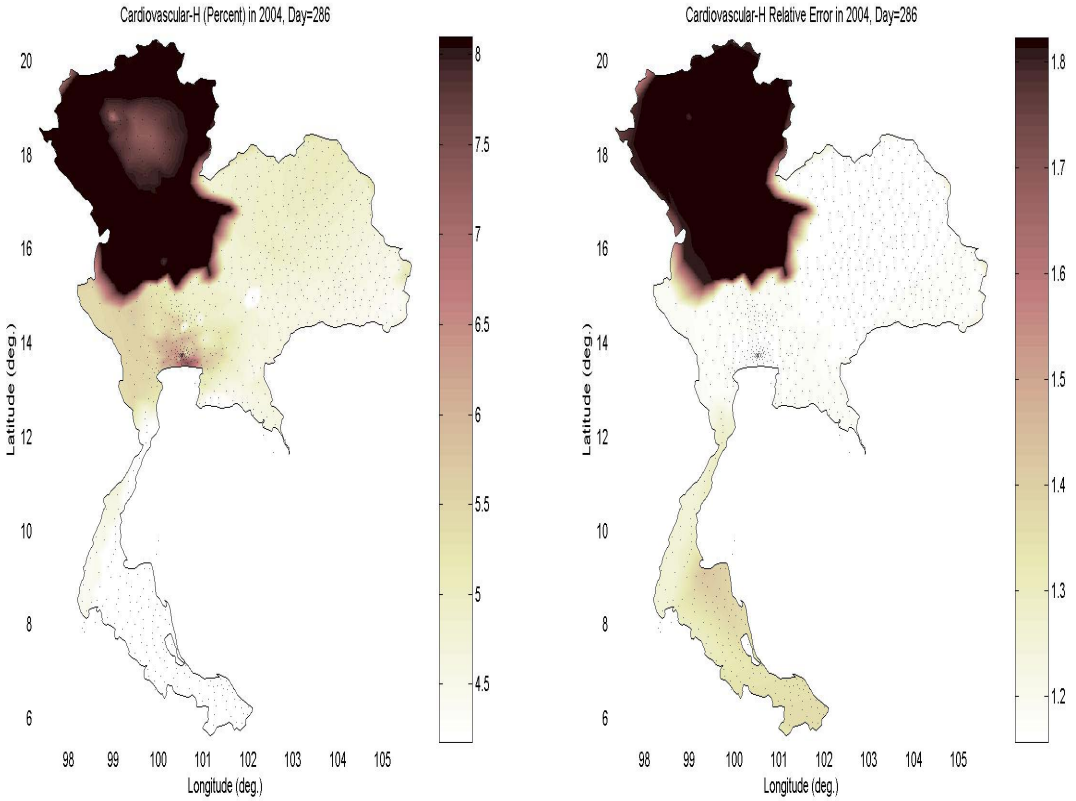

a) Cardiovascular mortality risk increase H b) Relative error σ_H/H

Figure 4.3 Maps of (a) the cardiovascular mortality risk increase (percent) and (b) the associated relative error on day 286 in 2004

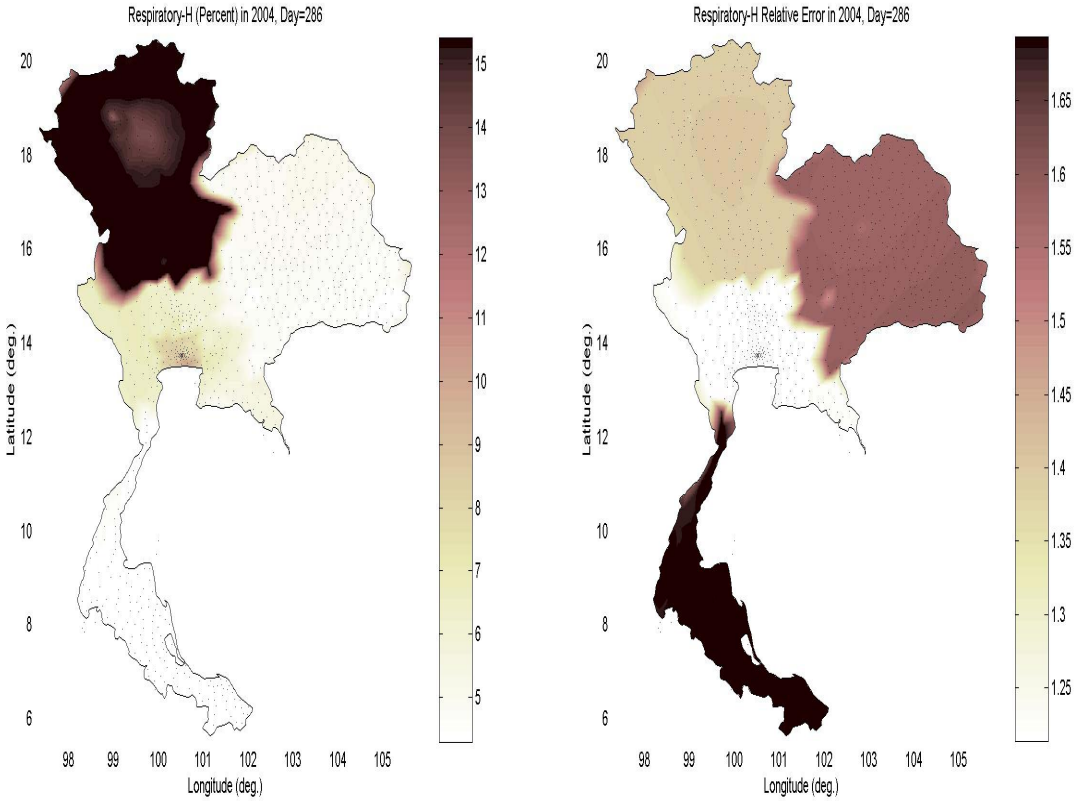

a) Respiratory mortality risk increase H b) Relative error σ_H/H

Figure 4.4 Maps of (a) the respiratory mortality risk increase (percent) and (b) the associated relative error on day 286 in 2004

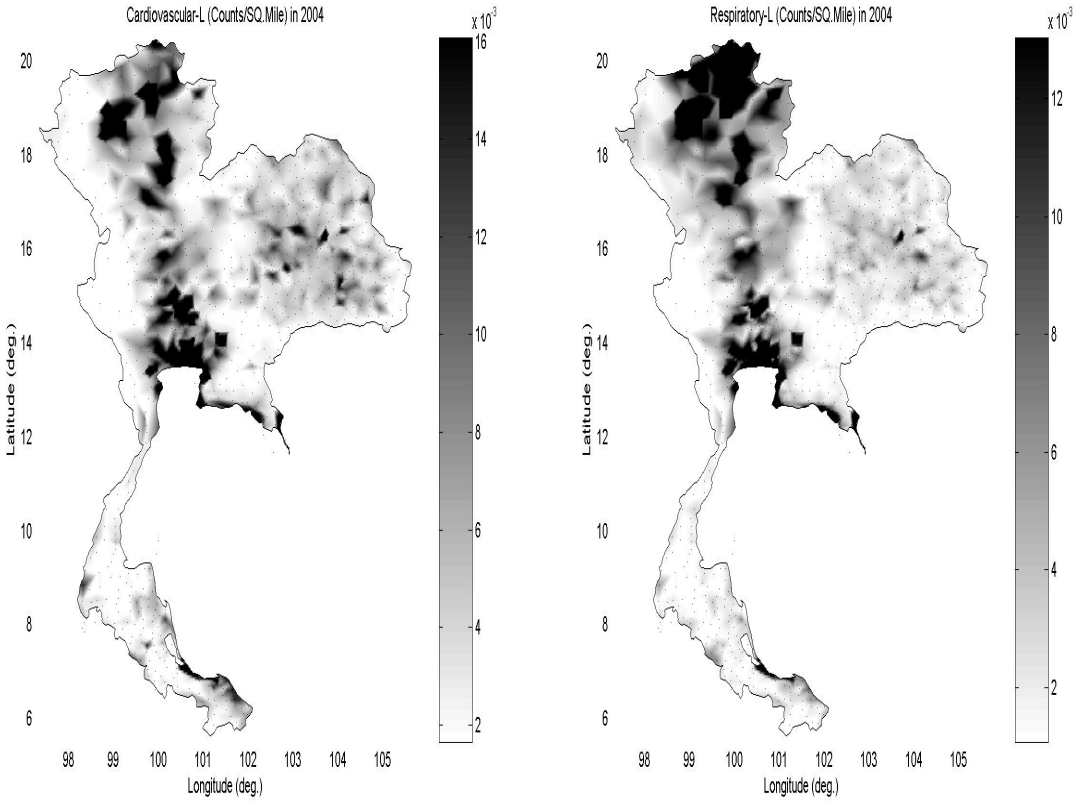

a) Cardiovascular mortality density b) Respiratory mortality density

Figure 4.5 Maps of (a) the cardiovascular and (b) respiratory yearly mortality density (deaths/sq.mile) in 2004

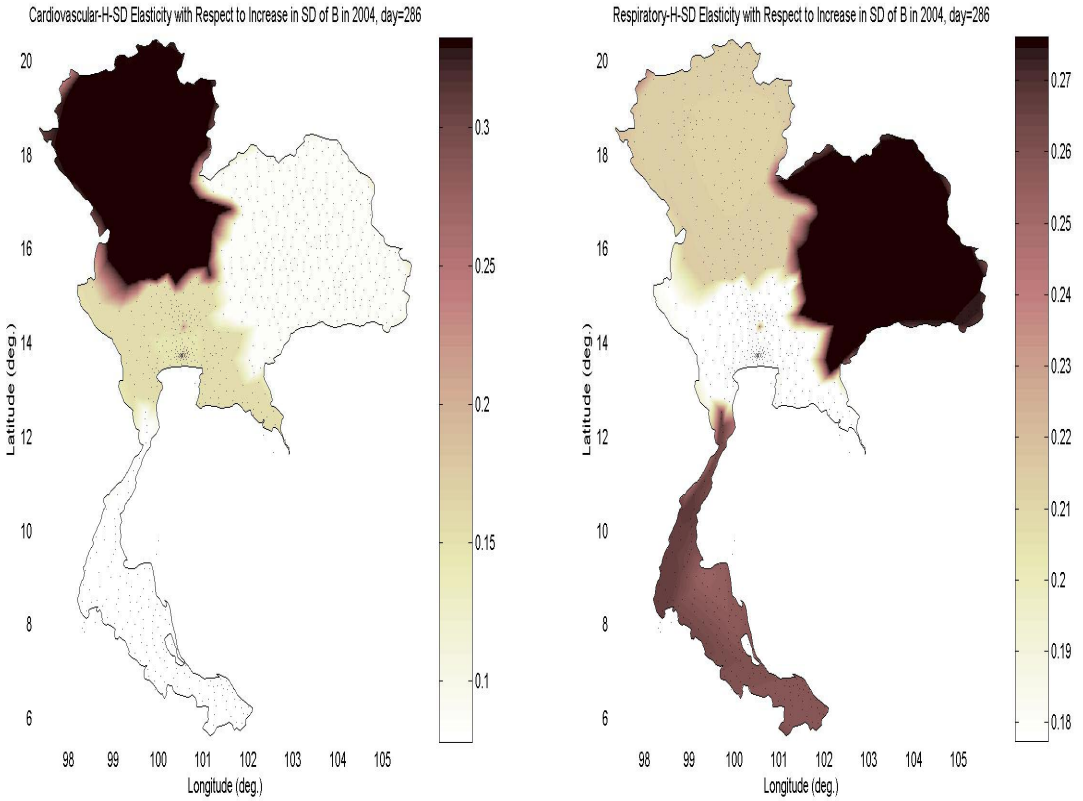

a) Cardiovascular-H SD elasticity $\rho_{\sigma_H}^{\sigma_B}$ b) Respiratory-H SD elasticity $\rho_{\sigma_H}^{\sigma_B}$

Figure 4.6 Maps of elasticity of σ_H with respect to σ_B on day 286 in 2004 for (a) cardiovascular, and (b) respiratory mortality.

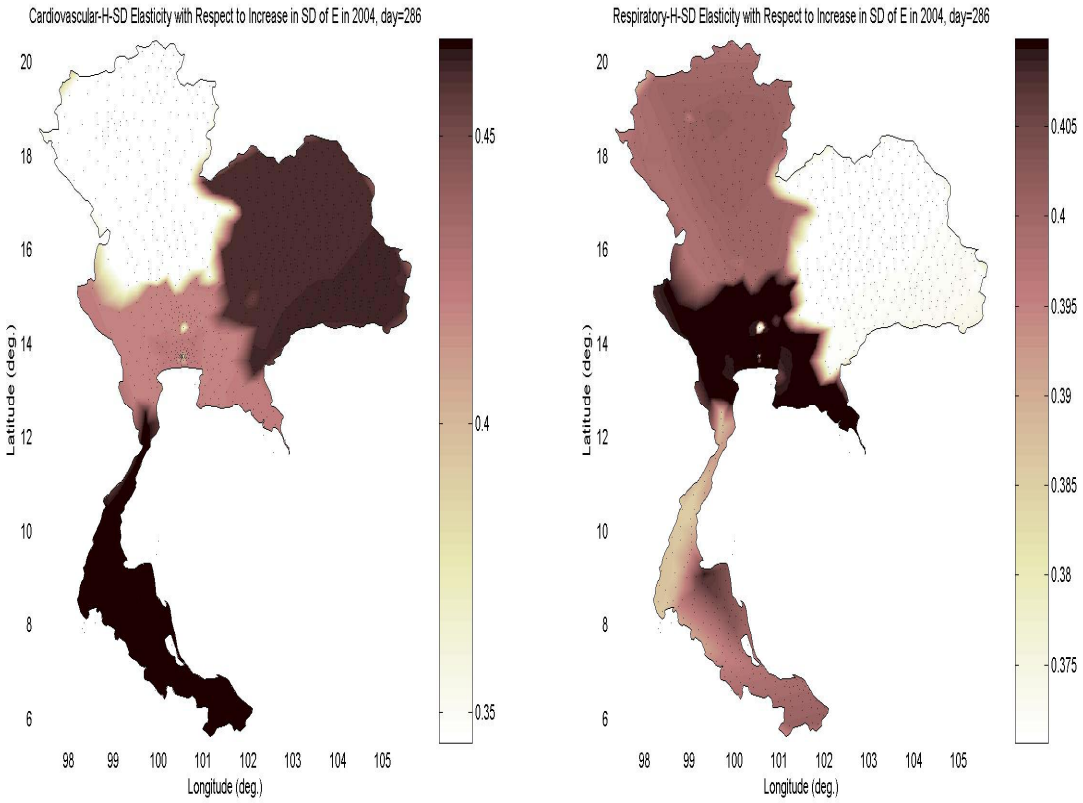

a) Cardiovascular-H SD elasticity $\rho_{\sigma_H}^{\sigma_E}$ b) Respiratory-H SD elasticity $\rho_{\sigma_H}^{\sigma_E}$

Figure 4.7 Maps of elasticity of σ_H with respect to σ_E on day 286 in 2004 for (a) cardiovascular, and (b) respiratory mortality.

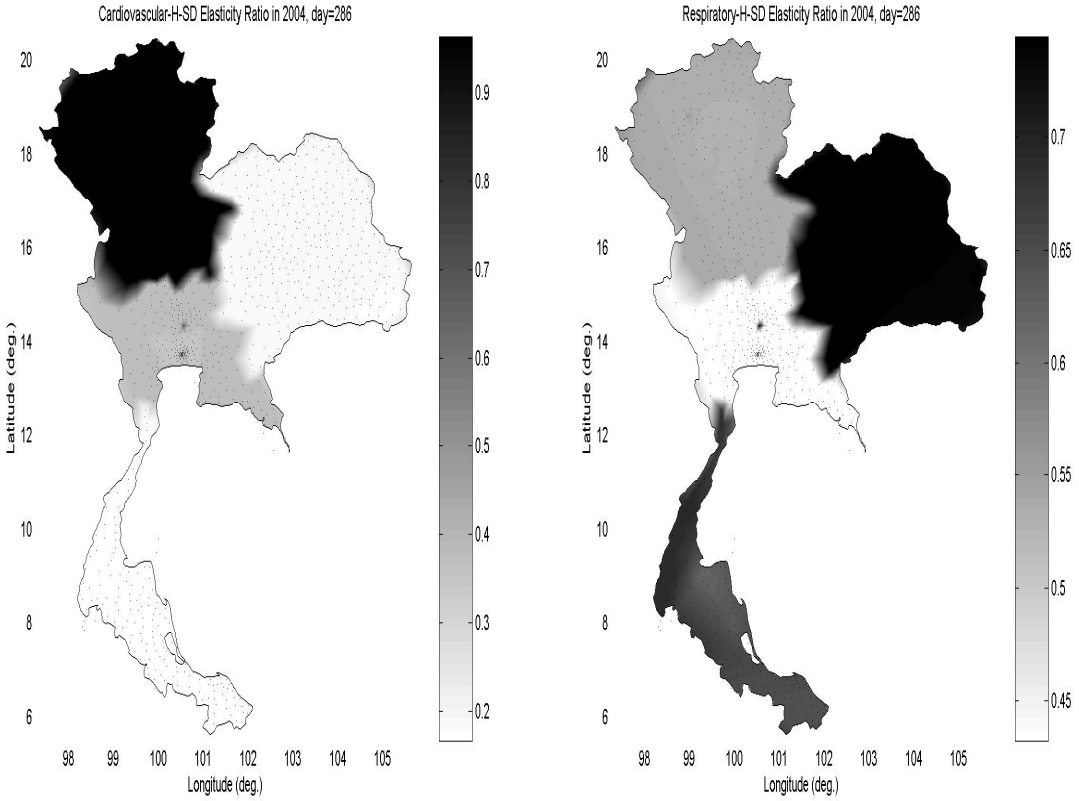

a) Cardiovascular-H SD elasticity ratio r_ρ b) Respiratory-H SD elasticity ratio r_ρ

Figure 4.8 Maps of elasticity ratio on day 286 in 2004 for (a) cardiovascular, and (b) respiratory mortality.

V. CONCLUSIONS

Summary of Findings

The spatiotemporal distribution of PM_{10} across Thailand exhibits a high natural space/time variability with combinations of spatial and temporal ranges of variability that are unique to Thailand. The usefulness and feasibility of the BME mapping analysis to model the space/time distribution of PM_{10} across Thailand was demonstrated. BME spatiotemporal maps of PM_{10} provide evidence that daily average levels on the worst day of each year of the 1998-2003 time period do not comply with the NAQQS standard in many parts of the country, including most of central region, and a small part of the Northern region. This finding is supported by BME maps of the daily maximum PM_{10} concentration, and BME non attainment maps for the daily average PM_{10} concentration. These results are consistent with economic growth and trends in fossil fuel consumption in the central region, indicating that transportation and industry are a major sources of PM_{10} in that region, while this is not clear for other regions of Thailand. The adequacy of the current monitoring network was assessed, and districts in the Northeastern region were suggested as targets for installing new monitoring stations in order to improve the monitoring network.

The second analysis of this dissertation was mainly aimed at investigating the effect of short-term exposure to PM_{10} on cardiovascular and respiratory mortality in different regions of Thailand. The analysis was conducted using a case-crossover design. This study adds to the

growing body of evidence linking PM_{10} with daily cardiopulmonary mortality. To our knowledge, this is the first case-crossover multi-location study of PM_{10} and cardiopulmonary mortality. The positive association between PM_{10} and cardiovascular mortality is found to be statistically significant in Bangkok and the central region, but not in the Northern region. Similar strength in the positive association between PM_{10} and respiratory mortality are found in the two non overlapping areas of Bangkok and the central region, however the association is statistically significant only in the Bangkok area. In the Northern region, the strength of the association was greatly elevated but not statistically significant. The pooled country odd ratio estimates show that an increase in PM_{10} is associated with statistically significant increase in cardiovascular mortality, but that the positive association with country wide respiratory mortality is not statistically significant.

The implementation of a holistochastic framework for risk assessment provides useful confidence intervals for the number of deaths from cardiovascular and respiratory causes that resulted from acute health response to short term exposure to PM_{10} in Thailand. An elasticity analysis of uncertainty suggests that future work should focus in improving the PM_{10} monitoring network in the Southern and Northeastern regions, where very few stations are located, as well as in the Northern region, where the network is still sparse, and that the resulting PM_{10} exposure maps be used to improve PM_{10}-mortality epidemiologic studies focusing on cardiovascular health endpoints in the Northern region and respiratory health endpoints in the Southern and Northeastern regions.

Strengths and Limitation

The analysis of the spatiotemporal distribution of PM_{10} across Thailand using the powerful BME mapping framework has provided realistic maps of the PM_{10} daily average and daily maximum concentrations, as well as maps delineating non-attainment areas. The BME mapping method provides a rigorous mathematical framework to process of a wide variety of knowledge bases, and leads to spatiotemporal representations of PM_{10} that are more realistic and accurate than those obtained with classical approaches not accounting for the composite space/time variability of the PM_{10} field or the uncertainties associated with the PM_{10} monitoring data.

The epidemiologic analysis of the PM_{10}-mortality association was conducted using a case-crossover design which has several limitations and strengths. The computational complexity of the conditional logistic regression algorithm limited the size of the dataset that could be analyzed. This limited the number of controls selected for each death, as well as the number of co-pollutants considered. However this did not limit the ability to study the association region by region, and country pooled estimates of odds ratio for the country were obtained using a meta analysis of the regional estimates of the association. The use of a bi-directional selection scheme of controls instead of a time-stratified selection scheme resulted in a small overlap bias of the estimate of the strength of the association, though this overlap bias was minimized by using only a 7 day difference between a death and its controls.

Lack and disparity of monitoring sites between regions result in high uncertainty in the exposure assessment in regions with poor monitoring networks. Furthermore, due to the limitation in the information available for geocoding each death cases, the exposure estimate for each death was obtained only for the centroid of the primary district reported in the address on the death record, leading to possible errors in assessing the exposure for individuals living at

different distances from the district centroid. However the 925 districts of Thailand provide the best spatial resolution possible for the mortality data available.

However, in spite of these weaknesses, this study presents strengths that make it of benefit to the air pollution epidemiology and risk assessment fields. Though the stated research goal stated of detecting regional effects was challenging, this analysis yields significant results because of the case-crossover design efficiently controls for personal and time trend confounders and has high statistical power.

Our case-crossover analysis utilized the space/time BME exposure mapping method to analyze a very rich PM_{10} dataset presenting strong gradients of exposure over both space and time, and experiencing some very high air pollution events. Estimates of the PM_{10} exposure where obtained at 925 district locations of Thailand, over for each day of a 6 year period. This results in a very large dataset of death records and associated exposure levels, which combined with the case crossover design providing excellent control for personal confounding factors, results in a very high statistical power. This statistical power was the basis for being able to stratify the dataset by regions, and obtaining regional estimates of the strength of the association between PM_{10} and cardiovascular and respiratory mortality. The statistical power of the dataset could be used in future work to investigate other strata of the population of Thailand.

Future Research Directions and Recommendations

The PM_{10} effects in the Northern region were found to be of particular interest. They are strongest for both cardiovascular and respiratory mortality. The impact of PM_{10} in that region resulted in more deaths from respiratory causes than deaths from cardiovascular causes. The lag

between exposure and maximum health effect was 2 days for both cardiovascular and pulmonary mortality in that region, though there were high uncertainties in these estimates. Future epidemiologic investigations would be useful to unravel the etiology of PM_{10} related cardiovascular and respiratory mortality in that region.

The uncertainty in the effect estimate in the Northeastern and Southern regions could be reduced in future works if conducted using only BME estimates of PM_{10} and deaths cases at districts in the proximity of existing monitoring sites, but over a longer study period than the period considered in the work. Another recommendation is that the Northeastern region be the target for installing new monitoring sites. Monitoring data from these new monitoring sites would allow to greatly improve estimates of the effect of PM_{10} in that region.

PM_{10} effect estimates stratified by age would address how the excess cardiovascular and respiratory deaths are distributed from one age group to another. This information would be particularly useful for risk assessment as it would allow to better quantify the number of life days lost, instead of the number of lives shortened.

An increasing number studies have demonstrated the relationship between $PM_{2.5}$ and cardiopulmonary mortality. As $PM_{2.5}$ data are being collected in Thailand, the same study design could be applied to examine its health effects.

APPENDICIES

APPENDIX A Geographic locations of air quality monitoring network of Thailand

	Station Name	Longitude	Latitude
1	MOSTE	100.53	13.76
2	Chula Hos 03C	100.54	13.73
3	Land Transport Dept	100.56	13.80
4	Prabadang Rehabilitation 08T	100.55	13.66
5	Ramkhamhaeng 09T	100.62	13.75
6	National Housing Authority 10T	100.66	13.77
7	Huai Khwant11T	100.57	13.77
8	None-tree Vitaya 12T	100.55	13.70
9	EGAT Dept. of Energy Affairs	100.52	13.80
10	Thonburi Highway Sist. 14T	100.33	13.70
11	Singharatpitayakom 15T	100.45	13.68
12	EGAT South Banglpk 16T	100.56	13.62
13	Prabdang Mineral Resources 17T	100.54	13.66
14	Samutprakan 18T	100.60	13.60
15	Bangplee Housing Authority 19T	100.80	13.57
16	Rangsit 20T	100.61	14.02
17	Ayuttaya 21T	100.57	14.35
18	Sukothai University 22T	100.54	13.90
19	Sanamchan Nakhonpathom 23T	100.06	13.83
20	Sarabure 24T	100.93	14.54
21	Kao Noy Saraburi 25T	100.92	14.52
22	Ratchaburi Engineer Dept 26T	99.87	13.40
23	Samutsakhon 27T	100.28	13.54
24	Pattaya A28	100.88	12.93
25	Pluak Dang 28T	101.27	12.89
26	MaptaPut 29T	101.17	12.71
27	Rayong 30T	101.27	12.68
28	Rayong 31T	101.14	12.73
29	Laem Chabang Chonburi 32T	100.93	13.08
30	Siracha Chonburi 33T	100.93	13.18
31	General Education Chonburi 34T	100.99	13.37
32	Chaing Mai 35T	98.97	18.84
33	Chaing Mai 36T	98.99	18.79
34	Lampang A37	99.51	18.29
35	Sob Pad A38	99.77	18.25
36	Tasee 39	99.76	18.42
37	Mae Moh 40	99.66	18.28
38	Nakhonsawan 41T	100.14	15.71
39	Suratthani 42T	99.27	9.15
40	Phuket M43	98.38	7.88
41	Hatyai New 44T	100.57	7.06
42	KhonKaen site#3	102.84	16.44
43	Nakhonratcharsima 47T	102.11	14.97
44	Wongwean 22	100.52	13.74

APPENDIX A (continued) Geographic location of air quality monitoring network in Thailand

	Station Name	Longitude	Latitude
45	Traffic Police Residence 53T	100.60	13.79
46	Dindang Housing Author	100.56	13.76
47	Esso Laem Chabang	100.92	13.12
48	Thai Oil Laem Chabang Chonburi	100.91	13.12
49	Wat Laem Chabng Chonburi	100.88	13.08
50	Ban Huafai	99.76	18.43
51	Hnongsua	100.68	14.13

APPENDIX B Locations of calculated centroids for all 925 district polygons

	District	Province	Longitude	Latitude	Code	Region[1]
1	Phra Nakhon	Bangkok	100.50	13.75	1001	1
2	Dusit	Bangkok	100.52	13.78	1002	1
3	Nong Chok	Bangkok	100.86	13.85	1003	1
4	Bang Rak	Bangkok	100.53	13.73	1004	1
5	Bang Khen	Bangkok	100.63	13.87	1005	1
6	Bang Kapi	Bangkok	100.64	13.77	1006	1
7	Pathum Wan	Bangkok	100.54	13.74	1007	1
8	Pom Prap Sattu Phai	Bangkok	100.51	13.75	1008	1
9	Phra Khanong	Bangkok	100.62	13.69	1009	1
10	Min Buri	Bangkok	100.76	13.81	1010	1
11	Lat Krabang	Bangkok	100.80	13.74	1011	1
12	Yan Nawa	Bangkok	100.54	13.69	1012	1
13	Samphanthawong	Bangkok	100.51	13.74	1013	1
14	Phaya Tai	Bangkok	100.55	13.78	1014	1
15	Thon Buri	Bangkok	100.49	13.71	1015	1
16	Bangkok Yai	Bangkok	100.48	13.73	1016	1
17	Huai Khwang	Bangkok	100.59	13.77	1017	1
18	Khlong San	Bangkok	100.51	13.72	1018	1
19	Taling Chan	Bangkok	100.44	13.77	1019	1
20	Bangkok Noi	Bangkok	100.48	13.76	1020	1
21	Bang Khun Thian	Bangkok	100.43	13.59	1021	1
22	Phasi Charoen	Bangkok	100.44	13.72	1022	1
23	Nong Khaem	Bangkok	100.36	13.69	1023	1
24	Rat Burana	Bangkok	100.50	13.67	1024	1
25	Bang Phlat	Bangkok	100.50	13.79	1025	1
26	Din Daeng	Bangkok	100.57	13.77	1026	1
27	Bueng Kum	Bangkok	100.65	13.81	1027	1
28	Sathon	Bangkok	100.54	13.71	1028	1
29	Bang Sue	Bangkok	100.53	13.82	1029	1
30	Chatuchak	Bangkok	100.57	13.82	1030	1
31	Bang Kho Laem	Bangkok	100.51	13.70	1031	1
32	Prawet	Bangkok	100.68	13.70	1032	1
33	Khlong Toei	Bangkok	100.58	13.71	1033	1
34	Suan Luang	Bangkok	100.63	13.72	1034	1
35	Chom Thong	Bangkok	100.47	13.69	1035	1
36	Don Mueang	Bangkok	100.60	13.92	1036	1
37	Ratchathewi	Bangkok	100.54	13.76	1037	1
38	Lat Phrao	Bangkok	100.62	13.83	1038	1
39	Watthana	Bangkok	100.59	13.73	1039	1
40	Bang Khae	Bangkok	100.40	13.71	1040	1
41	Lak Si	Bangkok	100.57	13.88	1041	1
42	Sai Mai	Bangkok	100.66	13.90	1042	1
43	Khan Na Yao	Bangkok	100.68	13.82	1043	1
44	Saphan Sung	Bangkok	100.69	13.76	1044	1
45	Wang Thong Laeng	Bangkok	100.61	13.78	1045	1
46	Khlong Sam Wa	Bangkok	100.74	13.87	1046	1
47	Bang Na	Bangkok	100.62	13.66	1047	1

APPENDIX B (continued) Locations of calculated centroids for all 925 district polygons.

	District	Province	Longitude	Latitude	Code	Region[1]
48	Thawi Watthana	Bangkok	100.37	13.77	1048	1
49	Thung Khru	Bangkok	100.50	13.63	1049	1
50	Bang Bon	Bangkok	100.40	13.66	1050	1
51	Mueang Samut Prakan	Samut Prakan	100.66	13.56	1101	1
52	Bang Bo	Samut Prakan	100.87	13.58	1102	1
53	Bang Phli	Samut Prakan	100.73	13.62	1103	1
54	Phra Pradaeng	Samut Prakan	100.56	13.65	1104	1
55	Phra Samut Chedi	Samut Prakan	100.52	13.55	1105	1
56	Bang Sao Thong	Samut Prakan	100.82	13.63	1106	1
57	Mueang Nonthaburi	Nonthaburi	100.50	13.86	1201	1
58	Bang Kruai	Nonthaburi	100.43	13.81	1202	1
59	Bang Yai	Nonthaburi	100.37	13.85	1203	1
60	Bang Bua Thong	Nonthaburi	100.40	13.93	1204	1
61	Sai Noi	Nonthaburi	100.31	14.01	1205	1
62	Pak Kret	Nonthaburi	100.50	13.93	1206	1
63	Khlong Luang	Pathum Thani	100.68	14.10	1301	1
64	Lam Luk Ka	Pathum Thani	100.79	13.98	1302	1
65	Lat Lum Kaeo	Pathum Thani	100.41	14.05	1303	1
66	Thanyaburi	Pathum Thani	100.76	14.03	1304	1
67	Mueang Pathum Thani	Pathum Thani	100.54	14.00	1305	1
68	Nong Suea	Pathum Thani	100.84	14.16	1306	1
69	Sam Khok	Pathum Thani	100.53	14.08	1307	1
70	Ban Phraek	Ayutthaya	100.55	14.64	1401	2
71	Bang Ban	Ayutthaya	100.47	14.38	1402	2
72	Bang Pahan	Ayutthaya	100.55	14.47	1403	2
73	Bang Pa-in	Ayutthaya	100.59	14.23	1404	2
74	Bang Say	Ayutthaya	100.30	14.32	1405	2
75	Maharat	Ayutthaya	100.54	14.57	1406	2
76	Lat Bua Luang	Ayutthaya	100.35	14.17	1407	2
77	Phachi	Ayutthaya	100.73	14.43	1408	2
78	Phak Hai	Ayutthaya	100.34	14.45	1409	2
79	Sena	Ayutthaya	100.38	14.29	1410	2
80	Tha Ruea	Ayutthaya	100.71	14.53	1411	2
81	Uthai	Ayutthaya	100.69	14.35	1412	2
82	Bang Sai	Ayutthaya	100.49	14.21	1413	2
83	Wang Noi	Ayutthaya	100.72	14.24	1414	2
84	Phra Nakhon Si Ayuttaya	Ayutthaya	100.56	14.35	1415	2
85	Nakhon Luang	Ayutthaya	100.63	14.47	1416	2
86	Chaiyo	Ang Thong	100.47	14.67	1501	2
87	Mueang Ang Thong	Ang Thong	100.45	14.58	1502	2
88	Pa Mok	Ang Thong	100.45	14.49	1503	2
89	Pho Thong	Ang Thong	100.35	14.67	1504	2
90	Wiset Chai Chan	Ang Thong	100.32	14.55	1505	2
91	Samko	Ang Thong	100.25	14.61	1506	2
92	Sawaeng Ha	Ang Thong	100.29	14.75	1507	2
93	Mueang Lop Buri	Lop BuriI	100.68	14.82	1601	2
94	Phatthana Nikhom	Lop BuriI	101.03	14.91	1602	2

APPENDIX B (continued) Locations of calculated centroids for all 925 district polygons.

	District	Province	Longitude	Latitude	Code	Region[1]
95	Khok Sumrong	Lop BuriI	100.78	15.04	1603	2
96	Chai Badan	Lop BuriI	101.12	15.19	1604	2
97	Tha Wung	Lop BuriI	100.51	14.83	1605	2
98	Ban Mi	Lop BuriI	100.56	15.07	1606	2
99	Tha Luang	Lop BuriI	101.20	15.05	1607	2
100	Sa Bot	Lop BuriI	100.89	15.25	1608	2
101	Khok Charoen	Lop BuriI	100.85	15.40	1609	2
102	Lam Sonthi	Lop BuriI	101.35	15.32	1610	2
103	Nong Muang	Lop BuriI	100.71	15.28	1611	2
104	Mueang Sing Buri	Sing Buri	100.40	14.89	1701	2
105	Bang Rachan	Sing Buri	100.28	14.90	1702	2
106	Khai Bang Rachan	Sing Buri	100.30	14.82	1703	2
107	Phrom Buri	Sing Buri	100.45	14.78	1704	2
108	Tha Chang	Sing Buri	100.39	14.78	1705	2
109	In Buri	Sing Buri	100.36	15.02	1706	2
110	Mueang Chai Nat	Chai Nat	100.14	15.19	1801	2
111	Manorom	Chai Nat	100.16	15.32	1802	2
112	Wat Sing	Chai Nat	99.98	15.21	1803	2
113	Sapphaya	Chai Nat	100.26	15.14	1804	2
114	Sankhaburi	Chai Nat	100.17	15.02	1805	2
115	Hankha	Chai Nat	99.96	15.05	1806	2
116	Nong Mamong	Chai Nat	99.83	15.23	1807	2
117	Noen Kham	Chai Nat	99.84	14.98	1808	2
118	Mueang Saraburi	Saraburi	100.93	14.50	1901	2
119	Kaeng Khoi	Saraburi	101.06	14.57	1902	2
120	Nong Khae	Saraburi	100.86	14.37	1903	2
121	Wihan Daeng	Saraburi	100.98	14.34	1904	2
122	Nong Saeng	Saraburi	100.81	14.48	1905	2
123	Ban Mo	Saraburi	100.73	14.61	1906	2
124	Don Phut	Saraburi	100.62	14.61	1907	2
125	Nong Don	Saraburi	100.70	14.69	1908	2
126	Phra Phutthabat	Saraburi	100.81	14.72	1909	2
127	Sao Hai	Saraburi	100.85	14.58	1910	2
128	Muak Lek	Saraburi	101.27	14.77	1911	2
129	Wang Mueng	Saraburi	101.14	14.83	1912	2
130	Cha Loem Pra Khiat	Saraburi	100.91	14.66	1913	2
131	Mueang Chon Buri	Chon Buri	101.00	13.34	2001	2
132	Ban Bueng	Chon Buri	101.18	13.25	2002	2
133	Nong Yai	Chon Buri	101.37	13.12	2003	2
134	Bang Lamung	Chon Buri	100.99	12.92	2004	2
135	Phan Thong	Chon Buri	101.09	13.45	2005	2
136	Phanat Nikhom	Chon Buri	101.22	13.47	2006	2
137	Si Racha	Chon Buri	101.05	13.13	2007	2
138	Ko Sichang	Chon Buri	100.81	13.15	2008	2
139	Sattahip	Chon Buri	100.92	12.72	2009	2
140	Bo Thong	Chon Buri	101.51	13.24	2010	2
141	Ko Chan	Chon Buri	101.38	13.40	2011	2

APPENDIX B (continued) Locations of calculated centroids for all 925 district polygons.

	District	Province	Longitude	Latitude	Code	Region[1]
142	Mueang Rayong	Rayong	101.35	12.72	2101	2
143	Ban Chang	Rayong	101.05	12.73	2102	2
144	Klaeng	Rayong	101.66	12.77	2103	2
145	Wang Chan	Rayong	101.53	12.98	2104	2
146	Ban Khai	Rayong	101.34	12.83	2105	2
147	Pluak Daeng	Rayong	101.24	12.97	2106	2
148	Khao Chamao	Rayong	101.68	12.97	2107	2
149	Nikhom Phatthana	Rayong	101.15	12.84	2108	2
150	Mueang Chanthaburi	Chanthaburi	102.12	12.60	2201	2
151	Khlung	Chanthaburi	102.30	12.54	2202	2
152	Tha Mai	Chanthaburi	101.98	12.73	2203	2
153	Pong Nam Ron	Chanthaburi	102.37	12.92	2204	2
154	Makham	Chanthaburi	102.23	12.73	2205	2
155	Laem Sing	Chanthaburi	102.12	12.46	2206	2
156	Soi Dao	Chanthaburi	102.24	13.17	2207	2
157	Kaeng Hang Maeo	Chanthaburi	101.89	13.10	2208	2
158	Na Yai Am	Chanthaburi	101.88	12.74	2209	2
159	Khao Khitchakut	Chanthaburi	102.10	12.93	2210	2
160	Mueang Trat	Trat	102.60	12.27	2301	2
161	Khlong Yai	Trat	102.83	11.93	2302	2
162	Khlao Saming	Trat	102.42	12.43	2303	2
163	Bo Rai	Trat	102.57	12.56	2304	2
164	Laem Ngop	Trat	102.37	12.22	2305	2
165	Ko Kut	Trat	102.56	11.68	2306	2
166	Ko Chang	Trat	102.34	12.04	2307	2
167	Mueang Chachoengsao	Chachoengsao	101.02	13.72	2401	2
168	Bang Khla	Chachoengsao	101.21	13.74	2402	2
169	Bang Nam Priao	Chachoengsao	101.03	13.88	2403	2
170	Bang Pakong	Chachoengsao	100.96	13.53	2404	2
171	Ban Pho	Chachoengsao	101.08	13.61	2405	2
172	Phanom Sarakham	Chachoengsao	101.41	13.75	2406	2
173	Ratchasan	Chachoengsao	101.28	13.79	2407	2
174	Sanam Chai Khet	Chachoengsao	101.64	13.64	2408	2
175	Plaeng Yao	Chachoengsao	101.34	13.57	2409	2
176	Tha Takaib	Chachoengsao	101.75	13.41	2410	2
177	Khlong Khuean	Chachoengsao	101.16	13.78	2411	2
178	Mueang Prachin Buri	Prachin Buri	101.39	14.10	2501	2
179	Kabin Buri	Prachin Buri	101.78	13.90	2502	2
180	Na Di	Prachin Buri	101.86	14.20	2503	2
181	Ban Sang	Prachin Buri	101.25	13.95	2506	2
182	Prachantakham	Prachin Buri	101.56	14.23	2507	2
183	Si Maha Phot	Prachin Buri	101.53	13.90	2508	2
184	Si Mahosot	Prachin Buri	101.42	13.89	2509	2
185	Mueang Nakhon Nayok	Nakhon Nayok	101.24	14.28	2601	2
186	Pak Phli	Nakhon Nayok	101.35	14.23	2602	2
187	Ban Na	Nakhon Nayok	101.07	14.27	2603	2
188	Ongkharak	Nakhon Nayok	101.01	14.07	2604	2

APPENDIX B (continued) Locations of calculated centroids for all 925 district polygons.

	District	Province	Longitude	Latitude	Code	Region[1]
189	Mueang Sa Kaeo	Sa Kaeo	102.11	13.93	2701	5
190	Khlong Hat	Sa Kaeo	102.28	13.48	2702	5
191	Ta Phraya	Sa Kaeo	102.72	14.06	2703	5
192	Wang Num Yen	Sa Kaeo	102.08	13.52	2704	5
193	Watthana Nakhon	Sa Kaeo	102.36	13.89	2705	5
194	Arunyaprathet	Sa Kaeo	102.48	13.69	2706	5
195	Kao Chakun	Sa Kaeo	102.03	13.64	2707	5
196	Khok Sung	Sa Kaeo	102.66	13.87	2708	5
197	Wang Sombun	Sa Kaeo	102.13	13.36	2709	5
198	Mueang Nakhon Ratchasima	Nakhon Ratchasima	102.10	14.97	3001	5
199	Khon Buri	Nakhon Ratchasima	102.22	14.38	3002	5
200	Soeng Sang	Nakhon Ratchasima	102.48	14.36	3003	5
201	Khong	Nakhon Ratchasima	102.29	15.43	3004	5
202	Ban Lueam	Nakhon Ratchasima	102.14	15.58	3005	5
203	Chakkarat	Nakhon Ratchasima	102.44	14.95	3006	5
204	Chok Chai	Nakhon Ratchasima	102.21	14.76	3007	5
205	Dan Khun Thot	Nakhon Ratchasima	101.69	15.21	3008	5
206	Non Thai	Nakhon Ratchasima	102.02	15.19	3009	5
207	Non Sung	Nakhon Ratchasima	102.28	15.21	3010	5
208	Kham Sakaesaeng	Nakhon Ratchasima	102.17	15.38	3011	5
209	Bua Yai	Nakhon Ratchasima	102.38	15.59	3012	5
210	Prathai	Nakhon Ratchasima	102.71	15.56	3013	5
211	Pak Thong Chai	Nakhon Ratchasima	101.95	14.66	3014	5
212	Phimai	Nakhon Ratchasima	102.55	15.25	3015	5
213	Huai Thalaeng	Nakhon Ratchasima	102.64	15.04	3016	5
214	Chum Phuang	Nakhon Ratchasima	102.75	15.25	3017	5
215	Sung Noen	Nakhon Ratchasima	101.83	14.86	3018	5
216	Kham Thale So	Nakhon Ratchasima	101.94	15.02	3019	5
217	Si Khiu	Nakhon Ratchasima	101.61	14.93	3020	5
218	Pak Chong	Nakhon Ratchasima	101.45	14.62	3021	5
219	Nong Bunnak	Nakhon Ratchasima	102.37	14.73	3022	5
220	Kaeng Sanam Nang	Nakhon Ratchasima	102.24	15.70	3023	5
221	Non Daeng	Nakhon Ratchasima	102.54	15.45	3024	5
222	Wang Nam Khiaw	Nakhon Ratchasima	101.86	14.45	3025	5
223	Te Pha Rak	Nakhon Ratchasima	101.51	15.29	3026	5
224	Muang Yang	Nakhon Ratchasima	102.89	15.44	3027	5
225	Phra Thong Kham	Nakhon Ratchasima	101.99	15.36	3028	5
226	Lam Tha Men Chai	Nakhon Ratchasima	102.89	15.30	3029	5
227	Bua Lai	Nakhon Ratchasima	102.52	15.67	3030	5
228	Sida	Nakhon Ratchasima	102.54	15.56	3031	5
229	Cha Loem Pra Khiat	Nakhon Ratchasima	102.29	14.97	3032	5
230	Mueang Buri Ram	Buri Ram	103.07	14.94	3101	5
231	Khu Mueang	Buri Ram	103.04	15.27	3102	5
232	Krasang	Buri Ram	103.32	14.94	3103	5
233	Nang Rong	Buri Ram	102.76	14.63	3104	5
234	Nong Ki	Buri Ram	102.54	14.71	3105	5
235	Lahan Sai	Buri Ram	102.89	14.33	3106	5

APPENDIX B (continued) Locations of calculated centroids for all 925 district polygons.

	District	Province	Longitude	Latitude	Code	Region[1]
236	Prakhon Chai	Buri Ram	103.06	14.61	3107	5
237	Ban Kruat	Buri Ram	103.12	14.39	3108	5
238	Phutthaisong	Buri Ram	103.00	15.53	3109	5
239	Lum Plaimat	Buri Ram	102.87	15.02	3110	5
240	Satuek	Buri Ram	103.32	15.23	3111	5
241	Pakham	Buri Ram	102.67	14.41	3112	5
242	Na Pho	Buri Ram	102.94	15.70	3113	5
243	Nong Hong	Buri Ram	102.67	14.86	3114	5
244	Phlapphla Chai	Buri Ram	103.17	14.73	3115	5
245	Huai Rat	Buri Ram	103.23	15.00	3116	5
246	Non Suwan	Buri Ram	102.58	14.56	3117	5
247	Chamni	Buri Ram	102.84	14.79	3118	5
248	Ban Mai Chaiyapot	Buri Ram	102.85	15.57	3119	5
249	Non Din Daeng	Buri Ram	102.69	14.23	3120	5
250	Ban Dan	Buri Ram	103.19	15.12	3121	5
251	Khaen Dong	Buri Ram	103.12	15.31	3122	5
252	Cha Roem Pra Khiat	Buri Ram	102.89	14.56	3123	5
253	Mueang Surin	Surin	103.51	14.88	3201	5
254	Chumphon Buri	Surin	103.37	15.38	3202	5
255	Tha Tum	Surin	103.65	15.31	3203	5
256	Chom Phra	Surin	103.58	15.14	3204	5
257	Prasat	Surin	103.42	14.63	3205	5
258	Kap Choeng	Surin	103.59	14.46	3206	5
259	Rattanaburi	Surin	103.91	15.34	3207	5
260	Sanom	Surin	103.78	15.18	3208	5
261	Sikhoraphum	Surin	103.78	14.95	3209	5
262	Sangkha	Surin	103.84	14.57	3210	5
263	Lamduan	Surin	103.69	14.72	3211	5
264	Samrong Thap	Surin	103.94	15.04	3212	5
265	Bua Ched	Surin	103.98	14.48	3213	5
266	Phanom Dongrak	Surin	103.31	14.43	3214	5
267	Sri Narong	Surin	103.89	14.79	3215	5
268	Khwao Sinarin	Surin	103.62	15.00	3216	5
269	Non Narai	Surin	103.91	15.19	3217	5
270	Mueang Si Sa Ket	Si Sa Ket	104.35	15.08	3301	5
271	Yang Chum Noi	Si Sa Ket	104.39	15.24	3302	5
272	Kanthararom	Si Sa Ket	104.58	15.12	3303	5
273	Kantharalak	Si Sa Ket	104.68	14.57	3304	5
274	Khukhan	Si Sa Ket	104.19	14.72	3305	5
275	Phrai Bueng	Si Sa Ket	104.35	14.77	3306	5
276	Prang Ku	Si Sa Ket	104.04	14.86	3307	5
277	Khun Han	Si Sa Ket	104.41	14.54	3308	5
278	Rasi Salai	Si Sa Ket	104.18	15.36	3309	5
279	Uthumphon Phisai	Si Sa Ket	104.16	15.12	3310	5
280	Bueng Bun	Si Sa Ket	104.07	15.30	3311	5
281	Huai Thap Thun	Si Sa Ket	104.04	15.02	3312	5
282	Non Khun	Si Sa Ket	104.70	14.90	3313	5

APPENDIX B (continued) Locations of calculated centroids for all 925 district polygons.

	District	Province	Longitude	Latitude	Code	Region[1]
283	Si Rattana	Si Sa Ket	104.49	14.79	3314	5
284	Nam Kliang	Si Sa Ket	104.53	14.92	3315	5
285	Wang Hin	Si Sa Ket	104.22	14.96	3316	5
286	Phu Sing	Si Sa Ket	104.15	14.49	3317	5
287	Mueang Chan	Si Sa Ket	104.03	15.18	3318	5
288	Benchalak	Si Sa Ket	104.72	14.78	3319	5
289	Phayu	Si Sa Ket	104.39	14.91	3320	5
290	Pho Si Suwan	Si Sa Ket	104.07	15.24	3321	5
291	Si La Lad	Si Sa Ket	104.10	15.50	3322	5
292	Mueang Ubon Ratchathani	Ubon Ratchathani	104.83	15.30	3401	5
293	Si Mueang Mai	Ubon Ratchathani	105.36	15.56	3402	5
294	Khong Chiam	Ubon Ratchathani	105.50	15.45	3403	5
295	Khueang Nai	Ubon Ratchathani	104.54	15.39	3404	5
296	Khemarat	Ubon Ratchathani	105.15	15.97	3405	5
297	Det Udom	Ubon Ratchathani	105.08	14.85	3407	5
298	Na Chaluai	Ubon Ratchathani	105.22	14.57	3408	5
299	Nam Yuen	Ubon Ratchathani	105.08	14.43	3409	5
300	Buntharik	Ubon Ratchathani	105.40	14.70	3410	5
301	Trakan Phuet Phon	Ubon Ratchathani	105.07	15.61	3411	5
302	Kut Kaopun	Ubon Ratchathani	105.05	15.82	3412	5
303	Muang Sam Sip	Ubon Ratchathani	104.73	15.52	3414	5
304	Warin Chamrap	Ubon Ratchathani	104.87	15.12	3415	5
305	Phibun Mangsahan	Ubon Ratchathani	105.24	15.15	3419	5
306	Tan Sum	Ubon Ratchathani	105.16	15.39	3420	5
307	Pho Sai	Ubon Ratchathani	105.34	15.76	3421	5
308	Samrong	Ubon Ratchathani	104.79	14.98	3422	5
309	Don Mot Daeng	Ubon Ratchathani	105.03	15.38	3424	5
310	Sirindhorn	Ubon Ratchathani	105.44	15.11	3425	5
311	Thung Si Udom	Ubon Ratchathani	104.93	14.74	3426	5
312	Na yia	Ubon Ratchathani	105.06	15.04	3429	5
313	Na Tan	Ubon Ratchathani	105.29	15.93	3430	5
314	Lao Suea Kok	Ubon Ratchathani	104.92	15.44	3431	5
315	Sawang Wirawong	Ubon Ratchathani	105.08	15.24	3432	5
316	Nam Khun	Ubon Ratchathani	104.91	14.55	3433	5
317	Mueang Yasothon	Yasothon	104.17	15.85	3501	5
318	Sai Mun	Yasothon	104.20	15.98	3502	5
319	Kut Chum	Yasothon	104.29	16.05	3503	5
320	Kham Khuen Kaeo	Yasothon	104.34	15.65	3504	5
321	Pa Tio	Yasothon	104.40	15.84	3505	5
322	Maha Chana Chai	Yasothon	104.26	15.51	3506	5
323	Kho Wang	Yasothon	104.34	15.38	3507	5
324	Loeng Nok Tha	Yasothon	104.52	16.20	3508	5
325	Thai Chaloen	Yasothon	104.45	16.07	3509	5
326	Mueang Chaiyaphum	Chaiyaphum	102.04	15.86	3601	5
327	Ban Khwao	Chaiyaphum	101.84	15.82	3602	5
328	Khon Sawan	Chaiyaphum	102.28	15.93	3603	5
329	Kaset Sombun	Chaiyaphum	101.92	16.27	3604	5

APPENDIX B (continued) Locations of calculated centroids for all 925 district polygons.

	District	Province	Longitude	Latitude	Code	Region[1]
330	Nong Bua Daeng	Chaiyaphum	101.63	16.19	3605	5
331	Chatturat	Chaiyaphum	101.85	15.58	3606	5
332	Bamnet Narong	Chaiyaphum	101.64	15.47	3607	5
333	Nong Bua Rawe	Chaiyaphum	101.63	15.82	3608	5
334	Thep Sathit	Chaiyaphum	101.48	15.58	3609	5
335	Phu Khiao	Chaiyaphum	102.16	16.36	3610	5
336	Ban Thaen	Chaiyaphum	102.35	16.38	3611	5
337	Kaeng Khro	Chaiyaphum	102.21	16.14	3612	5
338	Khon San	Chaiyaphum	101.71	16.54	3613	5
339	Phakdi Chumphon	Chaiyaphum	101.41	15.96	3614	5
340	Noen Sa-nga	Chaiyaphum	101.99	15.55	3615	5
341	Sup Yai	Chaiyaphum	101.64	15.60	3616	5
342	Mueang Amnat Charoen	Amnat Charoen	104.65	15.88	3701	5
343	Chanuman	Amnat Charoen	104.93	16.13	3702	5
344	Pathum Ratchawongsa	Amnat Charoen	104.91	15.90	3703	5
345	Phana	Amnat Charoen	104.86	15.67	3704	5
346	Senangkhanikhom	Amnat Charoen	104.69	16.05	3705	5
347	Hua Taphan	Amnat Charoen	104.53	15.68	3706	5
348	Lue Amnat	Amnat Charoen	104.71	15.71	3707	5
349	Mueang Nong Bua Lamphu	Nong Bua Lam Phu	102.40	17.15	3901	5
350	Na Klang	Nong Bua Lam Phu	102.22	17.32	3902	5
351	Non Sang	Nong Bua Lam Phu	102.53	16.90	3903	5
352	Si Bun Ruang	Nong Bua Lam Phu	102.21	17.00	3904	5
353	Suwannakhuha	Nong Bua Lam Phu	102.25	17.55	3905	5
354	Na Wang	Nong Bua Lam Phu	102.07	17.35	3906	5
355	Mueang Khon Kaen	Khon Kaen	102.81	16.46	4001	5
356	Ban Fang	Khon Kaen	102.62	16.49	4002	5
357	Phra Yuen	Khon Kaen	102.67	16.31	4003	5
358	Nong Ruea	Khon Kaen	102.45	16.49	4004	5
359	Chum Phae	Khon Kaen	102.10	16.62	4005	5
360	Si Chomphu	Khon Kaen	102.13	16.76	4006	5
361	Nam Phong	Khon Kaen	102.88	16.70	4007	5
362	Ubolratana	Khon Kaen	102.68	16.78	4008	5
363	Kranuan	Khon Kaen	103.08	16.75	4009	5
364	Ban Phai	Khon Kaen	102.78	16.04	4010	5
365	Puai Noi	Khon Kaen	102.87	15.89	4011	5
366	Phon	Khon Kaen	102.59	15.80	4012	5
367	Waeng Yai	Khon Kaen	102.46	15.92	4013	5
368	Waeng Noi	Khon Kaen	102.42	15.80	4014	5
369	Nong Song Hong	Khon Kaen	102.79	15.76	4015	5
370	Phu Wiang	Khon Kaen	102.41	16.68	4016	5
371	Mancha Khiri	Khon Kaen	102.52	16.21	4017	5
372	Chonnabot	Khon Kaen	102.56	16.02	4018	5
373	Khao Suan Kwang	Khon Kaen	102.78	16.92	4019	5
374	Phu Pha Man	Khon Kaen	101.87	16.72	4020	5
375	Sam Sung	Khon Kaen	103.06	16.56	4021	5
376	Khok Pho Chai	Khon Kaen	102.39	16.07	4022	5

APPENDIX B (continued) Locations of calculated centroids for all 925 district polygons.

	District	Province	Longitude	Latitude	Code	Region[1]
377	Nong Na Khum	Khon Kaen	102.32	16.81	4023	5
378	Ban Haet	Khon Kaen	102.77	16.20	4024	5
379	Non Sila	Khon Kaen	102.69	15.96	4025	5
380	Mueang Udon Thani	Udon Thani	102.79	17.39	4101	5
381	Kut Chap	Udon Thani	102.53	17.44	4102	5
382	Nong Wua So	Udon Thani	102.59	17.19	4103	5
383	Kumphawapi	Udon Thani	103.00	17.09	4104	5
384	Non Sa-at	Udon Thani	102.91	16.95	4105	5
385	Nong Han	Udon Thani	103.10	17.36	4106	5
386	Thung Fon	Udon Thani	103.22	17.49	4107	5
387	Chai Wan	Udon Thani	103.28	17.22	4108	5
388	Si That	Udon Thani	103.23	17.03	4109	5
389	Wang Sam Mo	Udon Thani	103.46	17.05	4110	5
390	Ban Dung	Udon Thani	103.26	17.71	4111	5
391	Ban Phu	Udon Thani	102.46	17.65	4117	5
392	Num Som	Udon Thani	102.18	17.75	4118	5
393	Phen	Udon Thani	102.93	17.66	4119	5
394	Sang Khom	Udon Thani	103.05	17.79	4120	5
395	Nong Saeng	Udon Thani	102.79	17.14	4121	5
396	Na Yung	Udon Thani	102.17	17.93	4122	5
397	Phibun Rak	Udon Thani	103.08	17.53	4123	5
398	Ku Kaeo	Udon Thani	103.16	17.17	4124	5
399	Prachak Silapakhom	Udon Thani	102.99	17.25	4125	5
400	Mueang Loei	Loei	101.72	17.54	4201	5
401	Na Duang	Loei	101.99	17.54	4202	5
402	Chiang Khan	Loei	101.74	17.82	4203	5
403	Pak Chom	Loei	101.96	17.92	4204	5
404	Dan Sai	Loei	101.23	17.22	4205	5
405	Na Haeo	Loei	101.00	17.44	4206	5
406	Phu Ruea	Loei	101.42	17.35	4207	5
407	Tha Li	Loei	101.44	17.61	4208	5
408	Wang Saphung	Loei	101.74	17.27	4209	5
409	Phu Kradueng	Loei	101.85	16.90	4210	5
410	Phu Luang	Loei	101.64	17.10	4211	5
411	Pha Khao	Loei	102.02	17.05	4212	5
412	A-rawan	Loei	101.98	17.29	4213	5
413	Nong Hin	Loei	101.83	17.08	4214	5
414	Mueang Nong Khai	Nong Khai	102.79	17.83	4301	5
415	Tha Bo	Nong Khai	102.56	17.80	4302	5
416	Bueng Kan	Nong Khai	103.63	18.30	4303	5
417	Phon Charoen	Nong Khai	103.65	18.07	4304	5
418	Phon Phisai	Nong Khai	103.13	17.95	4305	5
419	So Phisai	Nong Khai	103.45	18.14	4306	5
420	Si Chiang Mai	Nong Khai	102.50	17.94	4307	5
421	Sangkhom	Nong Khai	102.22	18.06	4308	5
422	Seka	Nong Khai	103.91	17.98	4309	5
423	Pak Khat	Nong Khai	103.34	18.28	4310	5

APPENDIX B (continued) Locations of calculated centroids for all 925 district polygons.

	District	Province	Longitude	Latitude	Code	Region[1]
424	Bueng Khong Long	Nong Khai	104.08	18.00	4311	5
425	Sri Wilai	Nong Khai	103.79	18.15	4312	5
426	Bueng Khla	Nong Khai	104.00	18.25	4313	5
427	Srakhai	Nong Khai	102.70	17.66	4314	5
428	Fao Rai	Nong Khai	103.30	18.00	4315	5
429	Rattanawapi	Nong Khai	103.24	18.19	4316	5
430	Pho Tak	Nong Khai	102.43	17.89	4317	5
431	Mueang Maha Sarakham	Maha Sarakham	103.31	16.12	4401	5
432	Kae Dam	Maha Sarakham	103.40	16.05	4402	5
433	Kosum Phisai	Maha Sarakham	103.00	16.25	4403	5
434	Kantharawichai	Maha Sarakham	103.27	16.28	4404	5
435	Chiang Yuen	Maha Sarakham	103.08	16.41	4405	5
436	Borabue	Maha Sarakham	103.13	15.99	4406	5
437	Na Chueak	Maha Sarakham	103.04	15.81	4407	5
438	Phayakkhaphum Phisa	Maha Sarakham	103.24	15.53	4408	5
439	Wapi Pathum	Maha Sarakham	103.35	15.86	4409	5
440	Na Dun	Maha Sarakham	103.24	15.73	4410	5
441	Yang Sisurat	Maha Sarakham	103.10	15.65	4411	5
442	Kut Rang	Maha Sarakham	102.96	16.04	4412	5
443	Chuen Chom	Maha Sarakham	103.15	16.54	4413	5
444	Mueang Roi Et	Roi Et	103.61	16.01	4501	5
445	Kaset Wisai	Roi Et	103.57	15.60	4502	5
446	Pathum Rat	Roi Et	103.39	15.62	4503	5
447	Chaturaphak Phiman	Roi Et	103.55	15.82	4504	5
448	Thawat Buri	Roi Et	103.78	16.03	4505	5
449	Phanom Phrai	Roi Et	104.08	15.69	4506	5
450	Phon Thong	Roi Et	103.96	16.29	4507	5
451	Pho Chai	Roi Et	103.80	16.32	4508	5
452	Nong Phok	Roi Et	104.22	16.30	4509	5
453	Selaphum	Roi Et	104.00	16.05	4510	5
454	Suwannaphum	Roi Et	103.81	15.60	4511	5
455	Mueang Suang	Roi Et	103.75	15.78	4512	5
456	Phon Sai	Roi Et	103.94	15.49	4513	5
457	At Samat	Roi Et	103.87	15.84	4514	5
458	Moei Wadi	Roi Et	104.11	16.37	4515	5
459	Sri Somdet	Roi Et	103.52	16.02	4516	5
460	Changhan	Roi Et	103.62	16.16	4517	5
461	Chiang Khwan	Roi Et	103.75	16.15	4518	5
462	Nong Hee	Roi Et	104.01	15.58	4519	5
463	Thung Kao Luang	Roi Et	103.87	15.99	4520	5
464	Mueang Kalasin	Kalasin	103.56	16.51	4601	5
465	Na Mon	Kalasin	103.80	16.58	4602	5
466	Kamalasai	Kalasin	103.61	16.28	4603	5
467	Rong Kham	Kalasin	103.72	16.29	4604	5
468	Kuchinarai	Kalasin	104.06	16.52	4605	5
469	Khao Wong	Kalasin	104.11	16.68	4606	5
470	Yang Talat	Kalasin	103.35	16.44	4607	5

APPENDIX B (continued) Locations of calculated centroids for all 925 district polygons.

	District	Province	Longitude	Latitude	Code	Region[1]
471	Huai Mek	Kalasin	103.24	16.59	4608	5
472	Sahatsakhan	Kalasin	103.58	16.72	4609	5
473	Kham Muang	Kalasin	103.65	16.95	4610	5
474	Tha Khantho	Kalasin	103.25	16.89	4611	5
475	Nong Kung Si	Kalasin	103.33	16.73	4612	5
476	Somdet	Kalasin	103.76	16.77	4613	5
477	Huai Phueng	Kalasin	103.89	16.68	4614	5
478	Sam Chai	Kalasin	103.53	16.88	4615	5
479	Na Khu	Kalasin	104.01	16.76	4616	5
480	Don Chan	Kalasin	103.72	16.47	4617	5
481	Khong Chai	Kalasin	103.48	16.26	4618	5
482	Mueang Sakon Nakhon	Sakon Nakhon	104.10	17.15	4701	5
483	Kusuman	Sakon Nakhon	104.27	17.35	4702	5
484	Kut Bak	Sakon Nakhon	103.75	17.08	4703	5
485	Phanna Nakhom	Sakon Nakhon	103.90	17.31	4704	5
486	Phang Khon	Sakon Nakhon	103.75	17.38	4705	5
487	Waritchaphum	Sakon Nakhon	103.61	17.26	4706	5
488	Nikhom Nam Un	Sakon Nakhon	103.72	17.18	4707	5
489	Wanon Niwat	Sakon Nakhon	103.74	17.62	4708	5
490	Kham Ta Kla	Sakon Nakhon	103.79	17.82	4709	5
491	Ban Muang	Sakon Nakhon	103.53	17.89	4710	5
492	Akat Amnuai	Sakon Nakhon	103.98	17.64	4711	5
493	Sawang Daen Din	Sakon Nakhon	103.45	17.45	4712	5
494	Song Dao	Sakon Nakhon	103.45	17.31	4713	5
495	Tao Ngoi	Sakon Nakhon	104.15	16.95	4714	5
496	Khok Si Suphan	Sakon Nakhon	104.31	17.03	4715	5
497	Charoen Sin	Sakon Nakhon	103.53	17.63	4716	5
498	Phon Na Kaew	Sakon Nakhon	104.31	17.21	4717	5
499	Phu Phan	Sakon Nakhon	103.91	16.97	4718	5
500	Mueang Nakhon Phanom	Nakhon Phanom	104.67	17.32	4801	5
501	Pla Pak	Nakhon Phanom	104.54	17.20	4802	5
502	Tha Uthen	Nakhon Phanom	104.51	17.60	4803	5
503	Ban Phaeng	Nakhon Phanom	104.23	17.87	4804	5
504	That Phanom	Nakhon Phanom	104.71	16.96	4805	5
505	Renu Nakhon	Nakhon Phanom	104.65	17.05	4806	5
506	Na Kae	Nakhon Phanom	104.51	16.94	4807	5
507	Si Songkhram	Nakhon Phanom	104.23	17.64	4808	5
508	Na Wa	Nakhon Phanom	104.10	17.50	4809	5
509	Phoe Sawan	Nakhon Phanom	104.41	17.47	4810	5
510	Na Thom	Nakhon Phanom	104.11	17.84	4811	5
511	Wang Yang	Nakhon Phanom	104.42	17.04	4812	5
512	Mueang Mukdahan	Mukdahan	104.63	16.55	4901	5
513	Nikom Kham Soi	Mukdahan	104.56	16.36	4902	5
514	Don Tan	Mukdahan	104.82	16.29	4903	5
515	Dong Luang	Mukdahan	104.35	16.80	4904	5
516	Khamcha-i	Mukdahan	104.35	16.61	4905	5
517	wan Yai	Mukdahan	104.73	16.72	4906	5

APPENDIX B (continued) Locations of calculated centroids for all 925 district polygons.

	District	Province	Longitude	Latitude	Code	Region[1]
518	Nong Sung	Mukdahan	104.34	16.45	4907	5
519	Mueang Chiang Mai	Chiang Mai	98.97	18.79	5001	3
520	Chom Thong	Chiang Mai	98.61	18.37	5002	3
521	Mae Chaem	Chiang Mai	98.31	18.67	5003	3
522	Chiang Dao	Chiang Mai	98.91	19.51	5004	3
523	Doi Saket	Chiang Mai	99.22	18.94	5005	3
524	Mae Taeng	Chiang Mai	98.86	19.18	5006	3
525	Mae Rim	Chiang Mai	98.88	18.94	5007	3
526	Samoeng	Chiang Mai	98.64	18.91	5008	3
527	Fang	Chiang Mai	99.17	19.88	5009	3
528	Mae Ai	Chiang Mai	99.34	20.00	5010	3
529	Phrao	Chiang Mai	99.22	19.29	5011	3
530	San Pa Tong	Chiang Mai	98.88	18.61	5012	3
531	San Kamphaeng	Chiang Mai	99.16	18.74	5013	3
532	San Sai	Chiang Mai	99.03	18.95	5014	3
533	Hang Dong	Chiang Mai	98.89	18.74	5015	3
534	Hot	Chiang Mai	98.48	18.12	5016	3
535	Doi Tao	Chiang Mai	98.66	17.90	5017	3
536	Omkoi	Chiang Mai	98.34	17.69	5018	3
537	Saraphi	Chiang Mai	99.02	18.69	5019	3
538	Wiang Haeng	Chiang Mai	98.66	19.59	5020	3
539	Chai Prakan	Chiang Mai	99.18	19.68	5021	3
540	Mae Wang	Chiang Mai	98.66	18.67	5022	3
541	Mae On	Chiang Mai	99.30	18.74	5023	3
542	Doi lo	Chiang Mai	98.76	18.53	5024	3
543	Mueang Lamphun	Lamphun	99.07	18.55	5101	3
544	Mae Tha	Lamphun	99.09	18.39	5102	3
545	Ban Hong	Lamphun	98.83	18.26	5103	3
546	Li	Lamphun	98.89	17.79	5104	3
547	Thung Hua Chang	Lamphun	99.06	17.98	5105	3
548	Pa Sang	Lamphun	98.89	18.42	5106	3
549	Ban Ti	Lamphun	99.16	18.65	5107	3
550	Wiang Nong Long	Lamphun	98.75	18.42	5108	3
551	Mueang Lamp Pang	Lampang	99.54	18.41	5201	3
552	Mae Mo	Lampang	99.83	18.40	5202	3
553	Ko Kha	Lampang	99.35	18.14	5203	3
554	Soem Ngam	Lampang	99.16	18.09	5204	3
555	Ngao	Lampang	99.93	18.75	5205	3
556	Chae Hom	Lampang	99.65	18.74	5206	3
557	Wang Nuea	Lampang	99.64	19.14	5207	3
558	Thoen	Lampang	99.29	17.56	5208	3
559	Mae Phrik	Lampang	99.06	17.50	5209	3
560	Mae Tha	Lampang	99.58	18.11	5210	3
561	Sop Prap	Lampang	99.34	17.89	5211	3
562	Hang Chat	Lampang	99.28	18.35	5212	3
563	Mueang Phan	Lampang	99.45	18.79	5213	3
564	Mueang Uttaradit	Uttaradit	100.18	17.69	5301	3

APPENDIX B (continued) Locations of calculated centroids for all 925 district polygons.

	District	Province	Longitude	Latitude	Code	Region[1]
565	Tron	Uttaradit	100.12	17.46	5302	3
566	Tha Pla	Uttaradit	100.47	17.86	5303	3
567	Nam Pat	Uttaradit	100.73	17.70	5304	3
568	Fak Tha	Uttaradit	100.89	18.00	5305	3
569	Ban Khok	Uttaradit	101.07	18.15	5306	3
570	Phichai	Uttaradit	100.13	17.30	5307	3
571	Lap Lae	Uttaradit	100.02	17.65	5308	3
572	Thong Saen Khan	Uttaradit	100.39	17.50	5309	3
573	Mueang Phrae	Phrae	100.25	18.11	5401	3
574	Rong Kwang	Phrae	100.38	18.33	5402	3
575	Long	Phrae	99.89	18.13	5403	3
576	Sung Men	Phrae	100.13	18.04	5404	3
577	Den Chai	Phrae	100.02	17.92	5405	3
578	Song	Phrae	100.22	18.58	5406	3
579	Wang Chin	Phrae	99.64	17.86	5407	3
580	Nong Muang Khai	Phrae	100.15	18.29	5408	3
581	Mueang Nan	Nan	100.68	18.88	5501	3
582	Mae Charim	Nan	101.11	18.71	5502	3
583	Ban Luang	Nan	100.46	18.87	5503	3
584	Na Noi	Nan	100.76	18.30	5504	3
585	Pua	Nan	101.01	19.14	5505	3
586	Tha Wang Pha	Nan	100.76	19.13	5506	3
587	Wiang Sa	Nan	100.71	18.56	5507	3
588	Thung Chang	Nan	100.93	19.47	5508	3
589	Chiang Klang	Nan	100.88	19.31	5509	3
590	No Muen	Nan	100.59	18.12	5510	3
591	Santi Suk	Nan	100.99	18.91	5511	3
592	Bo Kluea	Nan	101.21	19.09	5512	3
593	Song Khae	Nan	100.65	19.42	5513	3
594	Phu Phiang	Nan	100.87	18.78	5514	3
595	Cha Loem Pra Khiat	Nan	101.15	19.49	5515	3
596	Mueang Phayao	Phayao	99.87	19.14	5601	3
597	Chun	Phayao	100.15	19.37	5602	3
598	Chiang Kham	Phayao	100.34	19.47	5603	3
599	Chiang Muan	Phayao	100.28	18.94	5604	3
600	Dok Khamtai	Phayao	100.06	19.11	5605	3
601	Pong	Phayao	100.39	19.19	5606	3
602	Mae Chai	Phayao	99.80	19.38	5607	3
603	Phu Sang	Phayao	100.37	19.62	5608	3
604	Phu Kham Yao	Phayao	99.97	19.32	5609	3
605	Mueang Chiang Rai	Chiang Rai	99.79	19.92	5701	3
606	Wiang Chai	Chiang Rai	100.00	19.87	5702	3
607	Chiang Khong	Chiang Rai	100.34	20.14	5703	3
608	Thoeng	Chiang Rai	100.20	19.69	5704	3
609	Phan	Chiang Rai	99.76	19.57	5705	3
610	Pa Daet	Chiang Rai	99.98	19.51	5706	3
611	Mae Chan	Chiang Rai	99.86	20.18	5707	3

APPENDIX B (continued) Locations of calculated centroids for all 925 district polygons.

	District	Province	Longitude	Latitude	Code	Region[1]
612	Chiang Saen	Chiang Rai	100.16	20.26	5708	3
613	Mae Sai	Chiang Rai	99.92	20.36	5709	3
614	Mae Suai	Chiang Rai	99.48	19.69	5710	3
615	Wiang Pa Pao	Chiang Rai	99.44	19.29	5711	3
616	Phaya Mengrai	Chiang Rai	100.16	19.87	5712	3
617	Wiang Kaen	Chiang Rai	100.47	20.00	5713	3
618	Khun Tan	Chiang Rai	100.28	19.86	5714	3
619	Mae Fa Luang	Chiang Rai	99.64	20.23	5715	3
620	Mae Lao	Chiang Rai	99.71	19.77	5716	3
621	Wiang Chiang Roong	Chiang Rai	100.07	20.02	5717	3
622	Doi Luang	Chiang Rai	100.12	20.14	5718	3
623	Mueang Mae Hong Son	Mae Hong Son	98.02	19.28	5801	3
624	Khun Yuam	Mae Hong Son	97.90	18.83	5802	3
625	Pai	Mae Hong Son	98.42	19.32	5803	3
626	Mae Sariang	Mae Hong Son	97.78	18.28	5804	3
627	Mae La Noi	Mae Hong Son	97.99	18.48	5805	3
628	Sob Muei	Mae Hong Son	97.97	17.91	5806	3
629	Pang Mapha	Mae Hong Son	98.21	19.61	5807	3
630	Mueang Nakhon Sawan	Nakhon Sawan	100.10	15.72	6001	3
631	Krok Phra	Nakhon Sawan	100.02	15.58	6002	3
632	Chum Saeng	Nakhon Sawan	100.29	15.85	6003	3
633	Nong Bua	Nakhon Sawan	100.63	15.87	6004	3
634	Banphot Phisai	Nakhon Sawan	99.99	16.00	6005	3
635	Kao Lieo	Nakhon Sawan	100.10	15.89	6006	3
636	Takhli	Nakhon Sawan	100.38	15.26	6007	3
637	Tha Tako	Nakhon Sawan	100.46	15.66	6008	3
638	Phaisali	Nakhon Sawan	100.69	15.59	6009	3
639	Phayuha Khiri	Nakhon Sawan	100.22	15.51	6010	3
640	Lat Yao	Nakhon Sawan	99.78	15.77	6011	3
641	Tak Fa	Nakhon Sawan	100.47	15.38	6012	3
642	MaeWong	Nakhon Sawan	99.41	15.84	6013	3
643	Mae Poen	Nakhon Sawan	99.31	15.73	6014	3
644	Chum Ta Bong	Nakhon Sawan	99.52	15.68	6015	3
645	Mueang Uthai Thani	Uthai Thani	100.02	15.40	6101	3
646	Thap Than	Uthai Thani	99.83	15.49	6102	3
647	Sawang Arom	Uthai Thani	99.79	15.60	6103	3
648	Nong Chang	Uthai Thani	99.77	15.37	6104	3
649	Nong Khayang	Uthai Thani	99.95	15.35	6105	3
650	Ban Rai	Uthai Thani	99.33	15.25	6106	3
651	Lan Sak	Uthai Thani	99.47	15.52	6107	3
652	Huai Khot	Uthai Thani	99.53	15.32	6108	3
653	Mueang Kamphaeng Phet	Kamphaeng Phet	99.51	16.43	6201	3
654	Sai Ngam	Kamphaeng Phet	99.87	16.44	6202	3
655	Khlong Lan	Kamphaeng Phet	99.22	16.27	6203	3
656	Khanu Woralaksaburi	Kamphaeng Phet	99.69	16.01	6204	3
657	Khlong Khlung	Kamphaeng Phet	99.68	16.22	6205	3
658	Phran Kratai	Kamphaeng Phet	99.54	16.71	6206	3

APPENDIX B (continued) Locations of calculated centroids for all 925 district polygons.

	District	Province	Longitude	Latitude	Code	Region[1]
659	Lan Krabue	Kamphaeng Phet	99.87	16.60	6207	3
660	Saithong Wattana	Kamphaeng Phet	99.87	16.31	6208	3
661	Pang Sila Thong	Kamphaeng Phet	99.34	16.03	6209	3
662	Bung Samakkee	Kamphaeng Phet	99.97	16.22	6210	3
663	Kosamphi Nakhon	Kamphaeng Phet	99.35	16.61	6211	3
664	Mueang Tak	Tak	99.17	16.90	6301	3
665	Ban Tak	Tak	99.07	17.09	6302	3
666	Sam Ngao	Tak	98.83	17.39	6303	3
667	Mae Ramat	Tak	98.60	17.09	6304	3
668	Tha Song Yang	Tak	98.12	17.49	6305	3
669	Mae Sot	Tak	98.73	16.73	6306	3
670	Phop Phra	Tak	98.84	16.47	6307	3
671	Umphang	Tak	98.88	15.80	6308	3
672	Wang Chao	Tak	99.15	16.63	6309	3
673	Mueang Sukhothai	Sukhothai	99.78	17.02	6401	3
674	Ban Dan Lan Hoi	Sukhothai	99.50	17.06	6402	3
675	Khiri Mat	Sukhothai	99.74	16.83	6403	3
676	Kong Krailat	Sukhothai	99.98	16.93	6404	3
677	Si Satchanalai	Sukhothai	99.71	17.60	6405	3
678	Si Samrong	Sukhothai	99.73	17.17	6406	3
679	Sawankhalok	Sukhothai	99.84	17.29	6407	3
680	Si Nakhon	Sukhothai	99.96	17.39	6408	3
681	Thung Saliam	Sukhothai	99.55	17.36	6409	3
682	Mueang Phitsanulok	Phitsanulok	100.29	16.83	6501	3
683	Nakhon Thai	Phitsanulok	100.87	17.10	6502	3
684	Chat Trakan	Phitsanulok	100.68	17.39	6503	3
685	Bang Rakam	Phitsanulok	100.04	16.72	6504	3
686	Bang Krathum	Phitsanulok	100.35	16.59	6505	3
687	Phrom Phiram	Phitsanulok	100.15	17.07	6506	3
688	Wat Bot	Phitsanulok	100.37	17.15	6507	3
689	Wang Thong	Phitsanulok	100.58	16.82	6508	3
690	Noen Maprang	Phitsanulok	100.72	16.57	6509	3
691	Mueang Phichit	Phichit	100.37	16.41	6601	3
692	Wang Sai Phun	Phichit	100.54	16.38	6602	3
693	Pho Prathap Chang	Phichit	100.19	16.31	6603	3
694	Taphan Hin	Phichit	100.42	16.21	6604	3
695	Bang Mun Nak	Phichit	100.43	16.03	6605	3
696	Pho Thale	Phichit	100.25	16.06	6606	3
697	Sam Ngam	Phichit	100.13	16.47	6607	3
698	Tap Khlo	Phichit	100.60	16.19	6608	3
699	Sak Lek	Phichit	100.52	16.51	6609	3
700	Bueng Na Rang	Phichit	100.14	16.19	6610	3
701	Dong Cha Roen	Phichit	100.60	16.00	6611	3
702	Muang Phetchabun	Phetchabun	101.18	16.38	6701	3
703	Chondaeng	Phetchabun	100.83	16.11	6702	3
704	Lomsak	Phetchabun	101.31	16.73	6703	3
705	Lomkao	Phetchabun	101.26	16.97	6704	3

APPENDIX B (continued) Locations of calculated centroids for all 925 district polygons.

	District	Province	Longitude	Latitude	Code	Region[1]
706	Wachianburi	Phetchabun	101.09	15.65	6705	3
707	Sithep	Phetchabun	101.14	15.44	6706	3
708	Nongphai	Phetchabun	101.16	16.01	6707	3
709	Bung Samphan	Phetchabun	100.99	15.82	6708	3
710	Num Nao	Phetchabun	101.59	16.85	6709	3
711	Wang Pong	Phetchabun	100.81	16.34	6710	3
712	Khao Kho	Phetchabun	101.00	16.66	6711	3
713	Mueang Ratchaburi	Ratchaburi	99.78	13.54	7001	2
714	Chom Bueng	Ratchaburi	99.52	13.63	7002	2
715	Suan Phung	Ratchaburi	99.30	13.57	7003	2
716	Damnoen Saduak	Ratchaburi	99.97	13.56	7004	2
717	Ban Pong	Ratchaburi	99.81	13.81	7005	2
718	Bang Phae	Ratchaburi	99.98	13.68	7006	2
719	Photharam	Ratchaburi	99.76	13.70	7007	2
720	Pak Tho	Ratchaburi	99.66	13.35	7008	2
721	Wat Phleng	Ratchaburi	99.86	13.45	7009	2
722	Ban Kha	Ratchaburi	99.37	13.33	7010	2
723	Mueang Kanchanaburi	Kanchanaburi	99.32	14.07	7101	2
724	Sai Yok	Kanchanaburi	98.94	14.26	7102	2
725	Bo Phloi	Kanchanaburi	99.46	14.38	7103	2
726	Si Sawat	Kanchanaburi	99.13	14.67	7104	2
727	Tha Maka	Kanchanaburi	99.78	13.95	7105	2
728	Tha Muang	Kanchanaburi	99.61	13.91	7106	2
729	Thong Pha Phum	Kanchanaburi	98.69	14.83	7107	2
730	Sangkhla Buri	Kanchanaburi	98.53	15.19	7108	2
731	Phanom Thuan	Kanchanaburi	99.69	14.16	7109	2
732	Lao Khwan	Kanchanaburi	99.68	14.59	7110	2
733	Dan Makham Tia	Kanchanaburi	99.35	13.84	7111	2
734	Nong Prue	Kanchanaburi	99.40	14.68	7112	2
735	Huai Krachao	Kanchanaburi	99.68	14.34	7113	2
736	Mueang Suphan Buri	Suphan Buri	100.08	14.49	7201	2
737	Doem Bang Nang Buat	Suphan Buri	100.05	14.87	7202	2
738	Dan Chang	Suphan Buri	99.52	14.89	7203	2
739	Bang Pla Ma	Suphan Buri	100.15	14.35	7204	2
740	Si Prachan	Suphan Buri	100.15	14.64	7205	2
741	Don Chedi	Suphan Buri	99.95	14.64	7206	2
742	Song Phi Nong	Suphan Buri	99.99	14.19	7207	2
743	Samchuk	Suphan Buri	100.07	14.75	7208	2
744	Uthong	Suphan Buri	99.89	14.41	7209	2
745	Nong Ya Sai	Suphan Buri	99.85	14.77	7210	2
746	Mueang Nakhon Patho	Nakhon Pathom	100.02	13.82	7301	1
747	Kamphaeng Saen	Nakhon Pathom	99.97	14.03	7302	1
748	Nakhon Chai Si	Nakhon Pathom	100.18	13.82	7303	1
749	Don Tum	Nakhon Pathom	100.10	13.95	7304	1
750	Bang Len	Nakhon Pathom	100.19	14.05	7305	1
751	Sam Phran	Nakhon Pathom	100.22	13.72	7306	1
752	Phutthamonthon	Nakhon Pathom	100.29	13.83	7307	1

APPENDIX B (continued) Locations of calculated centroids for all 925 district polygons.

	District	Province	Longitude	Latitude	Code	Region[1]
753	Mueang Samut Sangkhron	Samut Sakhon	100.26	13.53	7401	1
754	Krathum Baen	Samut Sakhon	100.28	13.66	7402	1
755	Ban Phaeo	Samut Sakhon	100.12	13.59	7403	1
756	Mueang Samut Songkhram	Samut Songkhram	100.00	13.40	7501	2
757	Bang Khonthi	Samut Songkhram	99.95	13.47	7502	2
758	Umphawa	Samut Songkhram	99.91	13.36	7503	2
759	Mueang Phetchaburi	Phetchaburi	99.98	13.08	7601	2
760	Khao Yoi	Phetchaburi	99.81	13.24	7602	2
761	Nong Ya Plong	Phetchaburi	99.47	13.13	7603	2
762	Cha-am	Phetchaburi	99.89	12.75	7604	2
763	Tha Yang	Phetchaburi	99.78	12.82	7605	2
764	Ban Lat	Phetchaburi	99.84	13.05	7606	2
765	Ban Laem	Phetchaburi	99.99	13.18	7607	2
766	Kaeng Krachan	Phetchaburi	99.46	12.86	7608	2
767	Mueang Prachuap	Prachuap Khiri Khan	99.73	11.88	7701	4
768	Kui Buri	Prachuap Khiri Khan	99.75	12.11	7702	4
769	Thap Sakae	Prachuap Khiri Khan	99.57	11.55	7703	4
770	Bang Saphan	Prachuap Khiri Khan	99.44	11.29	7704	4
771	Bang Saphan Noi	Prachuap Khiri Khan	99.34	11.06	7705	4
772	Pran Buri	Prachuap Khiri Khan	99.70	12.38	7706	4
773	Hua Hin	Prachuap Khiri Khan	99.72	12.52	7707	4
774	Sam Roi Yod	Prachuap Khiri Khan	99.74	12.25	7708	4
775	Mueang Nakhon Si	Nakhon Si Thammarat	99.97	8.44	8001	4
776	Phrom Khiri	Nakhon Si Thammarat	99.79	8.54	8002	4
777	Lan Saka	Nakhon Si Thammarat	99.78	8.38	8003	4
778	Chawang	Nakhon Si Thammarat	99.52	8.48	8004	4
779	Phipun	Nakhon Si Thammarat	99.59	8.60	8005	4
780	Chian Yai	Nakhon Si Thammarat	100.16	8.12	8006	4
781	Cha-Uat	Nakhon Si Thammarat	99.99	7.96	8007	4
782	Tha Sala	Nakhon Si Thammarat	99.88	8.70	8008	4
783	Thung Song	Nakhon Si Thammarat	99.66	8.11	8009	4
784	Na Bon	Nakhon Si Thammarat	99.56	8.27	8010	4
785	Thung Yai	Nakhon Si Thammarat	99.38	8.29	8011	4
786	Pak Phanang	Nakhon Si Thammarat	100.16	8.31	8012	4
787	Ron Phibun	Nakhon Si Thammarat	99.90	8.19	8013	4
788	Sichon	Nakhon Si Thammarat	99.81	8.95	8014	4
789	Khanom	Nakhon Si Thammarat	99.81	9.20	8015	4
790	Hua Sai	Nakhon Si Thammarat	100.25	8.01	8016	4
791	Bang Khan	Nakhon Si Thammarat	99.48	8.00	8017	4
792	Tham Phannara	Nakhon Si Thammarat	99.37	8.47	8018	4
793	Chulaphorn	Nakhon Si Thammarat	99.86	8.07	8019	4
794	Phra Phrom	Nakhon Si Thammarat	99.94	8.32	8020	4
795	Nop Phi Tam	Nakhon Si Thammarat	99.68	8.76	8021	4
796	Chang Klang	Nakhon Si Thammarat	99.63	8.36	8022	4
797	Cha Loem Pra Khiat	Nakhon Si Thammarat	100.04	8.18	8023	4
798	Mueang Krabi	Krabi	98.87	8.14	8101	4
799	Khao Phanom	Krabi	99.12	8.26	8102	4

APPENDIX B (continued) Locations of calculated centroids for all 925 district polygons.

	District	Province	Longitude	Latitude	Code	Region[1]
800	Ko Lanta	Krabi	99.08	7.68	8103	4
801	Khlong Thom	Krabi	99.20	7.90	8104	4
802	Ao Luk	Krabi	98.76	8.39	8105	4
803	Plai Phraya	Krabi	98.83	8.54	8106	4
804	Lam Thap	Krabi	99.31	8.05	8107	4
805	Nuea Khlong	Krabi	99.04	8.02	8108	4
806	Mueang Phangnga	Phangnga	98.51	8.49	8201	4
807	Ko Yao	Phangnga	98.59	8.05	8202	4
808	Kapong	Phangnga	98.47	8.74	8203	4
809	Takua Thung	Phangnga	98.40	8.29	8204	4
810	Takua Pa	Phangnga	98.33	8.84	8205	4
811	Khura Buri	Phangnga	98.38	9.16	8206	4
812	Thap Put	Phangnga	98.63	8.53	8207	4
813	Thai Muang	Phangnga	98.31	8.50	8208	4
814	Mueang Phuket	Phuket	98.36	7.84	8301	4
815	Kathu	Phuket	98.31	7.92	8302	4
816	Thalang	Phuket	98.35	8.05	8303	4
817	Mueang Surat Thani	Surat Thani	99.33	9.10	8401	4
818	Kanchanadit	Surat Thani	99.54	9.07	8402	4
819	Don Sak	Surat Thani	99.70	9.19	8403	4
820	Ko Samui	Surat Thani	99.96	9.51	8404	4
821	Ko Pha-Ngan	Surat Thani	100.00	9.79	8405	4
822	Chaiya	Surat Thani	99.00	9.49	8406	4
823	Tha Chana	Surat Thani	99.05	9.61	8407	4
824	Khiri Rat Nikhom	Surat Thani	98.94	9.00	8408	4
825	Ban Ta Khun	Surat Thani	98.68	9.10	8409	4
826	Phanom	Surat Thani	98.70	8.80	8410	4
827	Tha Chang	Surat Thani	98.95	9.34	8411	4
828	Ban Na San	Surat Thani	99.40	8.80	8412	4
829	Ban Na Doem	Surat Thani	99.28	8.90	8413	4
830	Khian Sa	Surat Thani	99.11	8.73	8414	4
831	Wiang Sa	Surat Thani	99.36	8.62	8415	4
832	Phrasaeng	Surat Thani	99.11	8.55	8416	4
833	Phunphin	Surat Thani	99.14	9.02	8417	4
834	Chai Buri	Surat Thani	99.08	8.44	8418	4
835	Wipawadi	Surat Thani	98.88	9.23	8419	4
836	Mueang Ranong	Ranong	98.61	9.86	8501	4
837	La-un	Ranong	98.80	10.08	8502	4
838	Kapoe	Ranong	98.62	9.53	8503	4
839	Kra Buri	Ranong	98.85	10.46	8504	4
840	Suk Samran	Ranong	98.49	9.42	8505	4
841	Mueang Chumphon	Chumphon	99.10	10.46	8601	4
842	Tha Sae	Chumphon	99.10	10.77	8602	4
843	Pathio	Chumphon	99.34	10.81	8603	4
844	Lang Suan	Chumphon	99.05	9.94	8604	4
845	Lamae	Chumphon	99.04	9.76	8605	4
846	Phato	Chumphon	98.81	9.81	8606	4

APPENDIX B (continued) Locations of calculated centroids for all 925 district polygons.

	District	Province	Longitude	Latitude	Code	Region[1]
847	Sawi	Chumphon	99.03	10.25	8607	4
848	Thung Tako	Chumphon	99.05	10.09	8608	4
849	Mueang Songkhla	Songkhla	100.61	7.12	9001	4
850	Sathing Phra	Songkhla	100.42	7.48	9002	4
851	Chana	Songkhla	100.70	6.89	9003	4
852	Na Thawi	Songkhla	100.68	6.64	9004	4
853	Thepha	Songkhla	100.91	6.79	9005	4
854	Saba Yoi	Songkhla	100.91	6.53	9006	4
855	Ranot	Songkhla	100.28	7.80	9007	4
856	Krasae Sin	Songkhla	100.30	7.58	9008	4
857	Rattaphum	Songkhla	100.20	7.08	9009	4
858	Sadao	Songkhla	100.42	6.67	9010	4
859	Hat Yai	Songkhla	100.43	6.97	9011	4
860	Na Mom	Songkhla	100.58	6.96	9012	4
861	Khuan Niang	Songkhla	100.38	7.18	9013	4
862	Bang Kam	Songkhla	100.41	7.07	9014	4
863	Singhanakhon	Songkhla	100.49	7.26	9015	4
864	Khlong Hoi Khong	Songkhla	100.35	6.86	9016	4
865	Mueang Satun	Satun	99.93	6.62	9101	4
866	Khuan Don	Satun	100.13	6.77	9102	4
867	Khuan Kalong	Satun	100.05	6.91	9103	4
868	Tha Phae	Satun	99.92	6.79	9104	4
869	La-ngu	Satun	99.79	6.91	9105	4
870	Thung Wa	Satun	99.77	7.04	9106	4
871	Ma Nung	Satun	99.94	7.01	9107	4
872	Mueang Trang	Trang	99.63	7.61	9201	4
873	Kantang	Trang	99.48	7.40	9202	4
874	Yan Ta Khao	Trang	99.74	7.42	9203	4
875	Palian	Trang	99.80	7.23	9204	4
876	Sikao	Trang	99.37	7.59	9205	4
877	Huai Yot	Trang	99.61	7.79	9206	4
878	Wang Wiset	Trang	99.42	7.75	9207	4
879	Na Yong	Trang	99.75	7.56	9208	4
880	Ratsada	Trang	99.67	7.93	9209	4
881	Hat Samran	Trang	99.60	7.23	9210	4
882	Mueang Phatthalung	Phatthalung	100.10	7.61	9301	4
883	Kong Ra	Phatthalung	99.95	7.42	9302	4
884	Khao Chaison	Phatthalung	100.12	7.47	9303	4
885	Tamot	Phatthalung	100.04	7.28	9304	4
886	Khuan Khanun	Phatthalung	100.06	7.75	9305	4
887	Pak Phayun	Phatthalung	100.32	7.36	9306	4
888	Si Banphot	Phatthalung	99.86	7.69	9307	4
889	Pa Bon	Phatthalung	100.13	7.23	9308	4
890	Bang Kaeo	Phatthalung	100.19	7.42	9309	4
891	Pa Phayom	Phatthalung	99.87	7.83	9310	4
892	Sri Nakarin	Phatthalung	99.91	7.56	9311	4
893	Mueang Pattani	Pattani	101.27	6.85	9401	4

APPENDIX B (continued) Locations of calculated centroids for all 925 district polygons.

	District	Province	Longitude	Latitude	Code	Region[1]
894	Khok Pho	Pattani	101.12	6.70	9402	4
895	Nong Chik	Pattani	101.17	6.80	9403	4
896	Panare	Pattani	101.52	6.81	9404	4
897	Mayo	Pattani	101.40	6.71	9405	4
898	Thung Yang Daeng	Pattani	101.45	6.64	9406	4
899	Sai Buri	Pattani	101.58	6.70	9407	4
900	Mai Kaen	Pattani	101.67	6.63	9408	4
901	Yaring	Pattani	101.39	6.84	9409	4
902	Yarang	Pattani	101.31	6.70	9410	4
903	Kapho	Pattani	101.54	6.61	9411	4
904	Mae Lan	Pattani	101.23	6.67	9412	4
905	Mueang Yala	Yala	101.24	6.55	9501	4
906	Betong	Yala	101.23	5.86	9502	4
907	Bannang Sata	Yala	101.28	6.26	9503	4
908	Than To	Yala	101.26	6.08	9504	4
909	Yaha	Yala	101.12	6.40	9505	4
910	Raman	Yala	101.44	6.49	9506	4
911	Kabang	Yala	100.98	6.36	9507	4
912	Kongpinang	Yala	101.25	6.40	9508	4
913	Mueang Narathiwat	Narathiwat	101.82	6.40	9601	4
914	Tak Bai	Narathiwat	102.00	6.24	9602	4
915	Bacho	Narathiwat	101.65	6.55	9603	4
916	Yi-ngo	Narathiwat	101.71	6.42	9604	4
917	Ra-ngae	Narathiwat	101.71	6.25	9605	4
918	Rueso	Narathiwat	101.52	6.38	9606	4
919	Si Sakhon	Narathiwat	101.51	6.19	9607	4
920	Waeng	Narathiwat	101.86	5.89	9608	4
921	Sukhirin	Narathiwat	101.73	5.92	9609	4
922	Su-ngai Kolok	Narathiwat	101.99	6.07	9610	4
923	Su-ngai Padi	Narathiwat	101.90	6.10	9611	4
924	Chanae	Narathiwat	101.62	6.05	9612	4
925	Caoairong	Narathiwat	101.85	6.23	9613	4

[1]Region codes 1, 2, 3, 4, and 5 correspond to Bangkok and its vicinity, central, north, south, and northeast regions respectively

APPENDIX C Graphs of the region-specific pooled estimates of odds ratios by cause of death (i.e. ratio of the odds of death for a 1μg/m^3 increase in daily PM_{10}) showing results for (a) Bangkok and its vicinity, and for (b) central region.

(a)

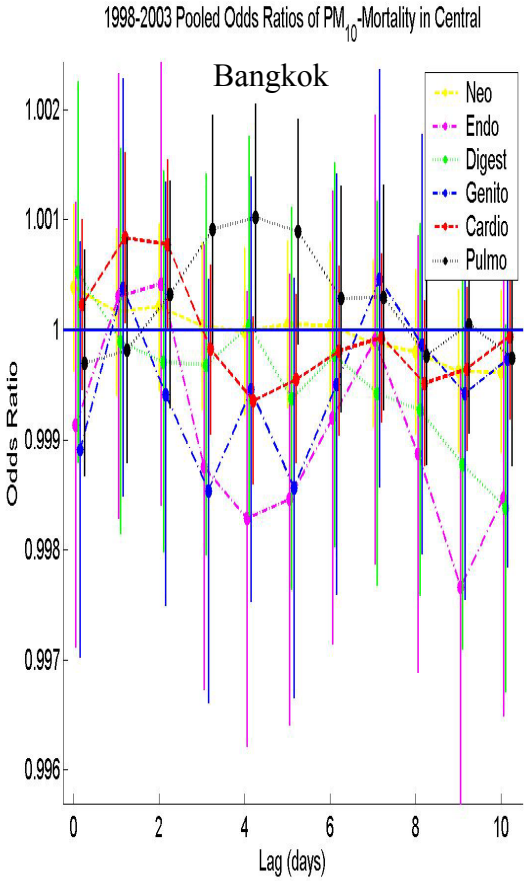

(b)

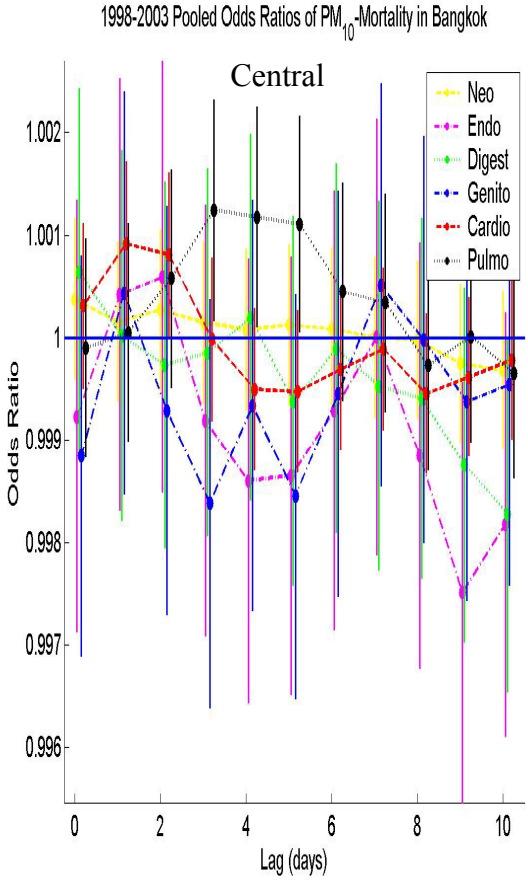

APPENDIX C (continued) Graphs of the region-specific pooled estimates of odds ratios by cause of death (i.e. ratio of the odds of death for a 1μg/m^3 increase in daily PM_{10}) showing results for (c) Northern region, and for (d) Southern region.

(c)

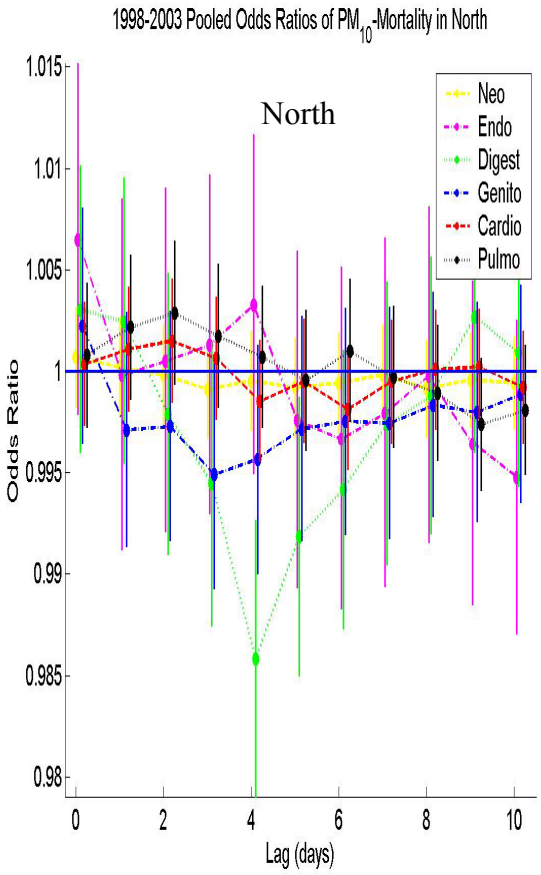

(d)

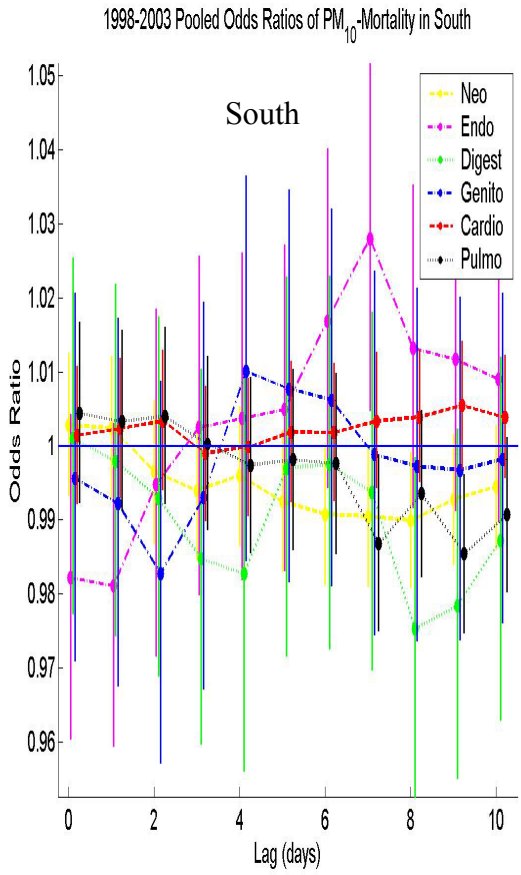

APPENDIX C (continued) Graph of the region-specific pooled estimates of odds ratios by cause of death (i.e. ratio of the odds of death for a 1μg/m^3 increase in daily PM_{10}) showing results for (e) Northeastern region.

(e)

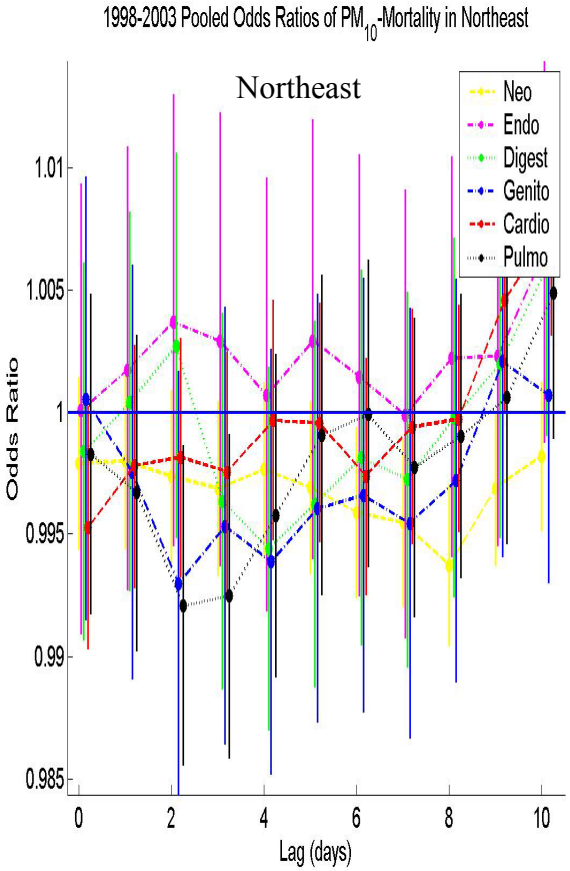

APPENDIX D Graphs of the region-specific and country-wide pooled estimates of the odds ratios showing results by region for (a) digestive mortality, and (b) genitourinary mortality.

(a)

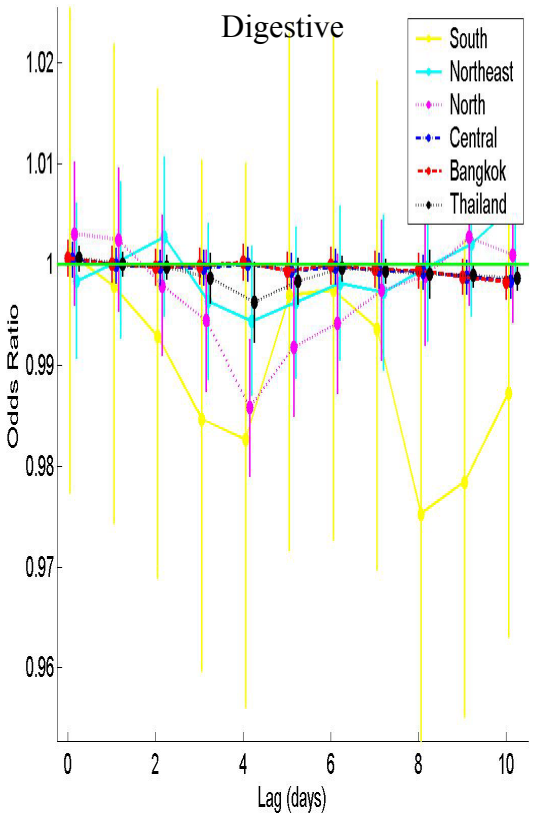

(b)

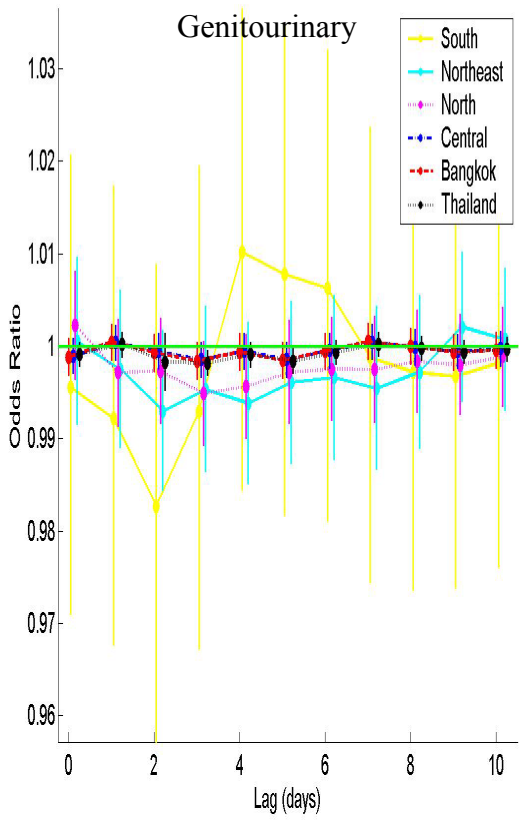

APPENDIX D (continued) Graphs of the region-specific and country-wide pooled estimates of the odds ratios showing results by region for (c) neoplasm mortality, and (d) endocrine, nutritional and metabolic mortality

(c)

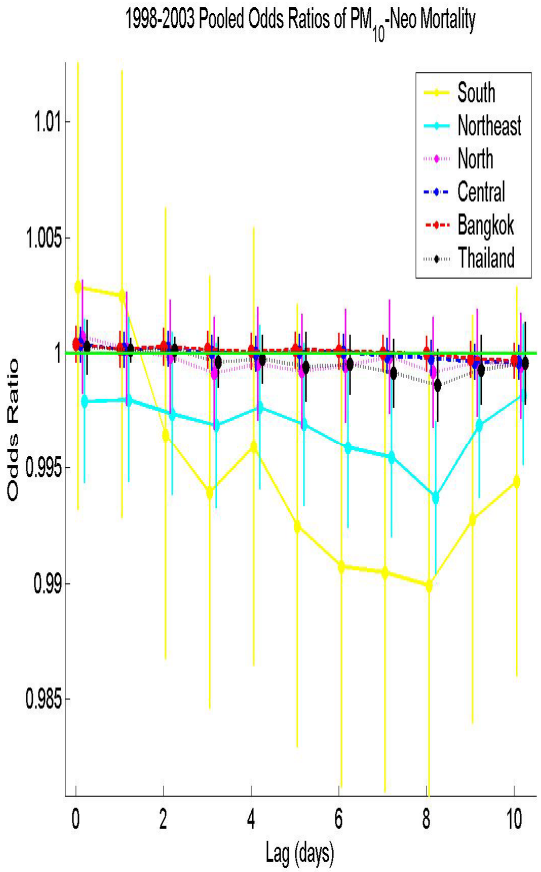

(d)